

AD-A133 366

REFRACTION OF WAVE PACKETS BY CURRENTS(U) FLORIDA INST  
OF TECH MELBOURNE DEPT OF OCEANOGRAPHY AND OCEAN  
ENGINEERING S K HORTON APR 82 TR-JEB-9

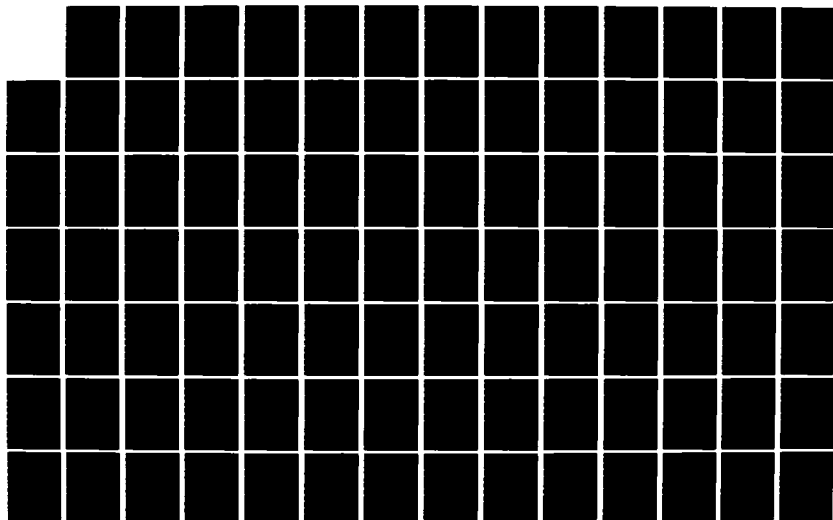
1/2

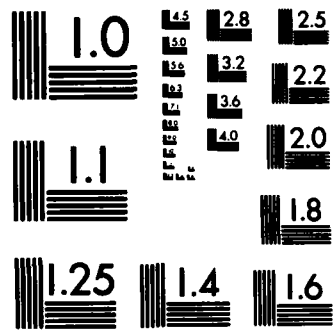
UNCLASSIFIED

N00014-80-C-0677

F/G 8/3

NL





MICROCOPY RESOLUTION TEST CHART  
NATIONAL BUREAU OF STANDARDS-1963-A

A133 366

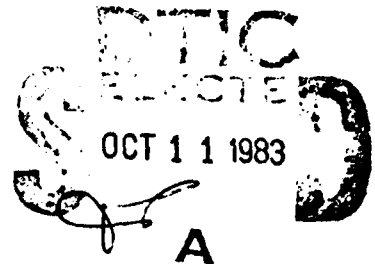
(12)

REFRACTION OF WAVE PACKETS BY CURRENTS

BY SHELLEY KAY HORTON

TECHNICAL REPORT NO. JEB-9  
DEPARTMENT OF OCEANOGRAPHY AND OCEAN ENGINEERING  
FLORIDA INSTITUTE OF TECHNOLOGY

APRIL, 1982



APPROVED FOR PUBLIC RELEASE;  
DISTRIBUTION UNLIMITED

DTIC FILE COPY

SPONSORED BY THE COASTAL SCIENCES PROGRAM,  
OFFICE OF NAVAL RESEARCH, CONTRACT NO. N00014-80-C-0677

83

THE FLORIDA STATE UNIVERSITY  
COLLEGE OF ARTS AND SCIENCES

REFRACTION OF WAVE PACKETS BY CURRENTS

by

SHELLEY KAY HORTON

A Thesis submitted to the  
Department of Oceanography  
in partial fulfillment of the  
requirements for the degree of  
Master of Science

Approved:

\_\_\_\_\_  
Professor Directing Thesis

\_\_\_\_\_  
\_\_\_\_\_  
\_\_\_\_\_

\_\_\_\_\_  
Chairman, Dept. of Oceanography

April, 1982

*[Faint, illegible text and a large handwritten 'A' are visible in this area.]*



## ABSTRACT

The refraction of wave packets by ocean, surface currents is investigated using a refraction method based on Snell's law with geometric group velocity  $G' = U' \cos \phi$  (Breeding, 1978) where  $U' = d\omega'/dk$ ,  $\phi$  is the difference in the direction of the wavelets and packets, and the prime denotes motion relative to the current. This refraction method requires curvature equations for the directions of the wavelets and wave packets, and an advection equation for the direction of the ray. Three equations are necessary, since after refraction the wavelet and packet directions differ, and a ray is not generally orthogonal to the wave fronts in a current. These equations are derived and applied to idealized current models. The current models are patterned after the Gulf Stream and the Circumpolar Current. Both parallel and curved current contours are considered. From this study, it was found that wave packets can be totally reflected or deflected from their original path by a current with the short period waves being affected to a greater extent than the long period waves. The curvature of a ray was found to have the same sign as the vorticity of the current and to increase as the vorticity increased. Rays were found to bend away from the current normal in a following current

and toward the current normal in an opposing current becoming perpendicular to the current speed contours if sufficient refraction occurred. Wave refraction was found to be the least for rays with small initial angles and for currents where  $u_{\max}/G_i$  (maximum current speed to initial geometric group speed) is small. Further, it was found that the change in the direction of a ray was greater than the change in the direction of the packet, which was greater than the change in the direction of the wavelets. The ray angle increased in a following current, and decreased in an opposing current. Critical angles were computed for parallel current speed contours. From an analysis of these angles, it was found that wave packets totally reflect before the wavelets, and at the same point as do the rays. Also, critical angles were found to be a function of the ratio  $u_t/G_i$  (current speed at the turning point to the initial geometric group speed), and to increase as this ratio decreased. Further, it was found that rays with initial angles less than 44 degrees would not be totally reflected by open ocean currents, since extremely large current speeds would be required. An analysis of rays in currents with curved contours indicated that some rays are focused, that some rays exit and re-enter the current, and that some rays may be trapped within the current. These are features which cannot occur with parallel currents. Three additional refraction methods were considered and compared to the method presented here. They were a monochromatic refraction method patterned after Arthur (1950), a wave packet refraction method, using conventional group speed, developed by Kenyon (1971), and a vorticity equation used by Teague (1974) and

presented by Kenyon (1971). It was found that there was very good agreement in the results of all the methods for small initial angles and small current speeds. However, differences between the results obtained by the different methods increased greatly for mid-range angles (30-75 degrees) and for large current speeds.

#### ACKNOWLEDGEMENT

The author wishes to thank the members of her committee, Dr. Raymond C. Staley, Dr. Ruby E. Krishnamurti, Dr. James J. O'Brien, Dr. William C. Burnette, and Dr. J. Ernest Breeding for their helpful review of the manuscript, and for their patience and understanding. A very special thanks to Dr. Breeding, who directed the research, for his guidance, advice, and constructive assistance. I also wish to thank Dr. David Thistle for filling in for Dr. Burnette when he was unable to attend committee meetings.

I would like to express my appreciation to the employees of the FIT Interactive Computing Facility under the direction of Dee Dee Pannell for their help and cooperation, especially to Mike Newell for invaluable help and advice with programming and other necessary computer functions. Thanks also to Kevin Hester.

I also wish to thank Helga Alexander for skillfully typing this manuscript.

This research was supported by the Coastal Sciences Program, Environmental Sciences Division, Office of Naval Research under Contract No. N00014-80-C-0677.

TABLE OF CONTENTS

|  | Page |
|--|------|
| ABSTRACT . . . . .   | ii   |
| ACKNOWLEDGEMENTS . . . . .   | v    |
| TABLE OF CONTENTS . . . . .  | vi   |
| LIST OF FIGURES . . . . .  | viii |
| LIST OF SYMBOLS . . . . .  | xi   |
| I. INTRODUCTION . . . . .  | 1    |
| II. BACKGROUND . . . . .   | 3    |
| III. THEORY . . . . .  | 9    |
| A. Curvature equations for wavelets and packets . . . . .                    | 9    |
| B. Advection equations for rays . . . . .                                    | 15   |
| C. Wavelet and packet directions . . . . .                                   | 16   |
| D. Physical properties of rays . . . . .                                     | 18   |
| E. Snell's law for wavelets and packets . . . . .                            | 19   |
| F. Critical angles . . . . .   | 23   |
| G. Vorticity equation . . . . .  | 28   |
| IV. CURRENT MODELS AND REFRACTION RESULTS . . . . .                          | 35   |
| A. Description of current models . . . . .                                   | 35   |
| B. Wave period . . . . .   | 39   |
| C. Properties of ray trajectories: parallel and<br>curved contours . . . . . | 39   |
| V. COMPARISON OF REFRACTION METHODS . . . . .                                | 78   |
| A. Monochromatic refraction . . . . .  | 78   |
| B. Vorticity approach . . . . .  | 79   |

|   | Page |
|---|------|
| V. COMPARISON OF REFRACTION METHODS (cont.)   |      |
| C. Kenyon's approach . . . . .                | 80   |
| D. Summary of refraction methods . . . . .    | 82   |
| VI. CONCLUSIONS AND RECOMMENDATIONS . . . . . | 86   |
| A. Conclusions . . . . .                      | 86   |
| B. Recommendations . . . . .                  | 92   |
| REFERENCES . . . . .                          | 95   |

## LIST OF FIGURES

| Figure  | Page |
|---|------|
| 1. Relationship between the incremental distances of the ray, wave packet, and wavelet . . . . .  | 17   |
| 2. Plot of critical angles vs. $u_r/G_i$ for wavelets and packets . . . . .   | 26   |
| 3. A blow-up of a section of Figure 2 which indicates the range of critical angles most likely to occur in the open oceans . . . . .                  | 27   |
| 4. The current profile for the Circumpolar Current models .   | 37   |
| 5. The current profile for the Gulf Stream Current models .   | 38   |
| 6. Annual significant period distribution from Daytona Beach, Florida . . . . .   | 40   |
| 7. Annual significant period distribution from Holden Beach, North Carolina . . . . .   | 41   |
| 8. Annual significant period distribution from Wrightsville Beach, North Carolina . . . . .   | 42   |
| 9. Variation in the values of $\rho$ , $\theta$ , and $\gamma$ along a ray in a following current. No reflection and $N = 0.366$ . . .                | 48   |
| 10. Variation in the values of $\rho$ , $\theta$ , and $\gamma$ along a ray in an opposing current. $N = 0.366$ . . . . .                             | 49   |
| 11. Variation in the values of $\rho$ , $\theta$ , and $\gamma$ along a ray in a following current. Total reflection occurs and $N = 0.366$ . . . . . | 50   |
| 12. Variation in the values of $\rho$ , $\theta$ , and $\gamma$ along a ray in a following current. No reflection and $N = 0.046$ . . .               | 51   |
| 13. Variation of the angles $\rho$ , $\theta$ , and $\gamma$ along a ray in a following current. Total reflection occurs and $N = 0.046$              | 52   |
| 14. Ray trajectories for 14 second period waves in a parallel, following current patterned after the Circumpolar Current                              | 53   |
| 15. Ray trajectories for 14 second period waves in a parallel, opposing current patterned after the Circumpolar Current                               | 54   |

| Figure   | Page |
|--|------|
| 16. Ray trajectories for 17 second period waves in a parallel, following current patterned after the Circumpolar Current                                   | 55   |
| 17. Ray trajectories for 17 second period waves in a parallel, opposing current patterned after the Circumpolar Current                                    | 56   |
| 18. Ray trajectories for 7 second period waves in a parallel, following current patterned after the Gulf Stream . . . .                                    | 57   |
| 19. Ray trajectories for 7 second period waves in a parallel, opposing current patterned after the Gulf Stream . . . .                                     | 58   |
| 20. Ray trajectories for 10 second period waves in a parallel, following current patterned after the Gulf Stream . . . .                                   | 59   |
| 21. Ray trajectories for 10 second period waves in a parallel, opposing current patterned after the Gulf Stream . . . .                                    | 60   |
| 22. Ray trajectories for 7 second period waves in a parallel, following current patterned after the Circumpolar Current                                    | 61   |
| 23. Ray trajectories for 14 second period waves in the Circumpolar Current model. The waves enter a following current from the inner radius side . . . . . | 62   |
| 24. Ray trajectories for 14 second period waves in the Circumpolar Current model. The waves enter a following current from the outer radius side . . . . . | 63   |
| 25. Ray trajectories for 14 second period waves in the Circumpolar Current model. The waves enter an opposing current from the inner radius side . . . . . | 64   |
| 26. Ray trajectories for 14 second period waves in the Circumpolar Current model. The waves enter an opposing current from the outer radius side . . . . . | 65   |
| 27. Ray trajectories for 17 second period waves in the Circumpolar Current model. The waves enter a following current from the inner radius side . . . . . | 66   |
| 28. Ray trajectories for 17 second period waves in the Circumpolar Current model. The waves enter a following current from the outer radius side . . . . . | 67   |
| 29. Ray trajectories for 17 second period waves in the Circumpolar Current model. The waves enter an opposing current from the inner radius side . . . . . | 68   |

| Figure   | Page |
|--|------|
| 30. Ray trajectories for 17 second period waves in the Circumpolar Current model. The waves enter an opposing current from the outer radius side . . . . . | 69   |
| 31. Ray trajectories for 7 second period waves in the curved Gulf Stream model. The waves enter a following current from the inner radius side . . . . .   | 70   |
| 32. Ray trajectories for 7 second period waves in the curved Gulf Stream model. The waves enter a following current from the outer radius side . . . . .   | 71   |
| 33. Ray trajectories for 7 second period waves in the curved Gulf Stream model. The waves enter an opposing current from the inner radius side . . . . .   | 72   |
| 34. Ray trajectories for 7 second period waves in the curved Gulf Stream model. The waves enter an opposing current from the outer radius side . . . . .   | 73   |
| 35. Ray trajectories for 10 second period waves in the curved Gulf Stream model. The waves enter a following current from the inner radius side . . . . .  | 74   |
| 36. Ray trajectories for 10 second period waves in the curved Gulf Stream model. The waves enter a following current from the outer radius side . . . . .  | 75   |
| 37. Ray trajectories for 10 second period waves in the curved Gulf Stream model. The waves enter an opposing current from the inner radius side . . . . .  | 76   |
| 38. Ray trajectories for 10 second period waves in the curved Gulf Stream model. The waves enter an opposing current from the outer radius side . . . . .  | 77   |
| 39. Rays computed using various refraction methods. $N = 0.366$  | 83   |
| 40. Rays computed using various refraction methods. $N = 0.091$  | 84   |
| 41. Rays computed using various refraction methods. $N = 0.046$  | 85   |

## LIST OF SYMBOLS

|             |   |
|-------------|---|
| A           | Wave amplitude  |
| C           | Ratio of current speed to phase speed                                       |
| c subscript | Denotes critical angle  |
| $ds_k$      | Incremental distance measured along the orthogonal to the wavelet crest     |
| $ds_m$      | Incremental distance measured along the orthogonal to the wave packet crest |
| $ds_r$      | Incremental distance along the ray  |
| $\hat{e}_k$ | Unit vector in the direction of $\vec{k}$                                   |
| $\hat{e}_m$ | Unit vector in the direction of $\vec{m}$                                   |
| $\hat{e}_r$ | Unit vector in the direction of $\vec{r}$                                   |
| exp         | Base of natural logarithm   |
| g           | Acceleration due to gravity   |
| G           | Geometric group speed relative to a fixed point                             |
| G'          | Geometric group speed relative to the current                               |
| i           | $\sqrt{-1}$   |
| $\hat{i}$   | Unit vector in the x-direction  |
| i subscript | Denotes incident wave   |
| $\hat{j}$   | Unit vector in the y-direction  |
| k           | Wave number of the wavelets   |
| $\hat{k}$   | Unit vector in the z-direction  |
| k subscript | Denotes wavelet component   |
| L           | Wavelength of the transmitted wave  |

|               |  |
|---------------|--|
| $L_0$         | Wavelength of the initial wave   |
| $m$           | Wave number of the wave packet   |
| $m$ subscript | Denotes wave packet component  |
| $M$           | Ratio of the current speed at the turning point to the initial geometric group speed |
| $N$           | Ratio of maximum speed of the current to the initial geometric group speed           |
| $\hat{n}_k$   | Unit vector perpendicular to $\hat{e}_k$   |
| $\hat{n}_r$   | Unit vector perpendicular to $\hat{e}_r$   |
| $P$           | Speed of the ray   |
| $\vec{r}$     | Position vector in a fixed coordinate system   |
| $\vec{r}'$    | Position vector in the coordinate system moving with the current                     |
| $R$           | Radius of curvature  |
| $t$           | Time   |
| $t$ subscript | Denotes transmitted wave   |
| $T$           | Wavelet period   |
| $u$           | Current speed  |
| $u_{cp}$      | Current speed of the Circumpolar Current   |
| $u_{gs}$      | Current speed of the Gulf Stream   |
| $u_{max}$     | Maximum current speed  |
| $U$           | Conventional group speed relative to a fixed point                                   |
| $U'$          | Conventional group speed relative to the current                                     |
| $V$           | Phase speed relative to a fixed point  |
| $V'$          | Phase speed relative to the current  |
| $W$           | Distance from the edge of the current in kilometers                                  |

|                  |  |
|------------------|--|
| $x,y$            | Cartesian coordinate system fixed in space   |
| $x',y'$          | Cartesian coordinate system moving with the current                                      |
| $x'',y''$        | Cartesian coordinate system rotated such that the $y''$ -axis is parallel to the current |
| $\gamma$         | Direction of the wavelet with respect to the x-axis                                      |
| $\Delta$         | Difference between wave components   |
| $\epsilon$       | One-half the frequency bandwidth   |
| $\zeta$          | Vertical component of the current vorticity  |
| $\eta$           | Vertical displacement of the sea surface   |
| $\theta$         | Direction of the wave packet with respect to the x-axis                                  |
| $\pi$            | 3.14159  |
| $\rho$           | Direction of the ray with respect to the x-axis  |
| $\sigma$         | Angular frequency of the wave packet relative to a fixed point                           |
| $\sigma'$        | Angular frequency of the wave packet relative to the current                             |
| $\tau$ subscript | Denotes value at the turning point   |
| $\phi$           | Difference in the direction of the wavelets and packets                                  |
| $\Omega$         | Average angular frequency of the wave packet   |
| $\omega$         | Angular frequency of the wavelets relative to a fixed point                              |
| $\omega'$        | Angular frequency of the wavelets relative to the current                                |
| $\nabla$         | Vector operator del  |

## I. INTRODUCTION

Ocean currents have been observed to cause changes in the direction, wavelength, and amplitude of surface gravity water waves which propagate through them. Several investigations have been made in which the interaction of currents and waves were analyzed. Some investigators used the monochromatic refraction approach for determining wave trajectories. This approach is based on Snell's law with phase velocity. The phase speed is defined as  $V = \omega/k$ , where  $\omega$  is the angular frequency of the wave and  $k$  is its wave number. Another approach which was used determines the refraction of wave groups and is based on the use of Snell's law with conventional group velocity where the conventional group speed  $U = d\omega/dk$  is defined as being in the same direction as the wavelets within the group. The approach taken in this study is to determine the refraction of wave packets using Snell's law with geometric group velocity. The geometric group speed is defined (Breeding, 1978) as  $G = U \cos(\theta - \gamma)$ . The angle  $\theta$  is the direction of the packet and  $\gamma$  is the direction of the wavelets within the packet. Both directions are defined with respect to the positive x-axis.

This study will be confined to idealized, steady, non-uniform currents in deep water. Deep water is defined as water of depth greater than one-half the wavelength of the waves.

In Chapter II, a brief history of work on wave refraction by currents is presented. In Chapter III, the theory used in this work to determine the refraction of wave packets by currents is developed. This consists of curvature equations for wavelets, packets, and rays, and an advection equation for rays. Also, the physical properties of rays, as well as Snell's law, and the critical angles for the wavelets, packets, and rays are discussed. Chapter IV contains descriptions of the current models used and the trajectories computed for these models. Trajectories from parallel and non-parallel current models are analyzed and compared. Chapter V contains a comparison and discussion of the results obtained in this study and the results obtained using the refraction methods of previous investigators. Lastly, Chapter VI contains the conclusions and recommendations.

## II. BACKGROUND

Johnson (1947) was one of the first to investigate the refraction of ocean waves by currents. He considered the refraction of deep water waves by a uniform current in which the waves moved with phase velocity. In Johnson's study wave fronts were constructed with orthogonals to the wave fronts. Johnson showed that the changes in the wavelength of a wave refracted by a current depended upon the ratio of the current speed to the wave's phase speed and upon its angle of incidence to the current. This relationship was expressed as

$$L/L_0 = (1 - C \sin \gamma)^{-2} \quad (1)$$

where  $L$  is the wavelength of the refracted wave,  $L_0$  is the wavelength of the initial wave,  $C$  is the ratio of the current speed to the phase speed, and  $\gamma$  is the angle the wave front initially makes with the boundary between the current and still water. Johnson concluded: a) that the wavelength, steepness, and direction of travel of a wave were significantly changed by its interaction with a current, b) that coastal currents could offer considerable protection against short period waves, and c) that waves can break within the current losing much of their energy and thus creating an area of relative calm beyond the discontinuity.

Arthur (1950) investigated the combined effects of current and bottom topography. He considered the refraction of ocean waves

by currents to be similar to the determination of the minimal flight path of an airplane. He adapted an equation derived by Zermelo (1931) for minimal flight paths. The air speed in Zermelo's equation, which would be analogous to the phase speed in wave refraction, was constant. Arthur extended this derivation to account for a variation in phase speed. He obtained the result

$$\frac{d\gamma}{dt} = - \frac{\partial(V' + u_k) \cos \gamma}{\partial y} + \frac{\partial(V' + u_k) \sin \gamma}{\partial x} \quad (2)$$

where  $x$  and  $y$  denote a Cartesian coordinate system,  $\gamma$  is the angle the wave direction makes with the positive  $x$ -axis,  $V'$  is the phase speed of the wave relative to the current,  $k = 2\pi/L$  is the wave number, and  $u_k = (\vec{k}/k) \cdot \vec{u}$  is the component of the current velocity  $\vec{u}$  in the direction of  $V'$ . Two additional equations were required to determine the wave path (ray) since, as Arthur pointed out, rays are generally not orthogonal to wave fronts in the presence of a current. These equations are

$$dx/dt = u_x + V' \cos \gamma \quad (3)$$

$$dy/dt = u_y + V' \sin \gamma$$

where  $u_x$  and  $u_y$  are the  $x$ - and  $y$ -components, respectively, of the current velocity. Arthur tested these equations on a model of a rip current. He found that waves which propagated against the current slowed down and thus lagged behind waves of the same period propagating in the surrounding still water. He also showed that caustics were formed within the current. These results were similar to those features observed for strong rip currents.

Kenyon (1971) investigated the refraction of wave groups by currents using the geometrical optics approximation. He determined rays by integrating the ray equations (Landau and Lifshitz, 1959)

$$\begin{aligned} \frac{d\vec{k}}{dt} &= -\nabla\omega \\ \frac{d\vec{r}}{dt} &= \nabla_{\vec{k}}\omega \end{aligned} \tag{4}$$

for certain boundary conditions. The vector  $\vec{r}$  is the position vector with respect to a fixed coordinate system,  $\omega$  is the angular frequency of a monochromatic wave,  $\nabla = (\partial/\partial x)\hat{i} + (\partial/\partial y)\hat{j}$ ,  $\nabla_{\vec{k}} = (\partial/\partial k_x)\hat{i} + (\partial/\partial k_y)\hat{j}$ , and  $\hat{i}$  and  $\hat{j}$  are unit vectors in the positive x and y directions, respectively. He also discussed the physical implications of an approximate radius of curvature equation developed by Landau and Lifshitz (1959) from equations (4) for sound waves propagating in a moving medium. In this equation, as stated by Kenyon (1971), the radius of curvature of a ray is  $R = U'/\zeta$  where  $U'$  is the conventional group speed relative to the current and  $\zeta$  is the vertical component of the current vorticity. This equation was not used by Kenyon (personal communication) to determine rays, but was used to discuss general properties of refraction by currents. Kenyon, however, did state that this equation would be a good approximate solution for ray paths when the maximum current speed was less than 5 percent of the initial group speed.

Kenyon (1971) used Gulf Stream and Circumpolar Current models to investigate the effects of refraction by a current. Kenyon concluded: a) waves could be reflected or deflected from their original paths by a current, b) rays, for waves which propagate with (against)

a variable current, bend in the direction of decreasing (increasing) current speed, and c) waves can be trapped about a local minimum or maximum in current speed. He also showed graphically what Arthur (1950) had implied: rays are not perpendicular to wave fronts when in a current.

Teague (1974) applied the radius of curvature expression developed by Landau and Lifshitz (1959) to wave groups propagating through a cyclonic eddy and a loop current. Teague showed that eddies and eddy type currents can have the effect of a giant lens focusing waves into caustics either within or beyond the boundary of the eddy.

Hayes (1980) applied Johnson's (1947) equation for the refraction of monochromatic waves by a current to data obtained for the Gulf Stream from the Marineland, Florida experiment (Shemdin et al., 1975). From the spectral wave data obtained, waves with dominant frequencies of 0.12 Hz. and 0.078 Hz. were observed near the western boundary of the Gulf Stream, and a dominant frequency of 0.12 Hz. was observed for waves in the shelf area west of the stream. In his monochromatic refraction model the 0.078 Hz. wave was reflected and the 0.12 Hz. wave passed through the current undergoing only slight refraction. These results were consistent with the data. However, an analysis based on the refraction of wave packets would also agree with the data. The 0.078 Hz. wave had an initial angle which exceeded the critical angle for either the monochromatic waves or the wave packets. The 0.12 Hz. wave approached the current at near normal incidence. For such angles of incidence,

there is little difference between the monochromatic refraction approach and the wave packet refraction approach. Thus, on the basis of Hayes' (1980) investigation it is not possible to determine the validity of either the monochromatic or the wave packet refraction methods.

When there is a variation of water depth, the traditional method of computing wave trajectories, either for monochromatic waves or wave groups, is to compute the paths using Snell's law with phase speed. The wave groups are assumed to have the same trajectories as the monochromatic waves. Breeding (1972, 1978, 1981) and Black (1979) have shown this traditional method to be incorrect when applied to the refraction of ocean waves. Breeding (1972 and 1978) used computed backtracks from directional wave data due to Hurricane Betsy (1965) and Hurricane Fifi (1974). Black used directional wave energy spectra determined from data obtained in the Gulf of Mexico due to Hurricane Eloise (1975). Both Breeding and Black found that the wave trajectories determined by a monochromatic refraction law were inconsistent with the data.

Breeding (1978) has proposed a refraction method for wave packets (wave groups) that has yielded results consistent with the data. He found that after refraction the packets and the wavelets within the packets no longer move in the same direction. This raises the question as to which refraction law should be used to determine the ray paths. Breeding (1978 and 1981) concluded that the refraction law given by Snell's law with geometric group velocity should be used in computing ray trajectories. The use of this refraction law has led to backtracks consistent with the directional

wave data and the known movements of Hurricanes Betsy (1965) and Fifi (1974). The geometric group velocity  $\vec{C}$  is used instead of the conventional group velocity  $\vec{U}$ , since the wavelet and packet directions differ and  $\vec{U}$  is defined as being in the same direction as the wavelets. The geometric group velocity reduces to the conventional group velocity when the wavelets and the packets are in the same direction. In this study, Breeding's method of wave packet refraction will be extended to apply to the refraction of wave packets by currents.

### III. THEORY

#### A. Curvature equations for wavelets and packets

The refraction of wave packets by a steadily moving, variable, deep water current can be computed by using curvature expressions for the wavelets and packets, and an advection expression for the ray. An expression for the ray by itself is not sufficient to determine the ray path. The wavelet and packet directions along the ray must also be determined since the trajectory of a wave packet depends on the direction of the wavelets within the packet (Breeding, 1978), and in the presence of a current, a ray generally is not normal to a wave front (Arthur, 1950, and Kenyon, 1971). The curvature expression for the wavelets and packets can be derived from the ray equations of geometrical optics. The ray equations for the wavelets and for the packets are

$$d\vec{k}/dt = -\nabla\omega \quad (5)$$

$$d\vec{m}/dt = -\nabla\sigma \quad (6)$$

where  $\omega$  is the average angular frequency of the component waves and  $\vec{k}$  is the corresponding wave number. The quantities  $\vec{m}$ , the wave number of the packet, and  $\sigma$ , the angular frequency of the packet, are defined by the incremental changes in  $\vec{k}$  and  $\omega$  as (Breeding, 1978)

$$\vec{m} = \Delta \vec{k} \quad (7)$$

$$\sigma = \Delta \omega \quad (8)$$

It should be noted that  $\Delta \vec{k}$  involves the difference in both magnitude and direction of the component wave numbers. It will be assumed that the changes in wave properties such as wavelength, direction, and amplitude vary slowly over distances of the order of a wavelength.

The angular frequency relation for wavelets  $\omega = vk$  is valid only for waves in a medium at rest. An angular frequency relationship for a moving medium was derived by Landau and Lifshitz (1959) for sound waves, and by Longuet-Higgins and Stewart (1960) for ocean waves.

Take a rectangular Cartesian coordinate system denoted by  $x, y$  fixed on the sea surface and a similar system denoted by  $x', y'$  moving with the medium (e.g., a current). In the primed system, where the medium appears to be at rest, the wave equation for the packets has the form (Breeding, 1981)

$$\eta = \exp\{i(\vec{k}' \cdot \vec{r}' - \omega' t)\} \int_{\Omega-\epsilon}^{\Omega+\epsilon} A(\omega) \exp\{i(\vec{m}' \cdot \vec{r}' - \sigma' t)\} d\omega \quad (9)$$

where  $\eta$  is the vertical displacement of the sea surface,  $\Omega$  is the average angular frequency of the packet,  $2\epsilon$  is the frequency bandwidth, and  $A$  is the amplitude of the waves. In equation (9) the quantity in front of the integral represents the motion of the wavelets. The quantity within the integral represents the motion of the packets. The position vector for the primed system  $\vec{r}'$  is

related to the position vector of the unprimed system  $\vec{r}$  by

$$\vec{r}' = \vec{r} - \vec{u}t \quad (10)$$

where  $\vec{u}$  is the velocity of the current. By substituting equation (10) into equation (9), the form of  $\eta$  in the unprimed system becomes

$$\eta = \exp\{i[\vec{k}' \cdot \vec{r} - (\vec{u} \cdot \vec{k}' + \omega')t]\} \int_{\Omega-\epsilon}^{\Omega+\epsilon} A(\omega) \exp\{i[\vec{m}' \cdot \vec{r} - (\vec{u} \cdot \vec{m}' + \sigma')t]\} d\omega \quad (11)$$

Also, in the unprimed system,  $\eta$  must have the form

$$\eta = \exp\{i(\vec{k} \cdot \vec{r} - \omega t)\} \int_{\Omega-\epsilon}^{\Omega+\epsilon} A(\omega) \exp\{i(\vec{m} \cdot \vec{r} - \sigma t)\} d\omega \quad (12)$$

Equations (11) and (12) must be equivalent for all time. In particular when  $t = 0$ , it is seen that  $|\vec{k}'| = |\vec{k}|$  and  $|\vec{m}'| = |\vec{m}|$ . Further, the angular frequencies in the fixed systems are seen to be defined by

$$\omega = \omega' + \vec{u} \cdot \vec{k} \quad (13)$$

$$\sigma = \sigma' + \vec{u} \cdot \vec{m} \quad (14)$$

Thus, the angular frequency of a wavelet or a packet in a moving medium is seen to be the sum of the angular frequency of the wave relative to the medium and the advection effect of the medium.

The curvature expressions for the wavelets and packets are derived from equations (5), (6), (13), and (14). The curvature

expression for the direction of the wavelets is obtained by substituting equation (13) into equation (5). This yields

$$d\vec{k}/dt = -k\nabla V' - \nabla(\vec{u} \cdot \vec{k}) \quad (15)$$

The second term on the right can be expanded using a vector identity to obtain

$$d\vec{k}/dt = -k\nabla V' - \vec{k} \cdot \nabla \vec{u} - \vec{k} \times (\nabla \times \vec{u}) - \vec{u} \cdot \nabla \vec{k} - \vec{u} \times (\nabla \times \vec{k}) \quad (16)$$

The fourth and last terms on the right-hand side of equation (16) are zero since  $\vec{k}$  and  $\vec{r}$  are independent variables. Hence, this equation simplifies to

$$d\vec{k}/dt = -k\nabla V' - \vec{k} \cdot \nabla \vec{u} - \vec{k} \times (\nabla \times \vec{u}) \quad (17)$$

An alternative expression for  $d\vec{k}/dt$  is

$$d\vec{k}/dt = k(d\hat{e}_k/dt) + \hat{e}_k(dk/dt) \quad (18)$$

where  $\hat{e}_k = \vec{k}/k$  represents a unit vector in the direction of  $\vec{k}$ .

Equations (17) and (18) can be combined and simplified to find

$$d\hat{e}_k/dt = -\nabla V' - \hat{e}_k \cdot \nabla \vec{u} - \hat{e}_k \times (\nabla \times \vec{u}) - \hat{e}_k/k(dk/dt) \quad (19)$$

A unit vector  $\hat{n}_k$  is taken tangent to the wavelet crest, i.e., perpendicular to  $\hat{e}_k$ . Thus

$$d\gamma/dt = \hat{n}_k \cdot d\hat{e}_k/dt \quad (20)$$

where  $\gamma$  denotes the direction of  $\vec{k}$  with respect to the positive x-axis. Equation (19) can be substituted into equation (20) to obtain

$$\frac{d\gamma}{dt} = \sin\gamma \frac{\partial(V' + u_k)}{\partial x} - \cos\gamma \frac{\partial(V' + u_k)}{\partial y} \quad (21)$$

where  $V'$  is the phase speed of the wavelet relative to the current and  $u_k = \hat{e}_k \cdot \vec{u}$ . This is the same equation used by Arthur (1950) to determine the paths of monochromatic waves. This equation is applicable to waves in any depth of water. Arthur applied it to shallow water waves. In this study it will be applied to deep water waves.

In deep water the wavelet speed can be expressed as  $V' = g/\omega'$ , where  $g$  is the acceleration due to gravity. The gradient of  $V'$  is expressed as

$$\nabla V' = -\frac{1}{k} \left( \frac{\partial \omega'}{\partial x} \hat{i} - \frac{\partial \omega'}{\partial y} \hat{j} \right) \quad (22)$$

substituting equation (13) into (22) leads to

$$\nabla V' = (\partial u_k / \partial x) \hat{i} + (\partial u_k / \partial y) \hat{j} \quad (23)$$

This value of  $\nabla V'$  can be substituted into equation (21) to obtain

$$\frac{d\gamma}{dt} = 2 \left( \frac{\partial u_k}{\partial x} \sin\gamma - \frac{\partial u_k}{\partial y} \cos\gamma \right) \quad (24)$$

Equation (24) can be expressed in a more convenient form by using

$u_k = u_x \cos\gamma + u_y \sin\gamma$ . This leads to

$$\frac{d\gamma}{dt} = 2 \left[ \sin^2 \gamma \frac{\partial u_y}{\partial x} + \sin\gamma \cos\gamma \left( \frac{\partial u_x}{\partial x} - \frac{\partial u_y}{\partial y} \right) - \cos^2 \gamma \frac{\partial u_x}{\partial y} \right] \quad (25)$$

Further, the arc length along the trajectory of an orthogonal to a wavelet crest is defined by  $ds_k = (V' + u_k)dt$ . As a result

equation (25) becomes

$$\frac{dy}{ds_k} = \frac{2}{V' + u_k} \left[ \sin^2 \gamma \frac{\partial u_y}{\partial x} + \sin \gamma \cos \gamma \left( \frac{\partial u_x}{\partial x} - \frac{\partial u_y}{\partial y} \right) - \cos^2 \gamma \frac{\partial u_x}{\partial y} \right] \quad (26)$$

This is the curvature equation which will be used to determine the change in the wavelet direction along a ray.

The curvature expression for the packets can be obtained by substituting equation (14) into equation (6). Following the same procedure as for the wavelets, the result is

$$\frac{d\theta}{ds_m} = \frac{1}{G' + u_m} \left[ \sin \theta \frac{\partial(G' + u_m)}{\partial x} - \cos \theta \frac{\partial(G' + u_m)}{\partial y} \right] \quad (27)$$

where  $\theta$  is the angle between  $\vec{m}$  and the positive x-axis,  $ds_m$  is the incremental distance measured along the orthogonals to the packet crest,  $G'$  is the geometric group velocity measured relative to the current, and  $u_m$  is the component of the current velocity in the direction of  $\vec{m}$ .

As was equation (21), equation (27) can be rewritten for the case of deep water waves. In deep water the geometric group velocity can be expressed as  $G' = \frac{1}{2}V'\cos\phi$ . Making this substitution for  $G'$  in equation (27) yields

$$\begin{aligned} \frac{d\theta}{ds_m} = \frac{1}{G' + u_m} & \left[ \sin^2 \theta \frac{\partial u_y}{\partial x} + \sin \theta \cos \theta \left( \frac{\partial u_x}{\partial x} - \frac{\partial u_y}{\partial y} \right) \right. \\ & - \cos^2 \theta \frac{\partial u_x}{\partial y} + \frac{1}{2} \cos \phi \left\{ \sin \theta \left( \cos \gamma \frac{\partial u_x}{\partial x} + \sin \gamma \frac{\partial u_y}{\partial x} \right) \right. \\ & \left. \left. - \cos \theta \left( \cos \gamma \frac{\partial u_x}{\partial y} + \sin \gamma \frac{\partial u_y}{\partial y} \right) \right\} \right] \quad (28) \end{aligned}$$

This is the curvature equation which will be used to determine the change in the packet direction along a ray.

#### B. Advection equation for rays

The determination of rays for wave packets can be obtained by taking Arthur's (1950) approach to wave refraction by currents. He recognized that refraction of surface waves by a current was due solely to advection. He thus determined the wavelet direction from equation (2) and the ray direction from the x- and y-components of the ray velocity (equations 3), which is the vector sum of the current velocity and the phase velocity. Ray paths were then determined by simultaneously solving these equations.

Rays for wave packets can be derived in a similar manner, except that both the wavelet and packet directions are required. The direction of the packets is given by equation (28), and the direction of the wavelets by equation (26). The ray velocity expressed in its component form is

$$\begin{aligned} dx/dt &= u_x + G' \cos\theta \\ dy/dt &= u_y + G' \sin\theta \end{aligned} \tag{29}$$

where  $u_x$  and  $u_y$  are the x- and y-components of the current velocity. Thus, the direction of the ray  $\rho$  is given by

$$\tan\rho = \frac{dy}{dx} = \frac{u_y + G' \sin\theta}{u_x + G' \cos\theta} \tag{30}$$

Ray paths for wave packets are determined by simultaneously solving equations (26), (28), and (29).

### C. Wavelet and packet directions

Wavelets, packets, and rays travel with different velocities and after refraction in different directions. This is an important fact which must be taken into account when computing trajectories. Even though the directions of the wavelets and packets differ from the direction of the ray, they are nevertheless carried along by the ray, and thus must reach the same speed contour as does the ray. To compensate for these differences in travel time and direction, the curvature equations for wavelets and packets must be multiplied by the ratios of the speeds and the cosines of the directions.

Consider a current with locally, parallel speed contours, and an  $x'', y''$ -coordinate system, such that the  $x''$ -axis is perpendicular to the contours (see Figure 1). It is thus seen that for the wavelets

$$ds_k = (P \cos \rho \, dt) / \cos \gamma \quad (31)$$

and for the packets

$$ds_m = (P \cos \rho \, dt) / \cos \theta \quad (32)$$

where  $\vec{P} = \vec{G}' + \vec{u}$  is the ray velocity.

These equations relate the incremental distances traveled by the wavelets or packets to that transversed by the ray. Substituting equation (31) into (26) and equation (32) into (28) results in the curvature expressions needed for computations of ray paths.

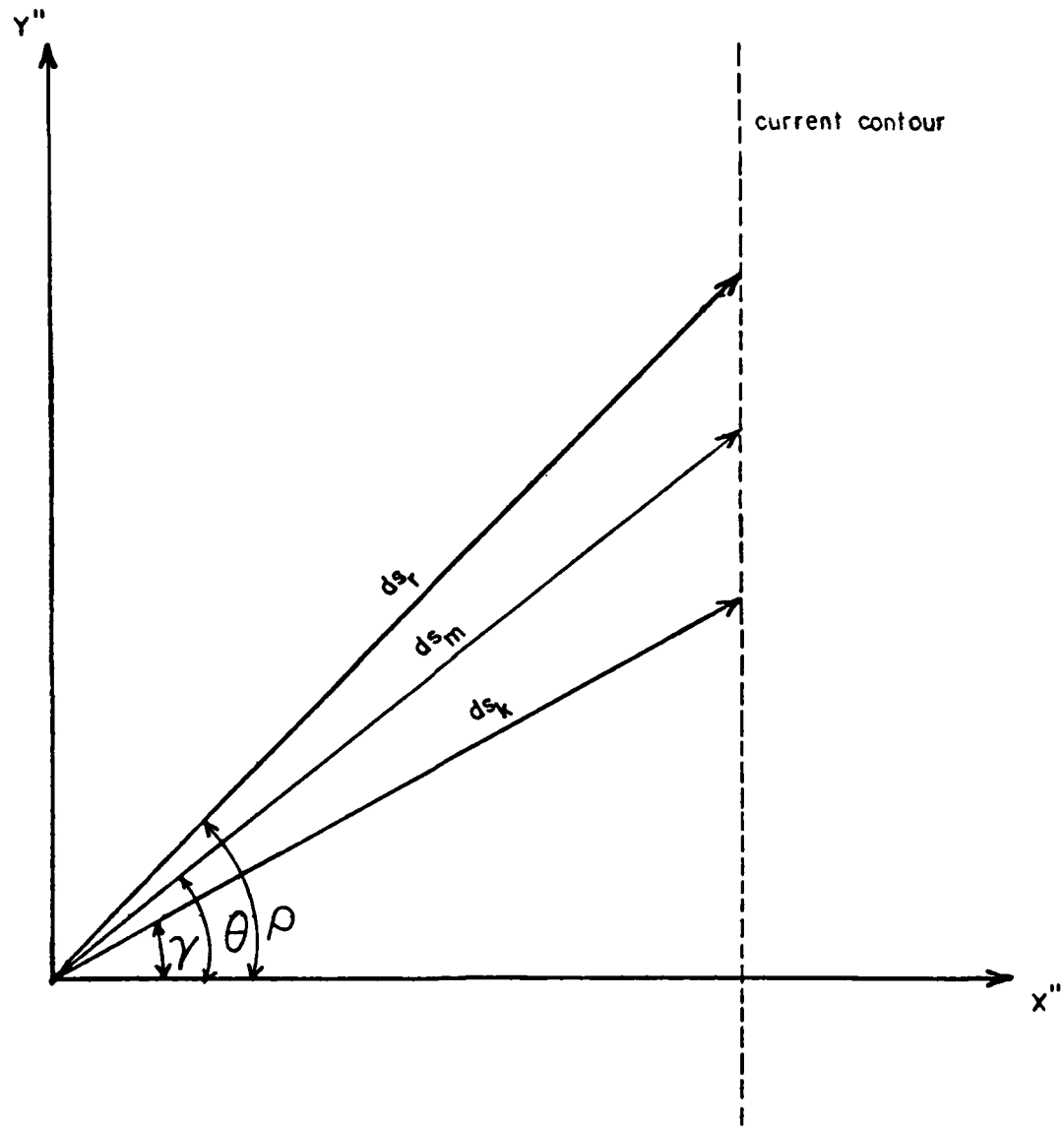


Figure 1. Relationship between the incremental distances for the ray ( $ds_r$ ), for the wave packet ( $ds_m$ ), and for the wavelets ( $ds_k$ ) between two points along the ray. The  $y''$ -axis is chosen to be parallel to the current speed contours.

#### D. Physical properties of rays

Some of the physical properties of wave rays can be deduced from equation (30). This equation can be written in a more convenient form by considering a variable, unidirectional current with parallel speed contours and xy-coordinate system such that the y-direction is parallel to the current. Equation (30) thus becomes

$$\tan\rho = u/(G'\cos\theta) + \tan\theta \quad (33)$$

From this result it is seen that  $\rho > \theta$  for a following current ( $u > 0$ ), that  $\rho < \theta$  for an opposing current ( $u < 0$ ), and that when  $\theta = 90$  degrees, the ray direction  $\rho = 90$  degrees. Thus when the packets reflect the rays must also reflect. Also, it is seen that if  $u \ll G'$  the ray and packet directions are almost equal.

Consideration of the instances when  $\rho$  or  $\theta$  are either 90 degrees or zero afford some interesting features. If  $\theta = 0$  degrees, i.e., the packets are perpendicular to the current contours, the direction of a ray varies only as  $u/G'$  varies. Thus, if the wavelets and packets enter a current at normal incidence, they remain normal to the current, but the ray direction changes as the current speed changes. If the current speed is constant the ray is a straight line. From the more general equation (30) for  $\rho = 90$  degrees, either  $u_x = G'_x = 0$  or  $u_x = -G'_x$ , provided the numerator is finite and does not vanish. So, at a turning point either the x-component of the current speed and group speed are zero or they balance each other. It has been found (Figures 14 thru 22) that for currents with parallel

contours, total reflection occurs for following currents only. Therefore, the first case applies and at a turning point the directions of the packet, current, and ray are all parallel to the y-axis. The second case will not occur for parallel contours, but if the contours are curved it is possible for the x-components of the speeds to balance each other. In a current with curved contours, it was found (Figures 26 and 30) that a ray in an opposing current can be totally reflected. When the turning point is reached under these circumstances, the ray direction and current direction exactly oppose each other. For  $\rho = 0$  degrees, either  $u_y = G'_y = 0$  or  $u_y = -G'_y$ , provided the denominator is finite and does not vanish. Only the second case is of interest. This result indicates that rays may become perpendicular to the current contours. It was found (Figures 19 and 21) that for opposing currents, rays are turned toward the normal to the current and in some instances become perpendicular to the current contours.

#### E. Snell's law for wavelets and packets

Snell's law expressions for wavelets and packets are derived by considering a current with parallel speed contours such that the magnitude of the current velocity varies across the current. Each current speed contour acts as a discontinuity to an approaching wave causing the wave to reflect and refract. The wavelet or packet must remain continuous across the discontinuity. Therefore, as an incident wave crest advances one wavelength the refracted wave crest also advances one wavelength. The wavelength changes as the wave

crosses the discontinuity, but the time, relative to a fixed coordinate system, required for the incident wave and refracted wave to advance one wavelength (i.e., the period) does not change. There is, however, a change in the wave period measured relative to the current.

The component of the wave number parallel to the boundary must be constant. Thus

$$k \sin\gamma = \text{constant} \quad (34)$$

where  $\gamma$  is the angle the wave crest makes with the boundary.

Both sides of equation (34) can be divided by  $\omega = Vk$ . Therefore

$$\frac{\sin\gamma}{V} = \text{constant} \quad (35)$$

where  $V$  is the phase speed relative to a fixed coordinate system.

The phase speed  $V$  can also be expressed as the sum of the phase speed relative to the current and the component of the current in the direction of  $\vec{k}$ , i.e.,

$$V = V' + u \sin\gamma \quad (36)$$

Then the refraction law for the wavelets can be stated as

$$\frac{\sin\gamma_t}{V'_t + u_t \sin\gamma_t} = \frac{\sin\gamma_i}{V'_i + u_i \sin\gamma_i} \quad (37)$$

where the subscript  $t$  denotes the transmitted wave and the subscript  $i$  denotes the incidence wave. If  $u_i = 0$  this result reduces to Johnson's (1947) equation (3) which is

$$\sin\gamma_t = \frac{\sin\gamma_i}{(1 - u \sin\gamma_i/V_i)^2} \quad (38)$$

It is clearly seen from this equation that the refracted angle for the wavelets is dependent upon the initial angle and the current speed ratio.

The Snell's law expression for packets is obtained in a similar manner. A crest which is determined by the interference maximum of the packet must be continuous across a boundary. Thus

$$m \sin\theta = \text{constant} \quad (39)$$

where  $\theta$  is the angle the packet crest makes with the boundary. In a fixed coordinate system,  $\sigma$ , the angular frequency of the packet, is a constant on both sides of the boundary. Thus, when both sides of equation (39) are divided by  $\sigma$  the result is

$$\frac{\sin\theta}{G} = \text{constant} \quad (40)$$

Further,  $G$  can be expressed as

$$G = G' + u \sin\theta \quad (41)$$

where  $G'$  is the geometric group speed relative to the current and  $u \sin\theta$  is the component of the current speed in the direction of  $\vec{m}$ . The refraction law for the packets can then be stated as

$$\frac{\sin\theta_t}{G'_t + u_t \sin\theta_t} = \frac{\sin\theta_i}{G'_i + u_i \sin\theta_i} \quad (42)$$

When there are no currents, equation (42) reduces to the results obtained by Stonely (1935) and Breeding (1978). Stonely used the

result to determine the direction of amplitude (group) fronts along monochromatic trajectories, whereas Breeding used the result to define wave packet trajectories. If  $u_i = 0$ , equation (42) can be rewritten as

$$\frac{\sin\theta_t}{G'_t + u_t \sin\theta_t} = \frac{\sin\theta_i}{G'_i} \quad (43)$$

Rearrangement of this equation leads to

$$\frac{G'_i - u_t \sin\theta_i}{\sin\theta_i} = \frac{G'_t}{\sin\theta_t} \quad (44)$$

Note that

$$G'_t = U'_t (\cos\theta_t \cos\gamma_t + \sin\theta_t \sin\gamma_t) \quad (45)$$

Therefore

$$\frac{G'_t}{\sin\theta_t} = U'_t (\text{ctn}\theta_t \cos\gamma_t + \sin\gamma_t) \quad (46)$$

Thus, substituting equation (46) into equation (44) yields

$$\text{ctn}\theta = \frac{G'_i - u_t \sin\theta_i - U'_t \sin\theta_i \sin\gamma_t}{U'_t \sin\theta_i \cos\gamma_t} \quad (47)$$

From this equation it is seen that the refracted angle for the packets is not solely determined from the initial wave quantities: period, angle, etc., but that certain transmitted wavelet values are also needed.

Equations (38) and (47) are useful in determining refracted angles and critical angles.

### F. Critical angles

A wavelet or a packet totally reflects when its transmitted angle equals 90 degrees. Thus, expressions for computing critical angles can be obtained by solving the Snell's law equations for the corresponding initial angles when the transmitted angle is 90 degrees.

For wavelets when  $\gamma_t = 90$  degrees equation (38) becomes

$$\frac{\sin\gamma_c}{(1 - u_\tau \sin\gamma_c / v_i)^2} = 1 \quad (48)$$

where  $\gamma_c$  is the critical angle for the wavelets and  $u_\tau$  is the current speed at the turning point. This equation can be rearranged and written as

$$\left(\frac{u_\tau}{v_i}\right)^2 \sin^2\gamma_c - \left(\frac{2u_\tau}{v_i} + 1\right) \sin\gamma_c + 1 = 0 \quad (49)$$

The quadratic equation can be used to solve this equation for  $\sin\gamma_c$ .

The result is

$$\sin\gamma_c = \frac{\left(2(u_\tau/v_i) + 1\right) - \sqrt{\left(2(u_\tau/v_i) + 1\right)^2 - 4(u_\tau/v_i)^2}}{2(u_\tau/v_i)^2} \quad (50)$$

Let  $M = u_\tau/G_i = 2u_\tau/v_i$  and substitute this into equation (50). It is found that

$$\sin\gamma_c = \left(2(M + 1) - 2\sqrt{2M + 1}\right)/M^2 \quad (51)$$

Thus, a critical angle for wavelets can be computed given a current speed to initial geometric group speed ratio. Critical angles for

wavelets are independent of period and shear.

From equation (47) for the packets, when  $\theta_t = 90$  degrees,  $\text{ctn}\theta_t = 0$  and it follows that

$$G_i - u_\tau \sin\theta_c - U'_\tau \sin\theta_c \sin\gamma_\tau = 0 \quad (52)$$

where  $\theta_c = \theta_i$  is the critical angle for the packets. Then

$$\sin\theta_c = \frac{G_i}{u_\tau + U'_\tau \sin\gamma_\tau} \quad (53)$$

If  $u_i = 0$ , (wavelets and packets are assumed parallel upon entering a current) then

$$\sin\theta_c = U'_\tau / (u_\tau + U'_\tau \sin\gamma_\tau) \quad (54)$$

This equation is not in a usable form. It is necessary to express  $\gamma_\tau$  as a function of  $\gamma_i$  where  $\gamma_i = \theta_c$ . Equation (54) can be written in a form independent of  $\gamma_i$ , if  $U'_\tau$  and  $\sin\gamma_\tau$  are expressed in terms of the initial wavelet values. Equation (38) expresses  $\gamma_\tau$  in terms of the initial wavelet values. The quantity  $U'_\tau$  can be expressed in terms of the initial values as follows

$$U'_\tau = \frac{1}{2} \sqrt{gL_\tau / 2\pi} \quad (55)$$

where  $L_\tau = L_i \sin\gamma_\tau / \sin\gamma_i$ . Making this substitution for  $L_\tau$ , and equation (38) for  $\sin\gamma_\tau$ , equation (55) becomes

$$U'_\tau = \frac{1}{2} \left\{ \frac{gL_i}{2\pi(1 - u \sin\gamma_i / V_i)^2} \right\}^{1/2} \quad (56)$$

The quantity  $V_i = gT_i^2 / 2\pi$  and  $u/V_i = \frac{1}{2}M$  where  $T_i$  denotes the

initial wave period. Thus, using these definitions for  $L_1$  and  $M$ , and rearranging terms, equation (56) becomes

$$U'_\tau = \frac{U'_1}{(1 - \frac{1}{2}M \sin \gamma_1)} \quad (57)$$

Equations (38) and (57) can be substituted into equation (54) to obtain

$$\sin \theta_c = \frac{U_1 (1 - \frac{1}{2}M \sin \gamma_1)^3}{u_\tau (1 - \frac{1}{2}M \sin \gamma_1)^3 + U_1 \sin \gamma_1} \quad (58)$$

Finally, since the wavelets and packets have the same initial direction it follows that  $\gamma_1 = \theta_c$ . Thus equation (58) can be written as

$$M^4 \sin^4 \theta_c - 7M^3 \sin^3 \theta_c + (18M^2 - 8) \sin^2 \theta_c - 20M \sin \theta_c + 8 = 0 \quad (59)$$

This is a quartic equation. In general, the expressions for the roots of such an equation are useless for computations (Sokolnikoff and Sokolnikoff, 1941). One thing which can be obtained from this equation is that the critical angles for packets are a function of  $U_\tau/G_1$  and are independent of period and shear as were the critical angles for the wavelets.

Often equations like (54) can be solved for specific values by iteration. The iteration process failed in this case due to non-convergence. Finally critical angles for packets were determined by trial and error using equations (47) and (54).

Figures 2 and 3 show graphically the critical angles obtained for wavelets and packets. From these figures it is seen that packets reflect at smaller angles of incidence than do the wavelets. Thus

CRITICAL ANGLES VS.  $U/G_i$   
FOR ALL WAVE PERIODS

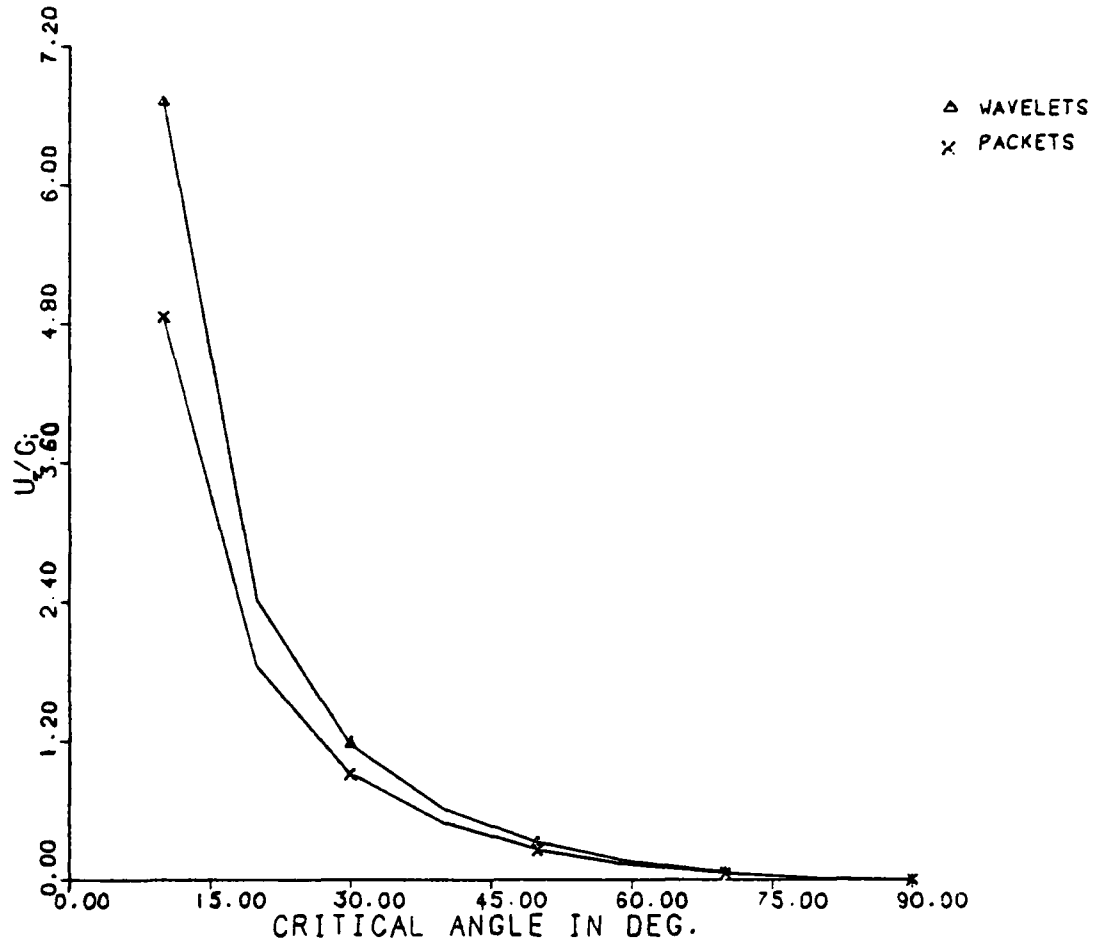


Figure 2. Plot of critical angles vs.  $u_T/G_i$  for wavelets and packets.

CRITICAL ANGLES VS.  $U_c/G_i$   
FOR ALL WAVE PERIODS

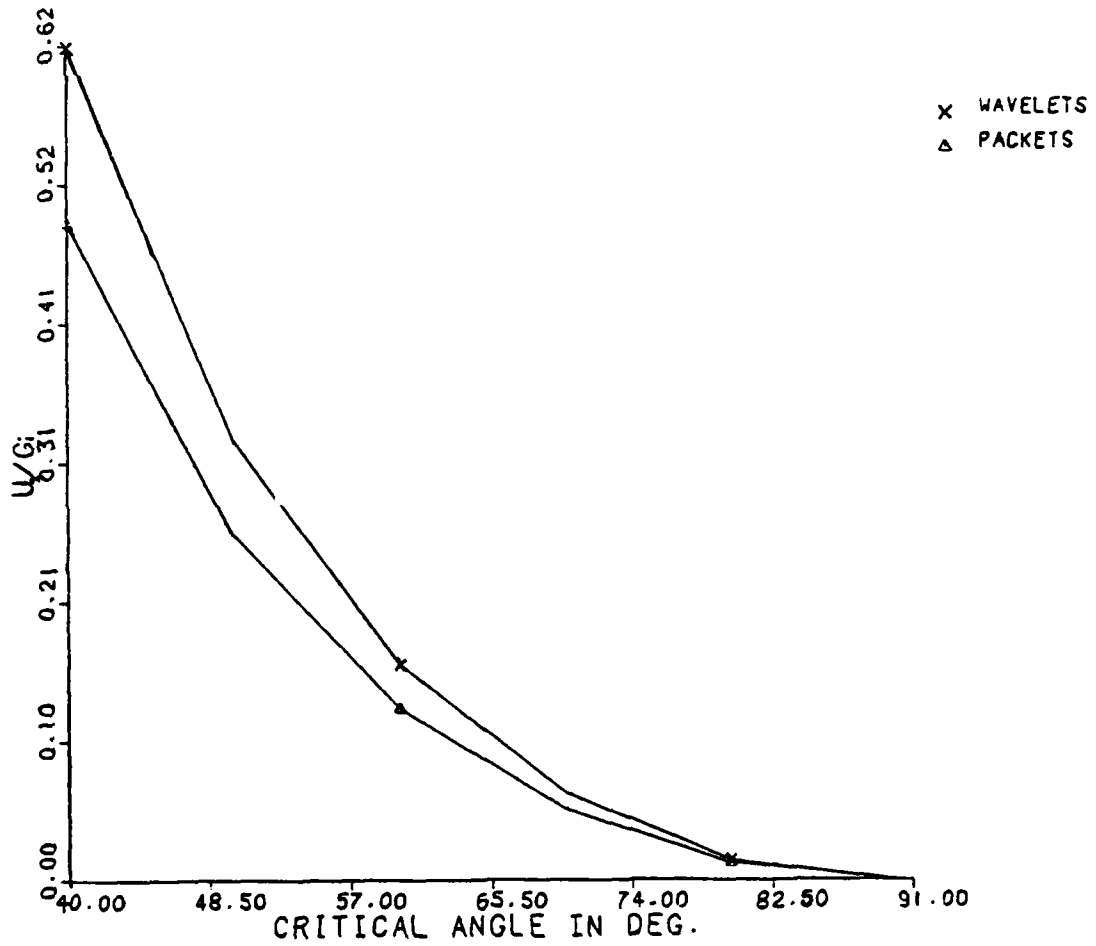


Figure 3. A blow-up of a section of Figure 2 which indicates the range of critical angles most likely to occur in the open ocean.

along a ray the packets reflect before the wavelets, and since the rays must reflect when the packets reflect (Section II.D.) it follows that the ray also reflects before the wavelets. It can also be seen that as the ratio  $u_T/G_i$  decreases the initial angle required for a ray to reflect increases and eventually the critical angles for wavelets, packets and rays become equal. Further, it is seen that very large values of  $u_T/G_i$  are required to reflect rays of small initial angle. For wave periods consistent with surface gravity waves (7 to 20 seconds) only rays with initial angles greater than 44 degrees will be reflected by open ocean currents. To reflect rays with initial angles less than 44 degrees, current speeds greater than two meters per second must be encountered. (The maximum speed of the Gulf Stream is 2 m/sec.)

Figure 3 is a blow-up of a section of Figure 2. This figure indicates the range of critical angles most likely to occur for surface gravity waves in the open ocean.

#### G. Vorticity equation

Another approach to determining ray paths for wave groups is to employ a curvature equation similar to the equation discussed by Kenyon (1971) and used by Teague (1974). This curvature equation involves the current vorticity and the conventional group speed. In this section, a curvature equation for rays of wave packets using geometric group speed will be developed and compared to the ray curvature equation mentioned by Kenyon and used by Teague. These curvature equations will be compared to the advection equation (30).

A ray curvature equation can be derived from equations (6) and (10) assuming that  $u \ll G'$ . The time derivative of equation (10) is

$$\vec{P} = G'(\vec{m}/m) + \vec{u} \quad (60)$$

where  $\vec{P}$  is the velocity of the ray. Multiplying equation (60) by  $m$  and taking the derivative of the result with respect to time yields

$$\frac{d(\vec{P}m)}{dt} = G' \frac{d\vec{m}}{dt} + \vec{m} \frac{dG'}{dt} + m \frac{d\vec{u}}{dt} + \vec{u} \frac{dm}{dt} \quad (61)$$

Equation (6) can be expanded and rewritten as

$$d\vec{m}/dt = -m\nabla G' - \vec{m} \cdot \nabla \vec{u} - \vec{m} \times (\nabla \times \vec{u}) \quad (62)$$

just as was done with equation (15) for the wavelets.

For steady state conditions  $\partial G'/\partial t = 0$  and  $\partial \vec{u}/\partial t = 0$ . Therefore, along a ray the total derivatives for  $G'$  and  $\vec{u}$  are

$$dG'/dt = \vec{P} \cdot \nabla G' \quad (63)$$

$$d\vec{u}/dt = \vec{P} \cdot \nabla \vec{u} \quad (64)$$

When (60) is substituted into (64), and only the first order term in  $\vec{u}$  is retained, it is found that

$$d\vec{u}/dt = G'(\vec{m}/m) \cdot \nabla \vec{u} \quad (65)$$

The substitution of equations (62), (63), and (65) into equation (61) yields

$$d(\vec{P}m)/dt = -G'm\nabla G' - G'\vec{m} \times (\nabla \times \vec{u}) + \vec{m}(\vec{P} \cdot \nabla G') + \vec{u} dm/dt \quad (66)$$

Since  $u \ll G'$  it can be assumed that  $P \approx G'$  and that the direction of  $\vec{m}$  is approximately the same as the direction of the ray. Then  $P$  can be substituted for  $G'$  in equation (66) and a unit vector in the direction of the ray, defined as  $\hat{e}_r = \vec{P}/P$ , can be substituted for the direction of  $\vec{m}$ . Then

$$d(\vec{P}m)/dt = -Pm\nabla G' - Pm\hat{e}_r \times (\nabla \times \vec{u}) + m\hat{e}_r (\vec{P} \cdot \nabla G') + \vec{u} dm/dt \quad (67)$$

Also

$$d(\vec{P}m)/dt = \hat{e}_r d(Pm)/dt + Pm(d\hat{e}_r/dt) \quad (68)$$

where  $\hat{e}_r$  and  $d\hat{e}_r/dt$  are perpendicular. Equations (67) and (68) can be combined to obtain

$$\begin{aligned} d\hat{e}_r/dt = & -\nabla G' - \hat{e}_r \times (\nabla \times \vec{u}) + (\vec{u}/Pm)(dm/dt) - (\hat{e}_r/Pm)d(Pm)/dt \\ & + (\hat{e}_r/P)(\vec{P} \cdot \nabla G') \end{aligned} \quad (69)$$

The third term on the right-hand side of this equation can be neglected since  $u \ll P$  and since the wave properties are assumed to change little over distances of the order of a wavelength.

The direction of the ray, i.e., the direction of  $\hat{e}_r$  with respect to the positive x-axis, is denoted by  $\rho$ . Then

$$d\rho/dt = \hat{n}_r \cdot (d\hat{e}_r/dt) = -\hat{n}_r \cdot \nabla G' - \hat{n}_r \cdot [\hat{e}_r \times (\nabla \times \vec{u})] \quad (70)$$

where  $\hat{n}_r$  is a unit vector perpendicular to  $\hat{e}_r$ .

For surface gravity waves, only the vertical component  $\zeta$  of the vorticity affects the ray trajectory. The z-component of  $(\nabla \times \vec{u})$  is given by

$$\zeta = \partial u_y / \partial x - \partial u_x / \partial y \quad (71)$$

Simplification of (70) leads to

$$d\rho/dt = \sin\rho (\partial G'/\partial x) - \cos\rho (\partial G'/\partial y) + \partial u_y / \partial x - \partial u_x / \partial y \quad (72)$$

Further, since  $ds_r \approx G'dt$ , where  $ds_r$  is an element of arc length along the ray, it is found that

$$\frac{d\rho}{ds_r} = \frac{1}{G'} \left[ \sin\rho \frac{\partial G'}{\partial x} - \cos\rho \frac{\partial G'}{\partial y} + \frac{\partial u_y}{\partial x} - \frac{\partial u_x}{\partial y} \right] \quad (73)$$

Equation (73) is the curvature equation for computing the rays of wave packets refracted by a current. This equation should be used in conjunction with the wavelet and packet curvature equations.

If  $\theta$  and  $\gamma$  are assumed to be in the same direction, and if the group speed  $U'$  is assumed to be constant along the ray, equation (73) will reduce to the curvature equation discussed by Kenyon (1971) and used by Teague (1974). That is

$$\frac{d\rho}{ds_r} = \frac{1}{U'} \left[ \frac{\partial u_y}{\partial x} - \frac{\partial u_x}{\partial y} \right] \quad (74)$$

This equation will determine ray paths, but only under very strict limitations.

The group speed  $U'$  is not constant even when  $u \ll U'$ , since a current causes a Doppler shift in the wave's frequency. However, if  $u/U'$  is very small, the changes in  $U'$  or  $G'$  along a ray will be quite small. Secondly,  $\theta$  and  $\gamma$  are not generally in the same direction due to refraction, but their difference would be small when  $u/U'$  is small.

A Snell's law type expression can be determined from equation (73), since Snell's law is the integrated form of the ray curvature equation. To integrate equation (73) it will be assumed that  $G'$  is constant along a ray, that the current has parallel speed contours, and that a Cartesian coordinate system with the y-axis parallel to the contours is used. Thus equation (73) can be expressed as

$$d\rho/ds_r = (1/G')(du/dx) \quad (75)$$

Separating variables and substituting  $\cos\rho$  for  $dx/ds_r$  equation (75) simplifies to

$$\cos\rho \, d\rho = du/G' \quad (76)$$

Integrating both sides of this equation yields

$$\sin\rho - u/G' = \text{constant} \quad (77)$$

This result is Snell's law for rays, and it can be expressed as

$$\sin\rho_i - u_i/G' = \sin\rho_t - u_t/G' \quad (78)$$

If  $u_i = 0$ , then

$$\sin\rho_t = \sin\rho_i + u_t/G' \quad (79)$$

When turning points and critical angles are considered, it is found that the critical angle equation for the rays has the form

$$\sin\rho_c = 1 - M \quad (80)$$

where  $\rho_c$  is the critical angle for the rays. This shows that the

critical angle for rays is a function of  $u_T/G_1$  just as was the critical angle for wavelets and packets.

Since critical angles for rays are the same as critical angles for packets, it should be possible to derive equation (80) from equation (53) when  $u \ll G'$  and when  $G'$  is constant. Thus, when  $\theta_c = 90$  degrees,  $G' = U' \sin \gamma_T$  and equation (53) can be rewritten as

$$\sin \theta_c = G' / (u_T + G') \quad (81)$$

and

$$\sin \theta_c = (1 + u_T/G')^{-1} \quad (82)$$

Equation (82) can be expanded to obtain

$$\sin \theta_c = 1 - u_T/G' + \dots \text{higher order terms} \quad (83)$$

Thus, neglecting the higher order terms, equation (53) reduces to equation (80).

Physical properties in addition to those discussed in Section III.D. become evident when equation (73) is viewed in the form

$$d\rho/ds_r = \zeta/G' \quad (84)$$

From this equation it can be seen that the curvature of a ray has the same sign as the vorticity of the current. Therefore, for a variable following (opposing) current, rays bend toward decreasing (increasing) current speed. Further, under the right conditions rays in a following (opposing) current may be trapped about a local minimum (maximum)

in current speed. It can also be seen that the curvature of a ray decreases with increasing geometric group speed (i.e., increasing period). So small period waves are affected to a greater extent by a current than are large period waves. These properties appear to occur (Section IV.C.) even when the assumptions made in obtaining equation (84) do not hold.

#### IV. CURRENT MODELS AND REFRACTION RESULTS

##### A. Description of current models

The refraction of wave packets by currents will be examined for four current models. Two of the current models will be patterned after the Gulf Stream. The other two models will be patterned after the Circumpolar Current. The Gulf Stream was chosen since it is the swiftest deep ocean current and since its effect on waves could greatly influence wave patterns off the east coast of the United States. The Circumpolar Current was chosen, since for the waves being considered its current speed to geometric group speed ratio is relatively small ( $< 0.1$ ), and since it affects a large portion of the Atlantic and Pacific Oceans.

Two parallel current models are considered. They are assumed to be unidirectional shear currents, uniform in the direction of flow, and independent of depth. One of the parallel current models has a maximum current speed of 50 cm/sec and a width of 1000 km. These values are representative of the Circumpolar Current. The current speed is assumed to have a parabolic profile such that its speed increases from zero at the edge of the current to its maximum value at the center of the current. The speed variation through the current is expressed by

$$u_{cp} = - 2 \times 10^{-4} (W^2 - 1000 W) \quad (85)$$

where  $u_{cp}$  is the speed of the current in cm/sec, and  $W$  is the distance from the edge of the current in km. The results obtained from this equation are plotted in Figure 4.

The parallel Gulf Stream model has a maximum current speed of 2 m/sec and a width of 100 km. This current model also has a parabolic profile such that the current speed increases from zero at the edge of the current to its maximum value at the center of the current. The speed across this current is expressed by

$$u_{gs} = - 8 \times 10^{-2}(W^2 - 100 W) \quad (86)$$

where  $u_{gs}$  is the speed of the current in cm/sec. The results obtained from this equation are shown in Figure 5.

The curved current models have the same current speed profiles and dimensions as the parallel currents, and are assumed to be independent of depth. However, their contours are assumed to be sections of horizontal, non-divergent circular rings. The Circumpolar Current is constructed so that its inner radius of curvature is 4000 km and its outer radius of curvature is 5000 km, similar to Kenyon's model. The curved Gulf Stream model has an inner radius of curvature of 500 km and an outer radius of curvature of 600 km, which roughly corresponds to the Gulf Stream off the coast of Georgia. To examine the refraction effect of non-parallel current contours the wave trajectories obtained for the curved current models can be compared with the rays determined for the corresponding parallel current models.

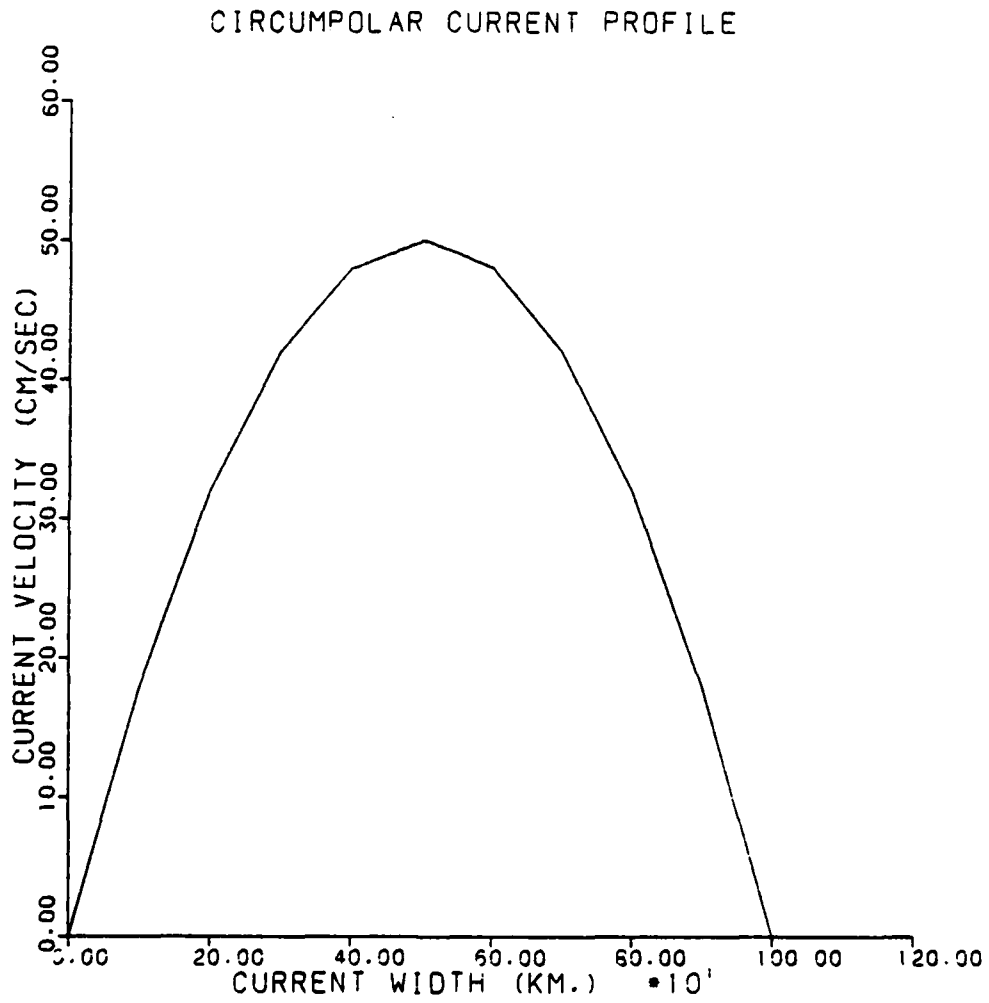


Figure 4. The current profile for the Circumpolar Current models.

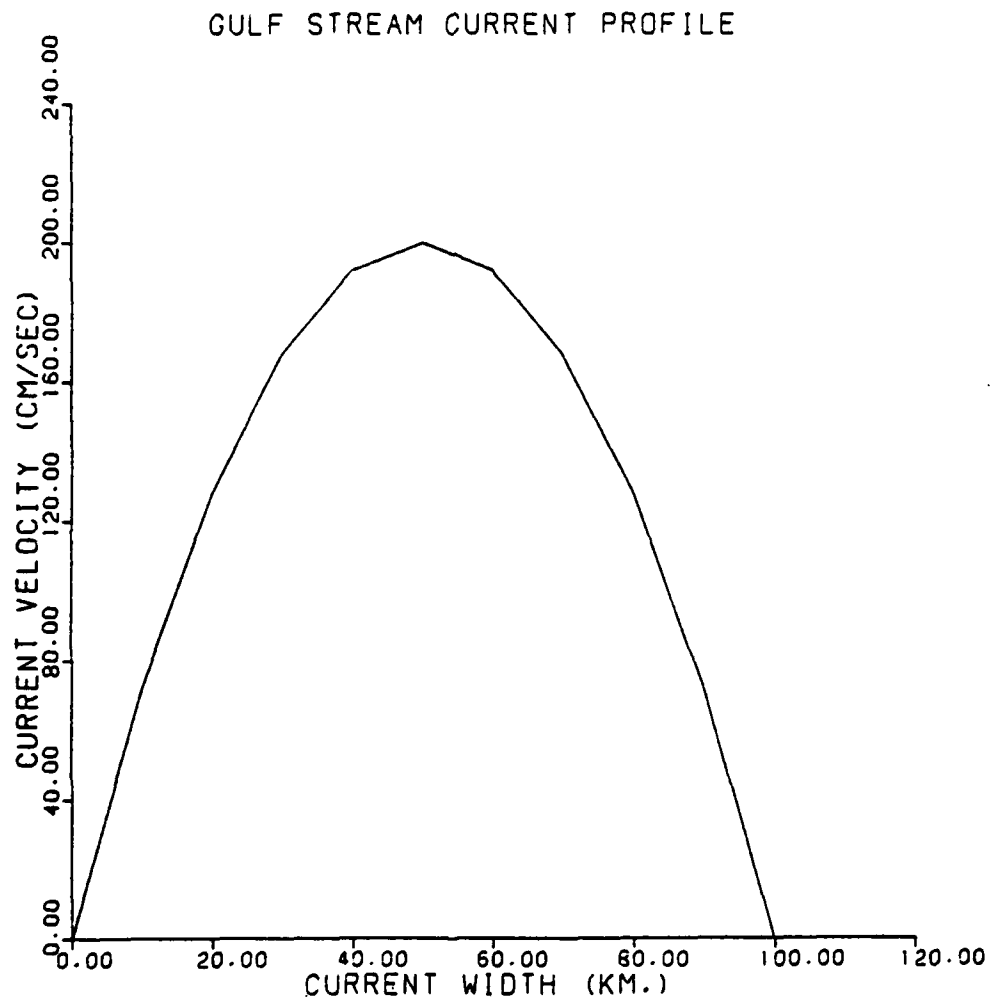


Figure 5. The current profile for the Gulf Stream current models.

### B. Wave period

In this study, waves of periods from seven to twenty seconds are considered. This is the significant range of periods found coastward of the Gulf Stream. Figures 6, 7, and 8 show the annual significant wave period distribution measured at sites off the east coast of the United States (Thompson, 1977). It is seen from these figures that swell wave periods peak near 10 seconds. In the Southern Ocean there are frequently large storms and a large fetch. As a result, longer period swell waves (15 to 20 seconds) are expected to be more prevalent in the Circumpolar Current than in the Gulf Stream.

### C. Properties of ray trajectories:

parallel and curved contours

In this section ray trajectories computed from equations (26), (28), and (30), are examined for waves in the current models previously described. For each model and wave period five initial angles are considered. The initial angles are 15, 30, 45, 60, and 75 degrees measured relative to the normal to the current contours.

The ray properties deduced from the theory in Section III.D. can be demonstrated through these trajectories. It was determined that  $\rho > \theta$  for a following current, that  $\rho < \theta$  for an opposing current, and that  $\rho = \theta = 90$  degrees at a turning point. These properties are presented graphically in Figures 9 thru 13 which show the variation in  $\rho$ ,  $\theta$ , and  $\gamma$  along some representative rays. Figure 9 depicts the values of the angles along a ray in a following current, and Figure 10 is for a ray in an opposing current. It is

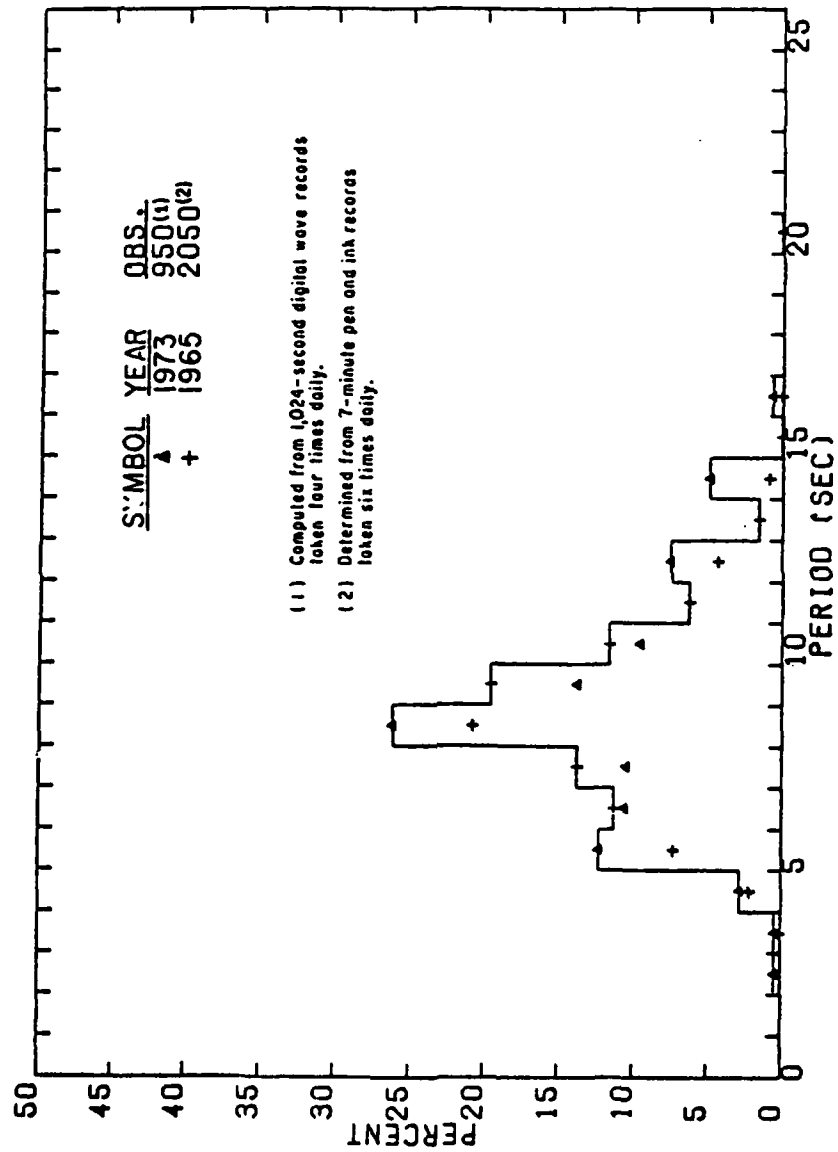
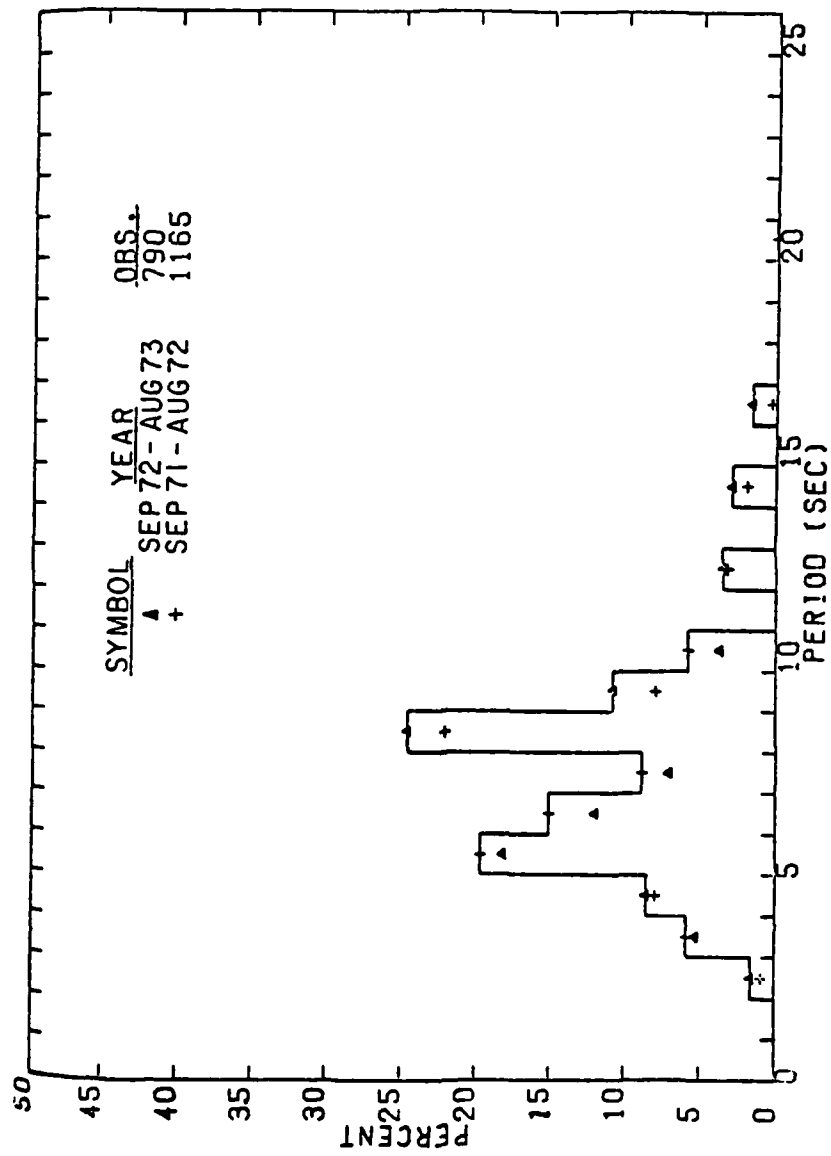


Figure 6. Annual significant period distribution from Daytona Beach, Florida. (Thompson, 1977)



| SYMBOL | YEAR            | OBS. |
|--------|-----------------|------|
| ▲      | SEP 72 - AUG 73 | 790  |
| +      | SEP 71 - AUG 72 | 1165 |

Figure 7. Annual significant period distribution from Holden Beach, North Carolina; computed from 1,024-second digital wave records taken four times daily. (Thompson, 1977)

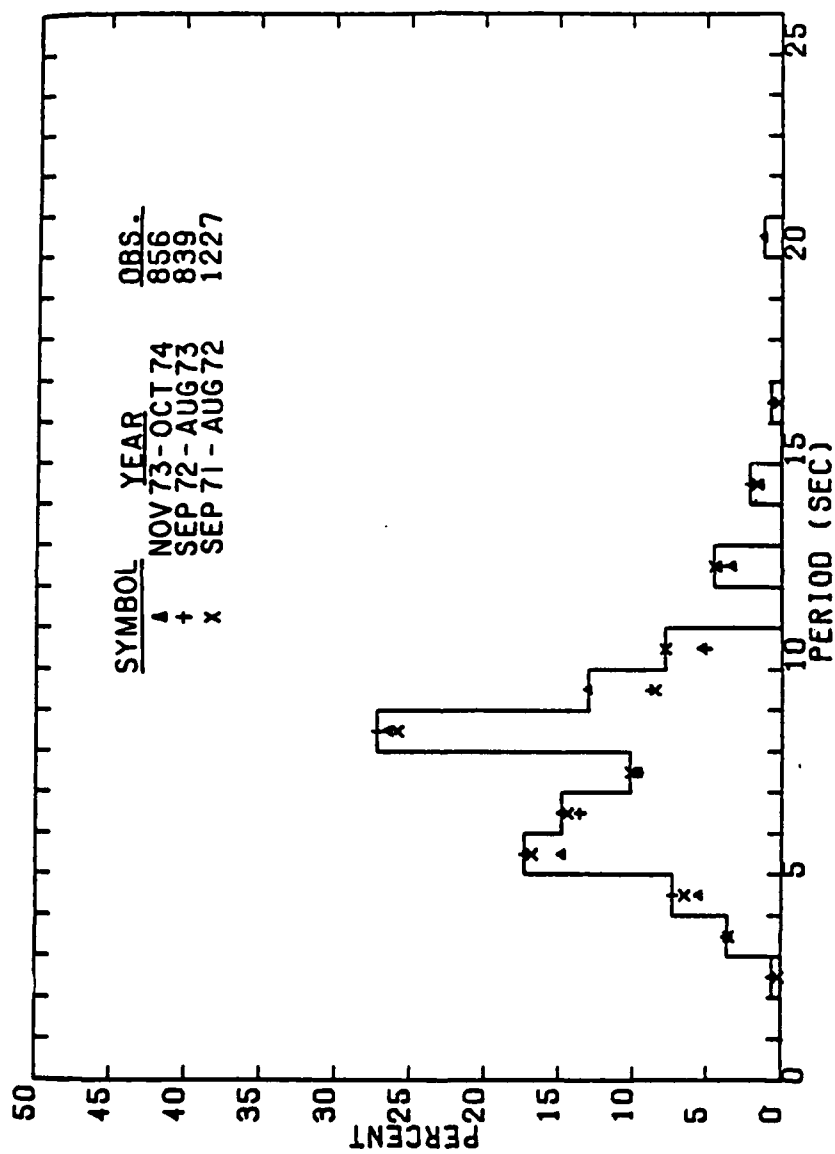


Figure 8. Annual significant period distributions from Wrightsville Beach, North Carolina; computed from 1,024-second digital wave records taken four times daily. (Thompson, 1977)

clearly seen that for the following current  $\rho > \theta$ , and that  $\rho < \theta$  for the opposing current. It is also seen that the angle  $\gamma$  changes the least of the three angles. This is because the speed of the wavelets is greater than that of the packets and rays. Thus, the wavelets are affected the least by the current. Figure 11 is an example of the variation in the angles along a ray which goes through a turning point. It is seen that when a ray totally reflects the values of  $\rho$  and  $\theta$  steadily increase, and reach 90 degrees at the turning point. The angle  $\gamma$ , however, is seen to increase to its maximum value at the turning point and then to decrease to its initial value. Due to the symmetry of the current models used  $\rho$ ,  $\theta$ , and  $\gamma$  have the same value when the ray exits the current as when it entered the current, except for  $\rho$  and  $\theta$  when the ray totally reflects.

It was also determined that when  $u \ll G'$  the values of  $\rho$  and  $\theta$  are nearly equal. In fact, it was found that in such cases  $\gamma$  is also nearly equal to  $\rho$  and  $\theta$ . An example of this is seen in Figure 12 where  $N = u_{\max}/G_1 = 0.046$ . For this ray  $\rho$  and  $\theta$  differ by no more than 1.5 degrees and  $\theta$  and  $\gamma$  differ by no more than 1 degree. However, in Figure 9, where  $N = 0.366$ ,  $\rho$  and  $\theta$  differ by about 12 degrees, and  $\theta$  and  $\gamma$  differ by about 4 degrees. This changes somewhat if the ray totally reflects (Figure 13). When there is a reflection  $\rho$  and  $\theta$  remain nearly equal, but  $\gamma$  deviates considerably from the other angles.

Further, at a turning point, it was determined that either  $u_x = G'_x = 0$  or  $u_x = -G'_x$ . The first case is seen to occur for rays which totally reflect in a following, parallel current. A good

example of this is presented in ray 5, Figure 14. At the turning point the ray, packet, and current directions become parallel. The second case occurs for curved currents. It was found that the x-component of current and wave packet velocities balanced each other in rays 4 and 5, Figures 26 and 30. Also, the current and ray directions were found to directly oppose each other. An interesting observation is that these rays reflect in an opposing current rather than in a following current.

Lastly, it was deduced in Section III.D. that in an opposing current rays can be turned so they would eventually become perpendicular to the current contours. This is seen in Figures 19 and 21, which show rays in the Gulf Stream. However, for the current model with the slower current speeds (50 cm/sec maximum) there is not sufficient refraction to cause the rays to become perpendicular to the contours (Figures 15 and 17).

Some ray properties were deduced in Section III.G. from the vorticity equation which is an approximate equation useful only when  $u \ll G'$ . Even so, it is apparent from the trajectories that these properties are general and occur even when  $u/G'$  is as large as 0.366. In accordance with equation (84) rays are bent away from the current normal in a following current, and toward the current normal in an opposing current. The rays in Figures 18 and 19 clearly demonstrate these results. Also, it was determined that the curvature of a ray increases as the vorticity increases and as the wave period decreases. The average vorticity of the current shown in Figure 22 is  $1 \times 10^{-6} \text{ sec}^{-1}$ . The average vorticity of the current shown in Figure 18 is  $4 \times 10^{-5} \text{ sec}^{-1}$ . The wave period is seven

seconds for the rays in both figures. It is clear that the curvature of the rays shown in Figure 18 is greater than the curvature of the rays shown in Figure 22. In Figures 18 and 20 the average vorticity of the current is  $4 \times 10^{-5} \text{ sec}^{-1}$ . The wave periods, however, differ in these figures. Seven second period wave rays are depicted in Figure 18 and 10 second period wave rays are shown in Figure 20. The rays with the smaller period are seen to have the greater curvature.

Ray trajectories computed for the parallel current models are shown in Figures 14 thru 21. For the parallel current patterned after the Circumpolar Current, wave periods of 14 and 17 seconds were considered. These periods correspond to  $N$  values of 0.046 and 0.038, respectively. In Figures 14 thru 17 it is seen that little refraction occurs for these values of  $N$ . It is also seen that only rays with large initial angles are totally reflected, as was indicated in Figure 2. The critical angle computed when  $N$  is 0.046 is 71 degrees. When  $N$  is 0.038 the critical angle is 74 degrees. The rays shown in Figures 14 and 16 are consistent with these results.

Ray trajectories for the current model patterned after the Gulf Stream are shown in Figures 18 thru 21. Wave periods of 7 and 10 seconds are considered. These periods correspond to  $N$  values of 0.366 and 0.256, respectively. The rays in this current are seen to undergo considerable refraction. The critical angles computed for these rays are 44 degrees when  $N$  is 0.366 and 50 degrees when  $N$  is 0.256.

Ray trajectories computed using the curved current models are shown in Figures 23 thru 38. It is evident from these figures that

the trajectories for waves in curved currents can be considerably different from the trajectories for waves in parallel currents even though the current speed profile and current dimensions are the same. This can be explained by the greater variation in current vorticity which occurs for curved currents compared to parallel currents.

With curved currents the side from which the ray enters the current becomes important. With parallel currents it is only necessary to distinguish between following and opposing currents, since the symmetry of the currents results in the same trajectories no matter from which side of the current the waves enter. With the curved currents this is not so. The trajectories of waves which enter from the inner radius side of the current are different from the trajectories which enter from the outer radius side. This can be seen in Figures 23 and 24 and in Figures 31 and 32. It is also seen that the critical angles are different for the inner radius side than for the outer radius side. For example, in Figure 23 the critical angles for these rays must be greater than 75 degrees. In Figure 24, the critical angle is found to be less than 60 degrees. A similar result is seen in the other figures. Thus, the critical angle for waves which enter a curved current from the inner radius side is larger than the critical angle for waves which enter from the outer radius side given the same wave period and current speed profile. These critical angles differ from those computed for parallel currents (Figure 2). The critical angles for rays which enter from the inner radius side are greater than the critical angles determined for the same waves in a parallel

current. The critical angles for rays which enter from the outer radius side are less than those determined for parallel currents.

The refraction of wave packets by curved currents can result in some very interesting rays. For example, rays may, due to the configuration of the current, pass through the current and then re-enter the current further downstream or upstream. This is seen to occur for ray 3 in Figures 26 and 30. This can occur for either a following or an opposing current, but only if the ray exits the current on the inner radius side. It can also be observed from these figures that rays may go through several inflection points (ray 4), and that rays may be focused into a particular area (rays 4 and 5). Comparison of Figures 26 and 30 indicates that the area into which the rays are focused moves further away from the entry point of the waves into the current as the wave period of the rays increases. One might say that the focal length increases as the wave period increases. Very large period waves ( $\approx 20$  seconds) would be focused outside of the current.

Ray 3, Figure 32; rays 4 and 5, Figures 34 and 38; and ray 4, Figure 25 are seen to abruptly stop within the current. This occurs due to numerical problems which come about when  $G'$  goes to zero. After a total reflection, it has been shown that  $\theta$  and  $\gamma$  differ considerably. In these rays, this difference results in  $G'$  becoming zero. Further study will be needed to determine what happens to the ray when this occurs.

VARIATION IN RHO, THETA & GAMMA  
ALONG A RAY

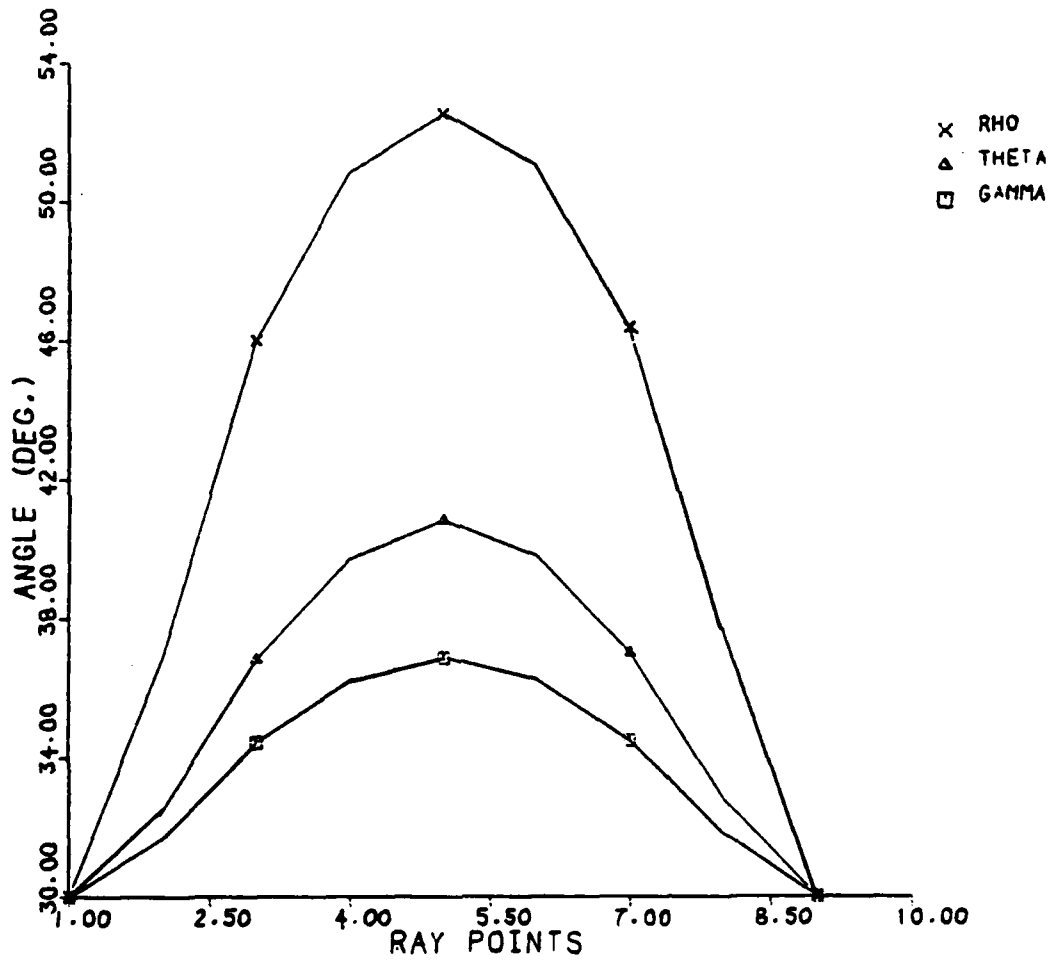


Figure 9. The variation in the values of the angles  $\rho$ ,  $\theta$ , and  $\gamma$  along ray 2 in Figure 18. This ray has an initial angle of 30 degrees, and passes through a following current without reflection. ( $N = 0.366$ )

VARIATION IN RHO, THETA & GAMMA  
ALONG A RAY

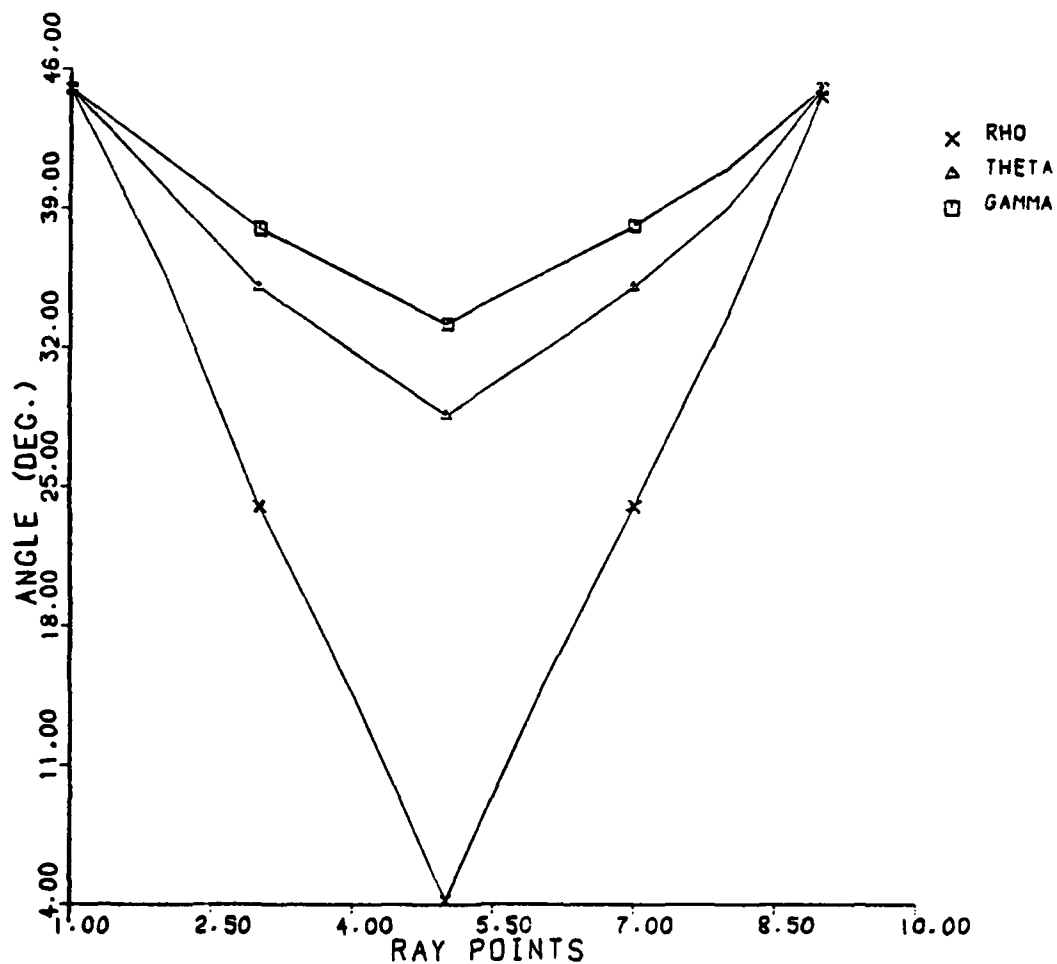


Figure 10. The variation in the values of the angles  $\rho$ ,  $\theta$ , and  $\gamma$  along ray 3 in Figure 19. This ray has an initial angle of 45 degrees, and passes through an opposing current. ( $N = 0.366$ )

VARIATION IN RHO, THETA & GAMMA  
ALONG A RAY

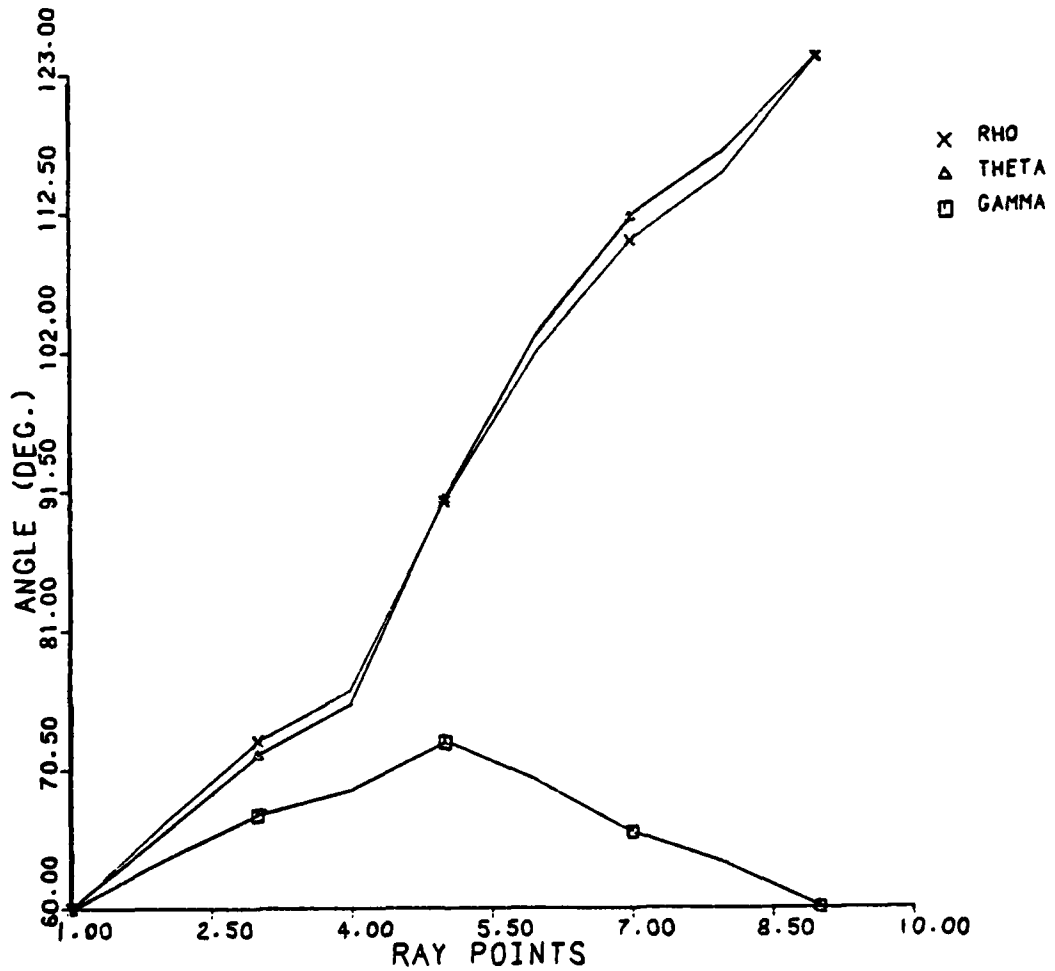


Figure 11. The variation in the values of the angles  $\rho$ ,  $\theta$ , and  $\gamma$  along ray 4 in Figure 18. This ray has an initial angle of 60 degrees. This ray is reflected. ( $N = 0.366$ )

VARIATION IN RHO, THETA & GAMMA  
ALONG A RAY

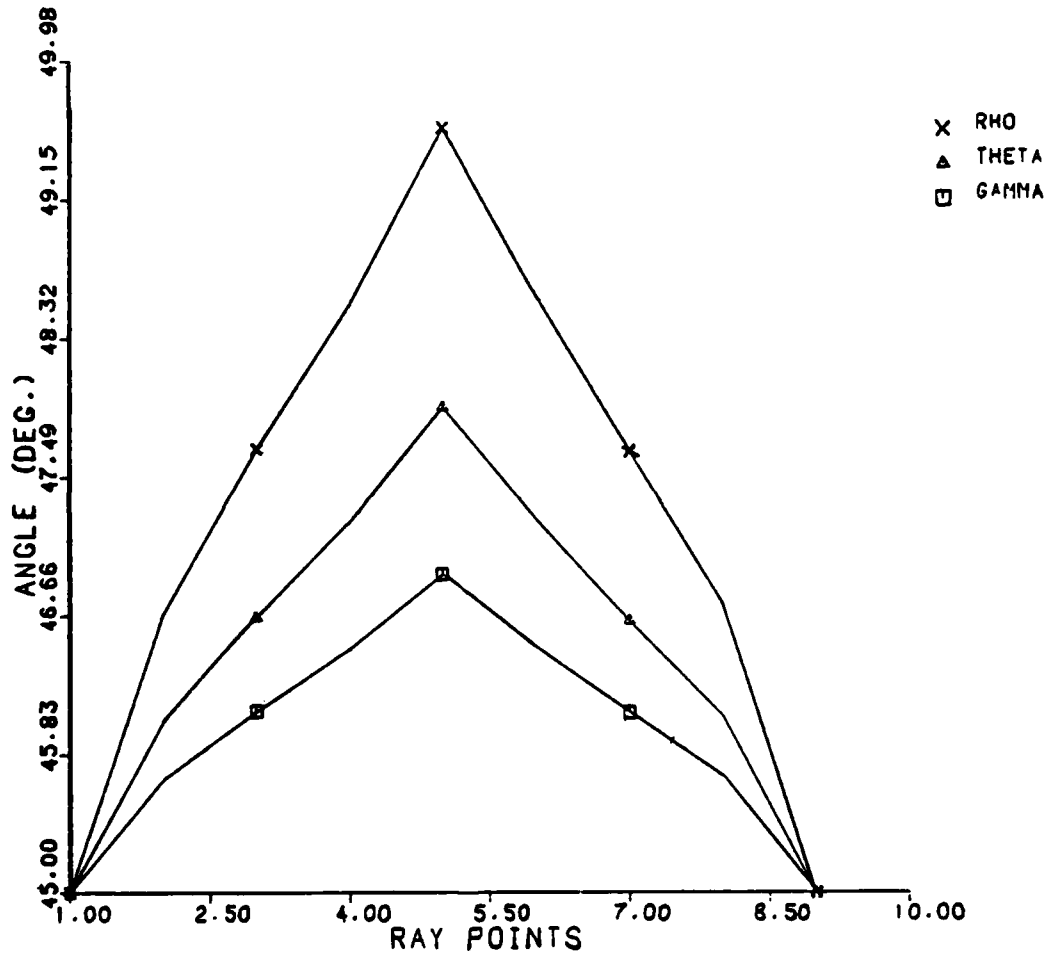


Figure 12. The variation in the values of the angles  $\rho$ ,  $\theta$ , and  $\gamma$  along ray 4 in Figure 14. This ray has an initial angle of 45 degrees and passes through a following current without reflection. ( $N = 0.046$ )

VARIATION IN RHO, THETA & GAMMA  
ALONG A RAY

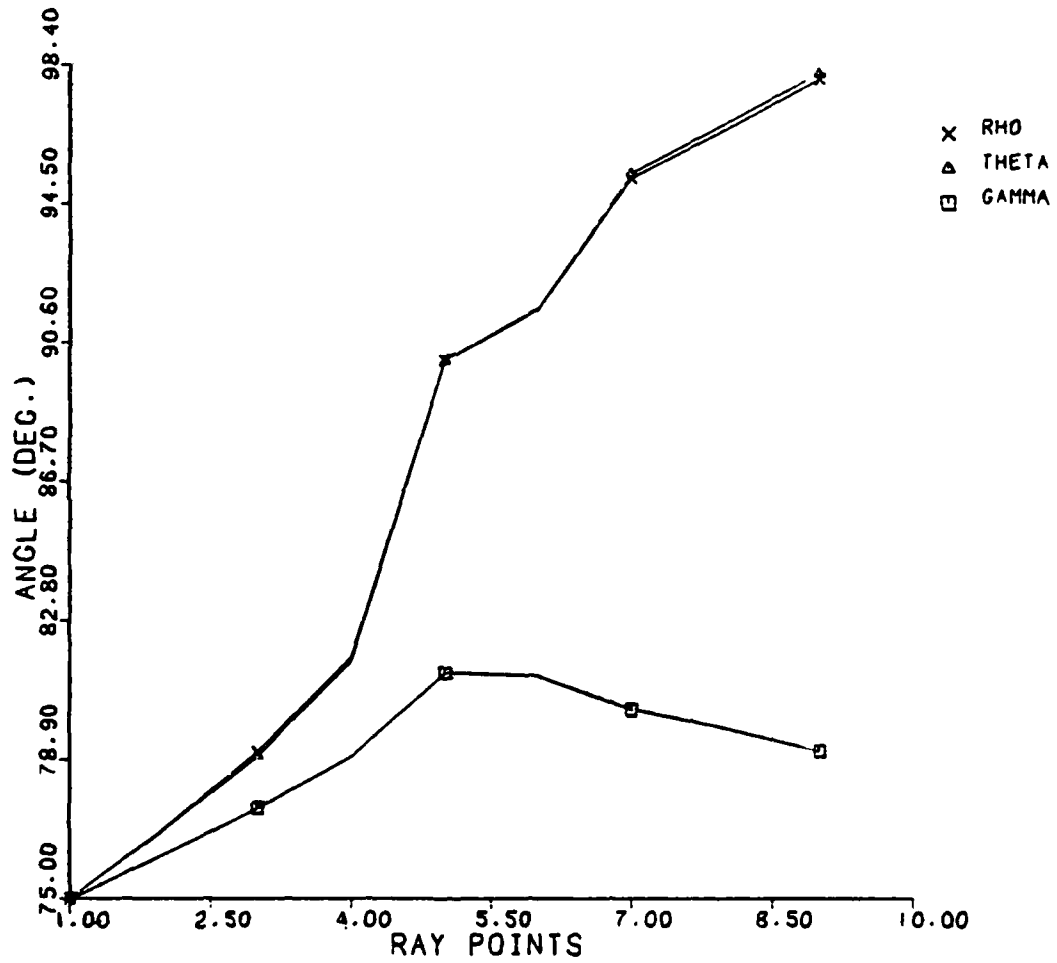


Figure 13. The variation in the values of the angles  $\rho$ ,  $\theta$ , and  $\gamma$  along ray 5 in Figure 14. This ray has an initial angle of 75 degrees and is totally reflected. ( $N = 0.046$ )

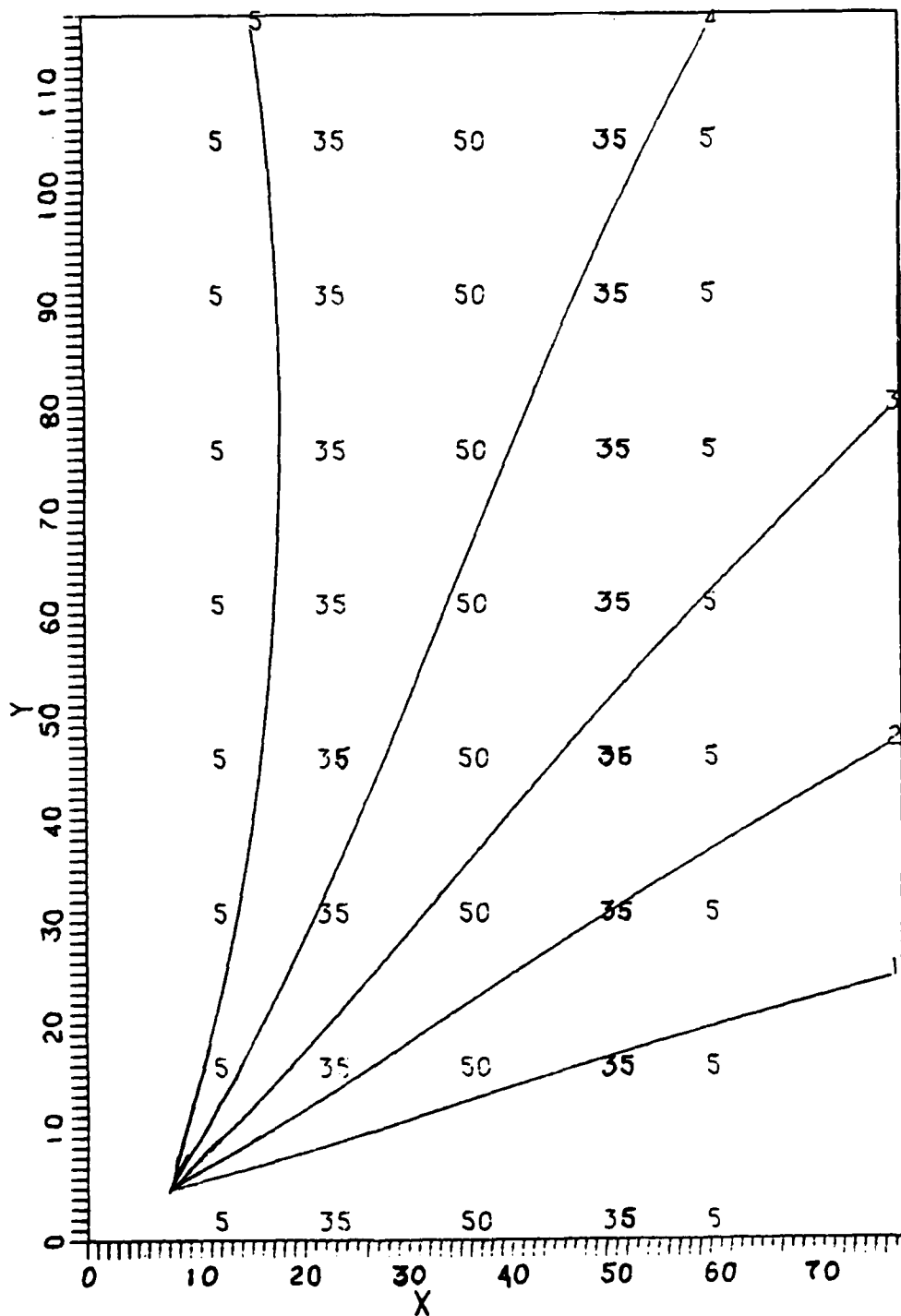


Figure 14. Ray trajectories for 14 second period waves in a following current. The current model used was the parallel model patterned after the Circumpolar Current. Current speeds are shown in cm/sec,  $N = 0.046$ , and the positive y-axis is in the direction of the current. Grid spacing is 20 km.

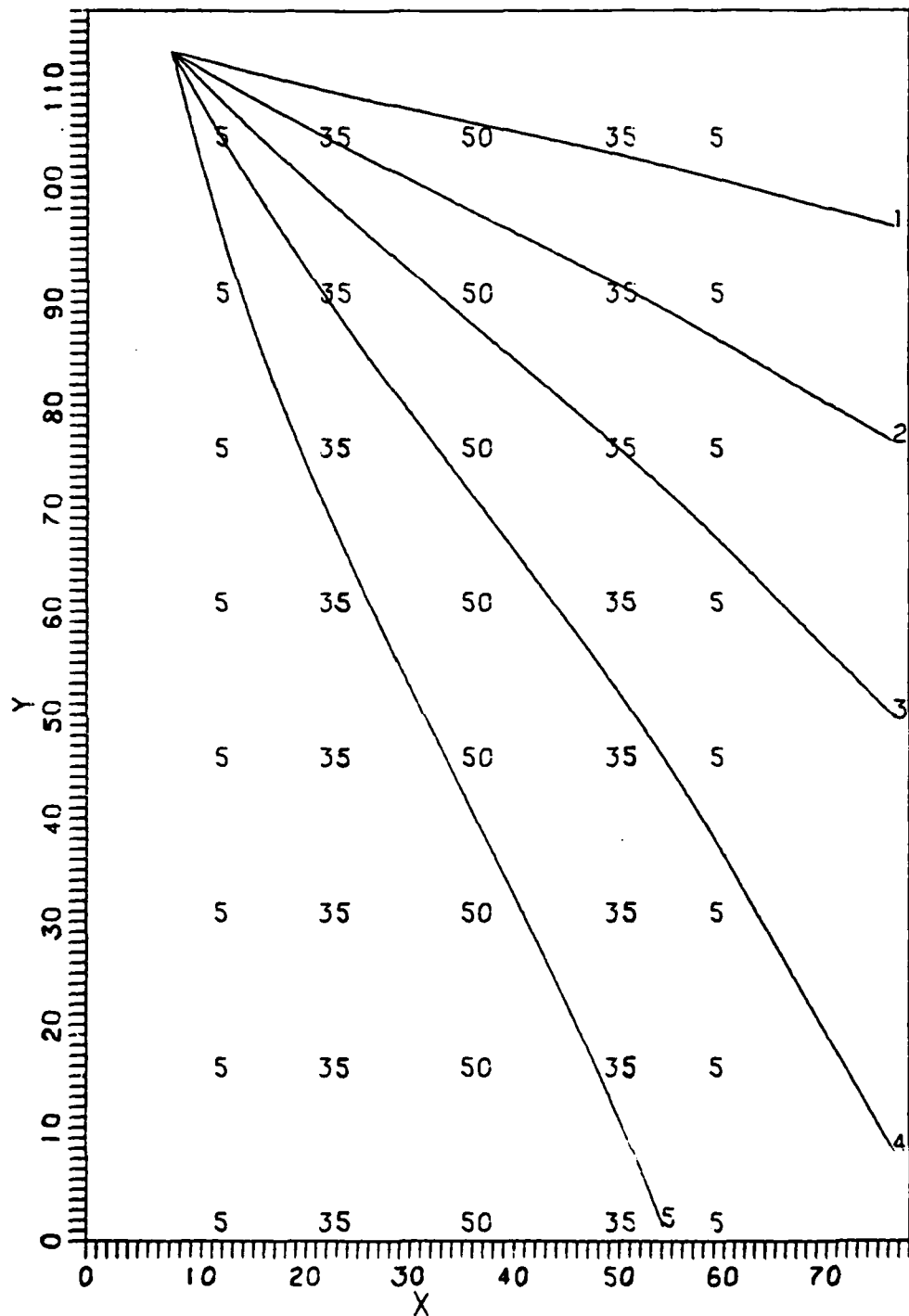


Figure 15. Ray trajectories for 14 second period waves in an opposing current. The current model used was the parallel model patterned after the Circumpolar Current. Current speeds are shown in cm/sec,  $N = 0.046$ , and the positive y-axis is in the direction of the current. Grid spacing is 20 km.

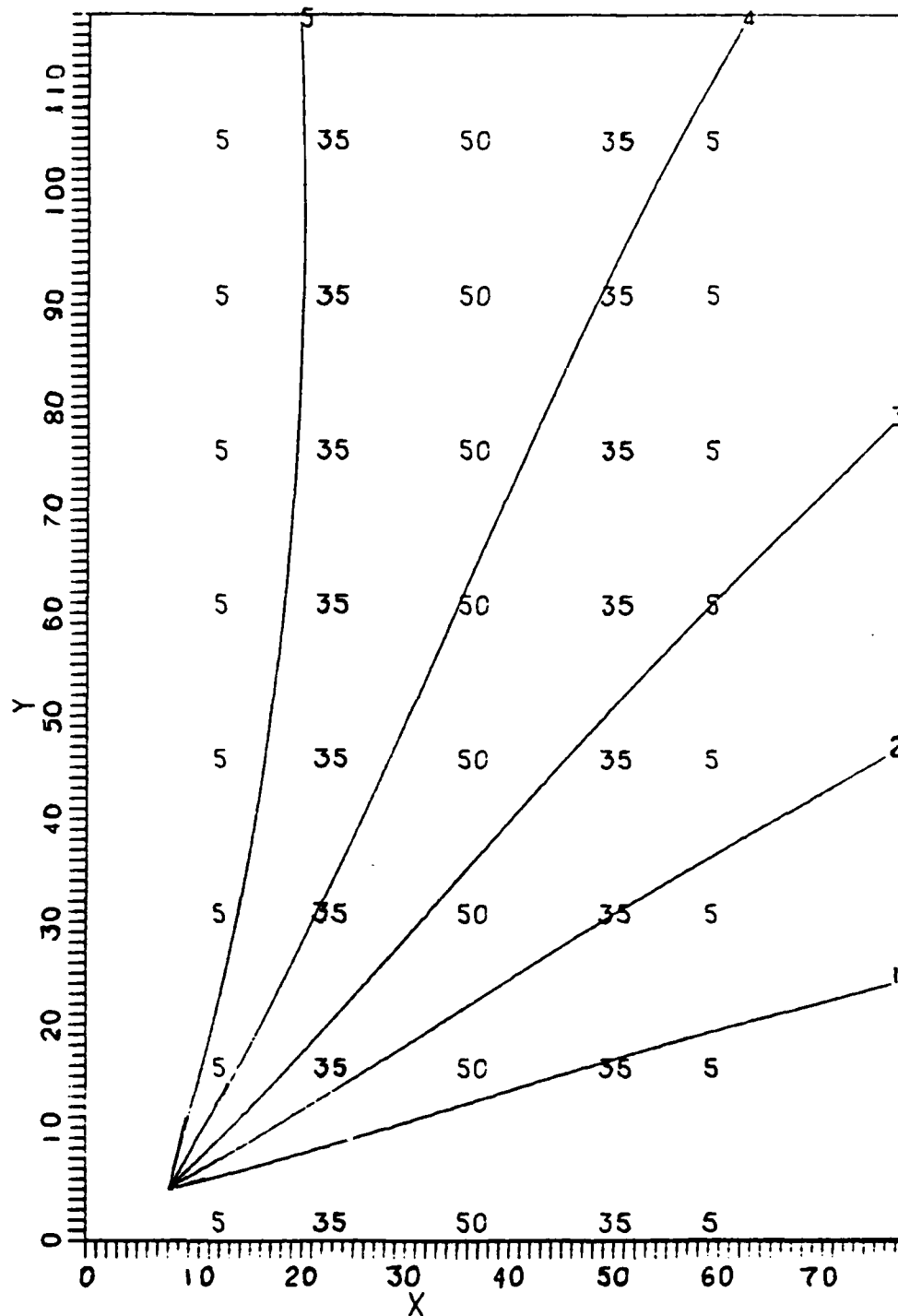


Figure 16. Ray trajectories for 17 second period waves in a following current. The current model used was the parallel model patterned after the Circumpolar Current. Current speeds are shown in cm/sec,  $N = 0.038$ , and the positive y-axis is in the direction of the current. Grid spacing is 20 km.

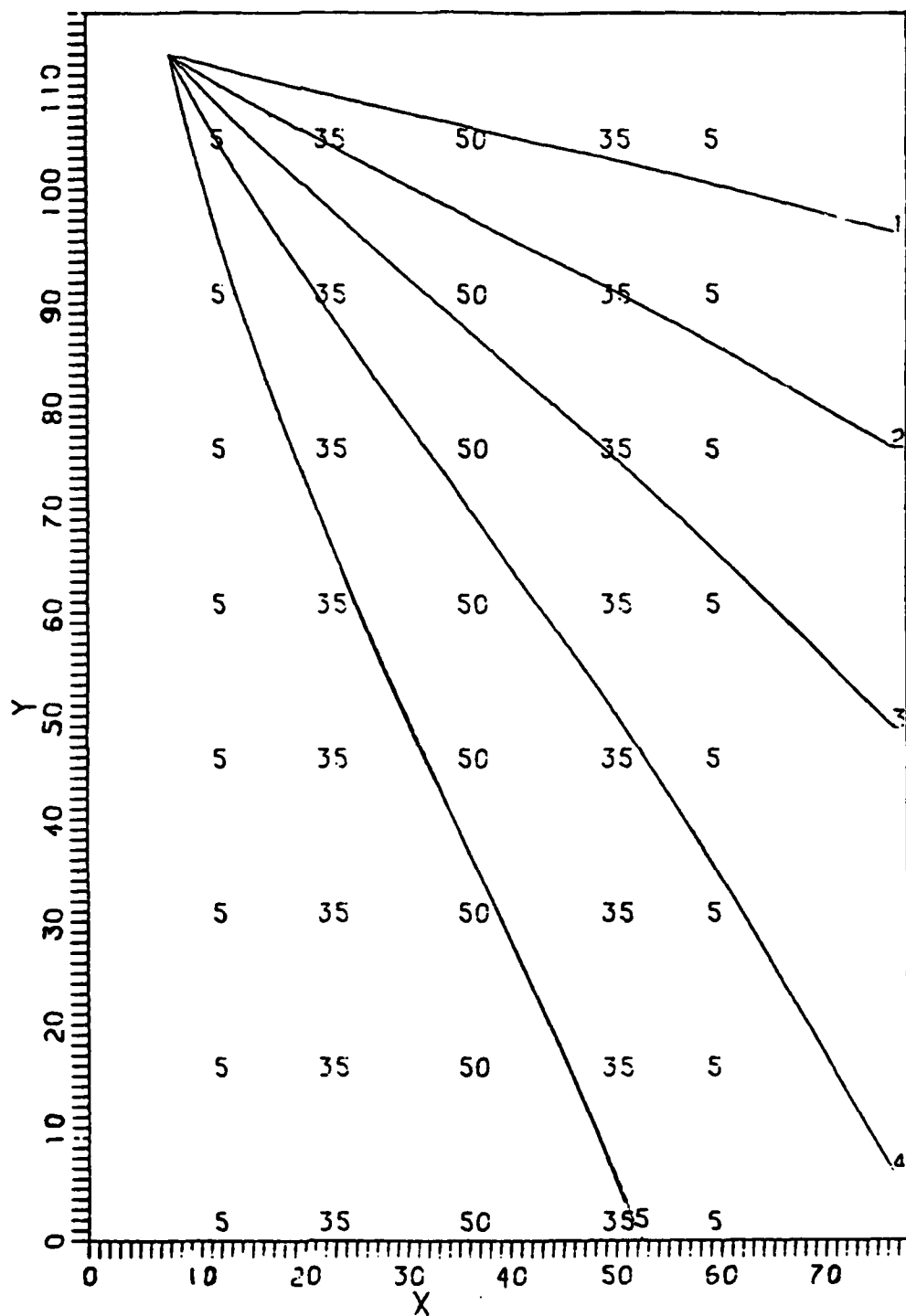


Figure 17. Ray trajectories for 17 second period waves in an opposing current. The current model used was the parallel model patterned after the Circumpolar Current. Current speeds are shown in cm/sec,  $N = 0.038$ , and the positive y-axis is in the direction of the current. Grid spacing is 20 km.

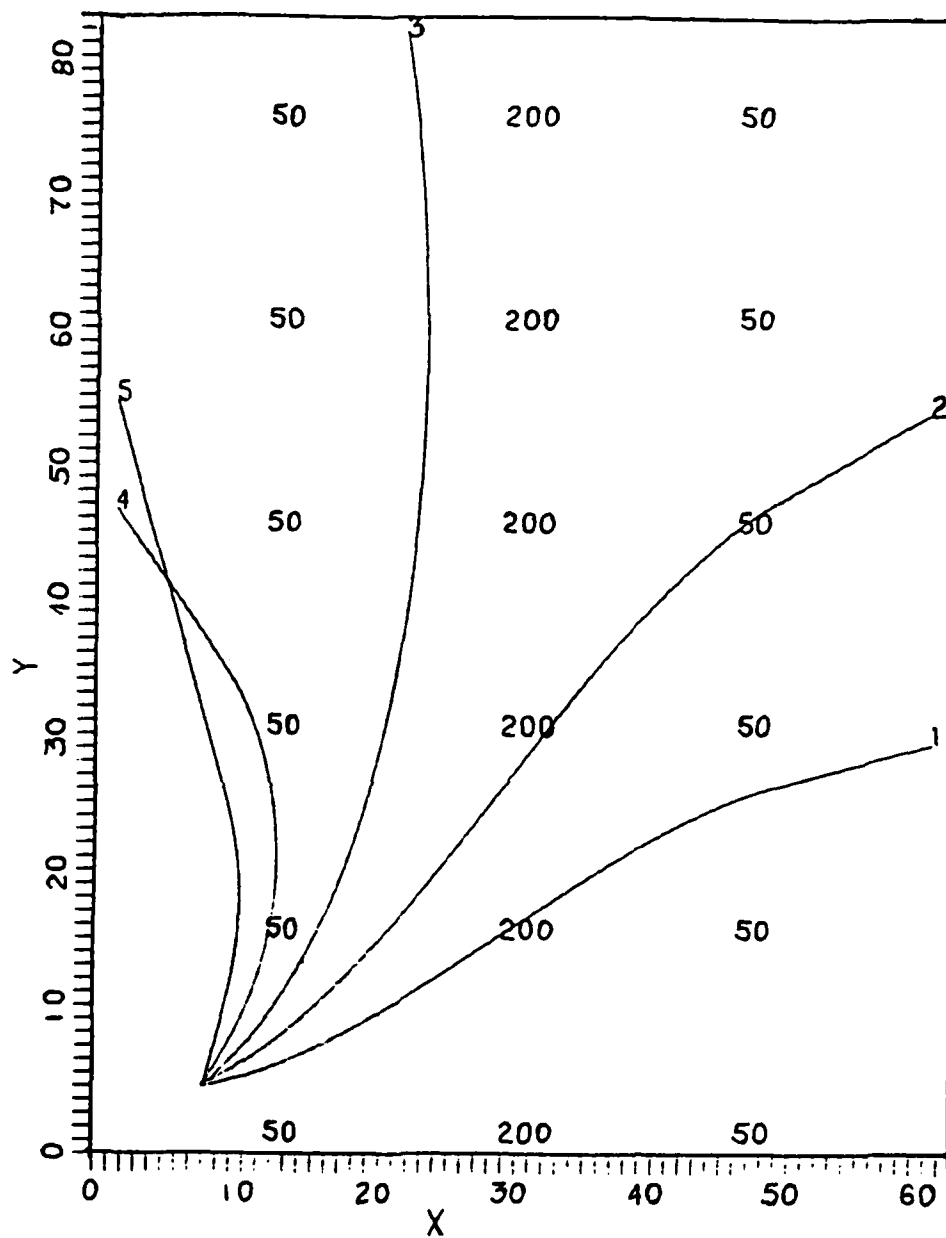


Figure 18. Ray trajectories for 7 second period waves in a following current. The current model used was the parallel model patterned after the Gulf Stream. Current speeds are shown in cm/sec,  $N = 0.366$ , and the positive y-axis is in the direction of the current. Grid spacing is 2.5 km.

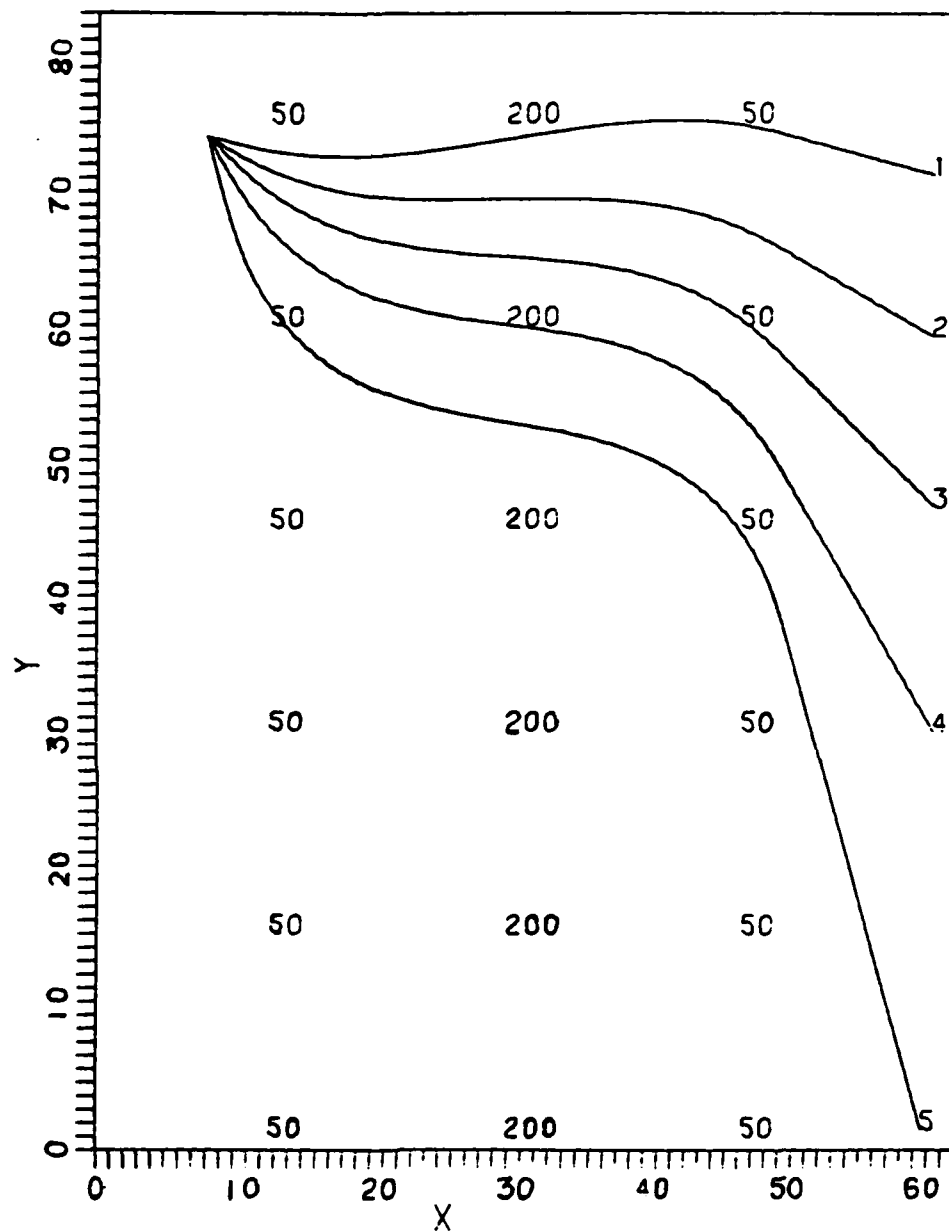


Figure 19. Ray trajectories for 7 second period waves in an opposing current. The current model used was the parallel model patterned after the Gulf Stream. Current speeds are shown in cm/sec,  $N = 0.366$ , and the positive y-axis is in the direction of the current. Grid spacing is 2.5 km.

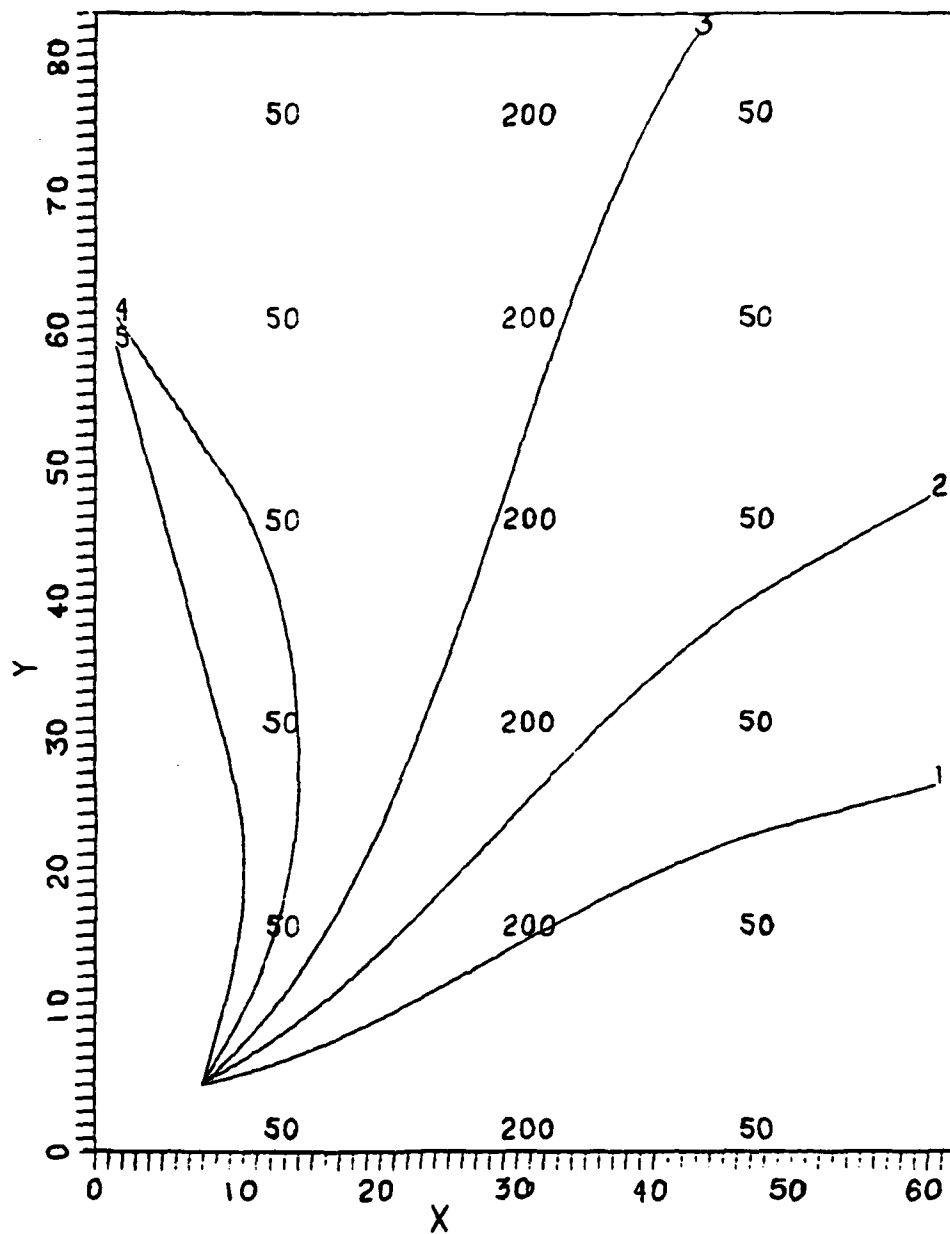


Figure 20. Ray trajectories for 10 second period waves in a following current. The current model used was the parallel model patterned after the Gulf Stream. Current speeds are shown in cm/sec,  $N = 0.256$ , and the positive  $y$ -axis is in the direction of the current. Grid spacing is 2.5 km.

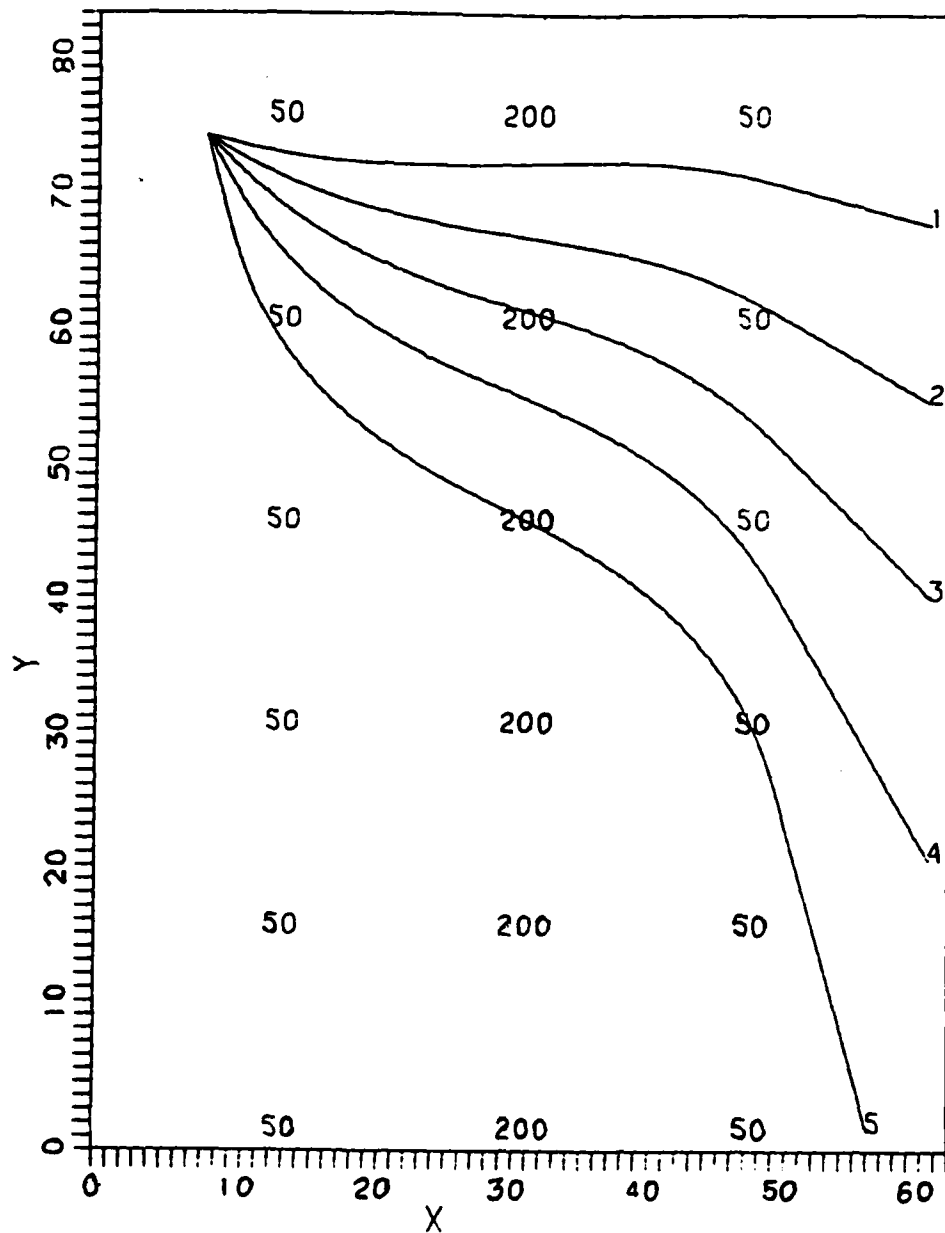


Figure 21. Ray trajectories for 10 second period waves in an opposing current. The current model used was the parallel model patterned after the Gulf Stream. Current speeds are shown in cm/sec,  $N = 0.256$ , and the positive y-axis is in the direction of the current. Grid spacing is 2.5 km.

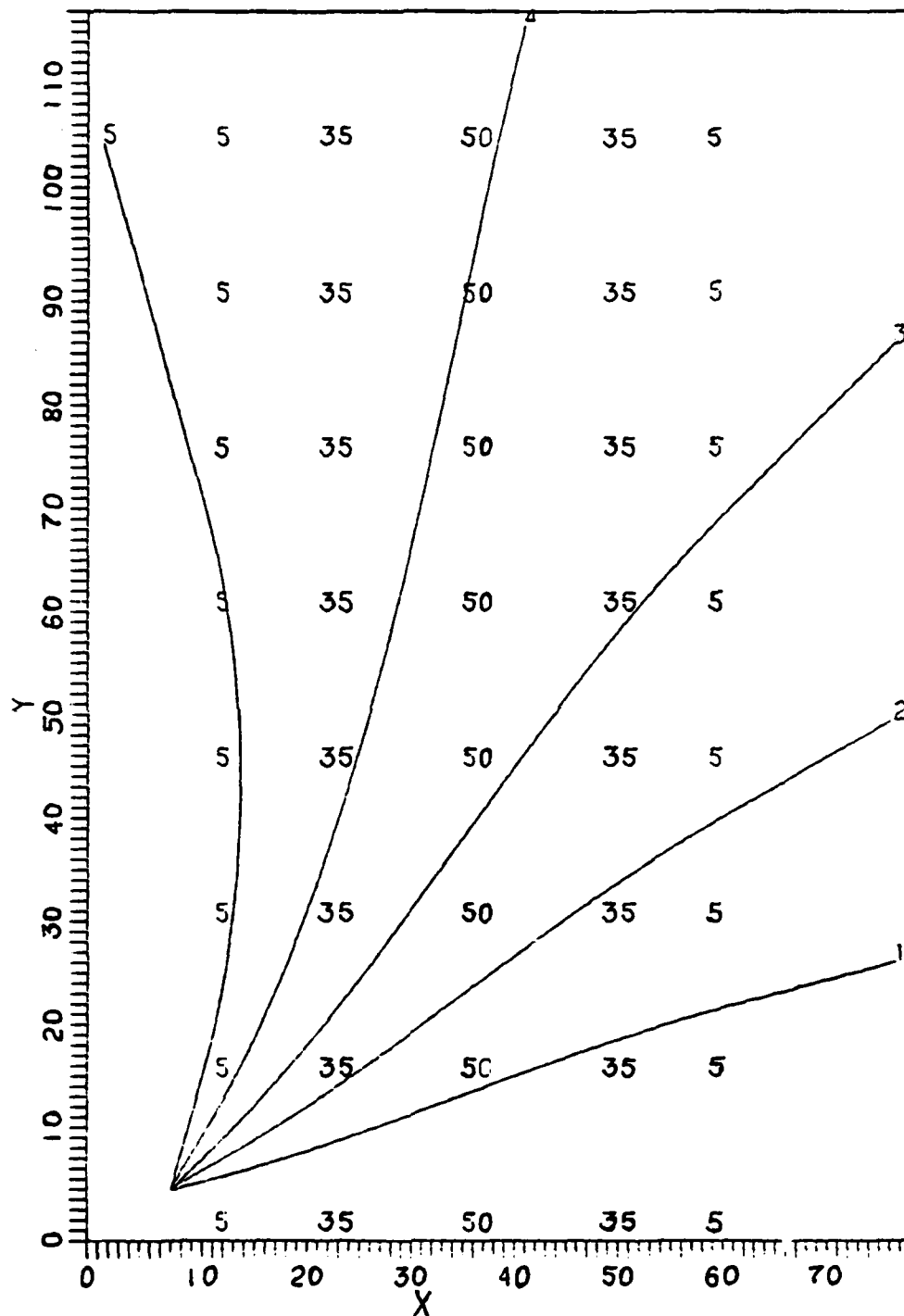


Figure 22. Ray trajectories for 7 second period waves in a following current. The current model used was the parallel model patterned after the Circumpolar Current. Current speeds are shown in cm/sec,  $N = 0.091$ , and the positive y-axis is in the direction of the current. Grid spacing is 20 km.

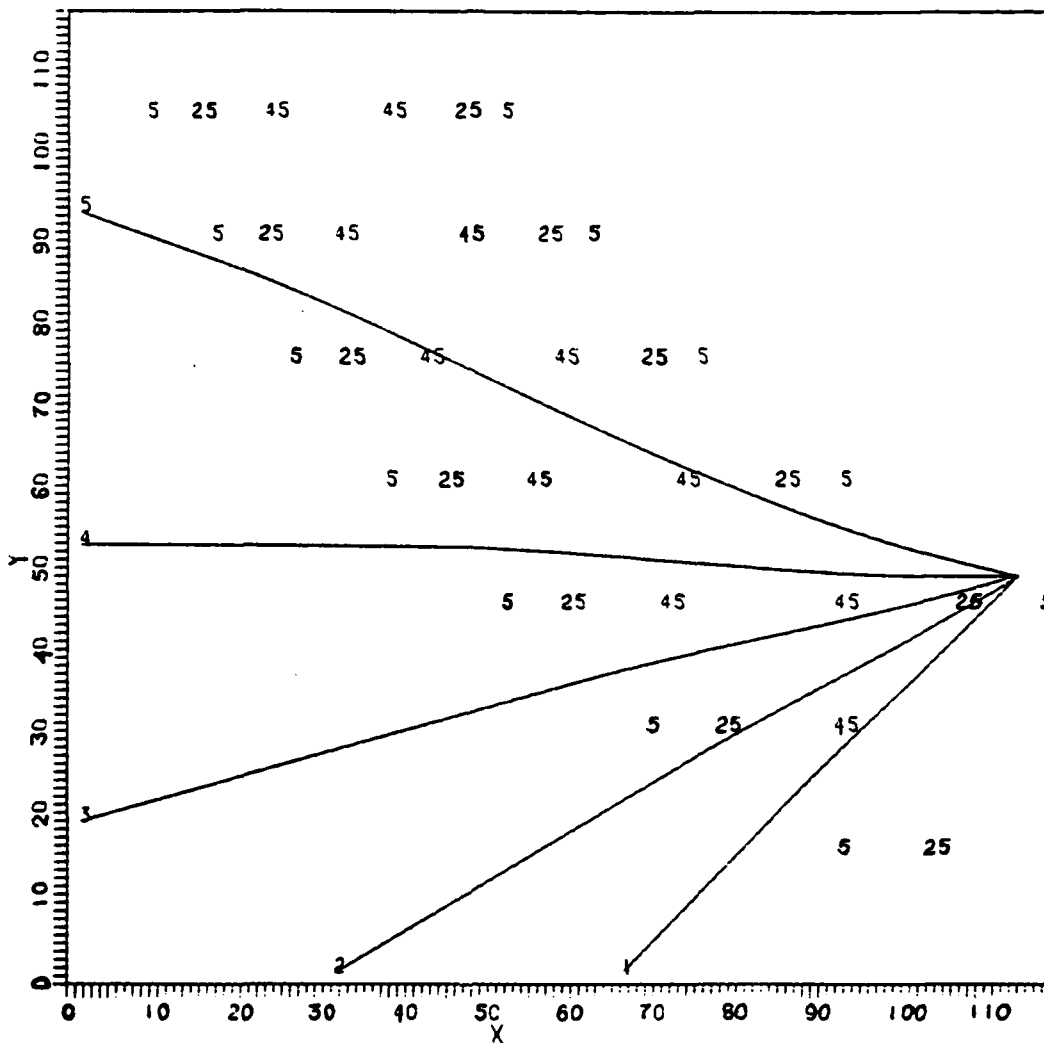


Figure 23. Ray trajectories for 14 second period waves in the Circumpolar Current model. The waves enter a following current from the inner radius side. Current speeds are given in cm/sec and  $N = 0.046$ . Grid spacing is 20 km.

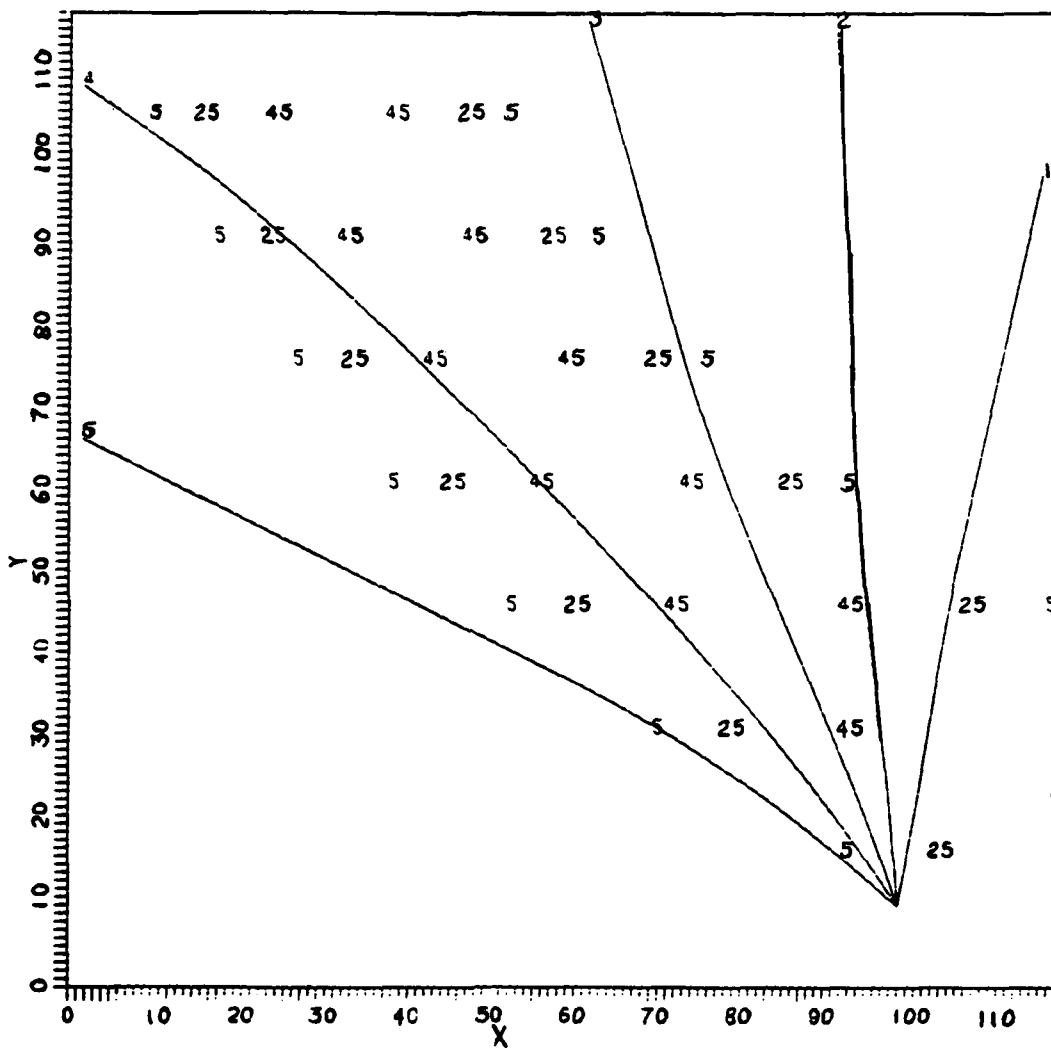


Figure 24. Ray trajectories for 14 second period waves in the Circumpolar Current model. The waves enter a following current from the outer radius side. Current speeds are given in cm/sec and  $N = 0.046$ . Grid spacing is 20 km.

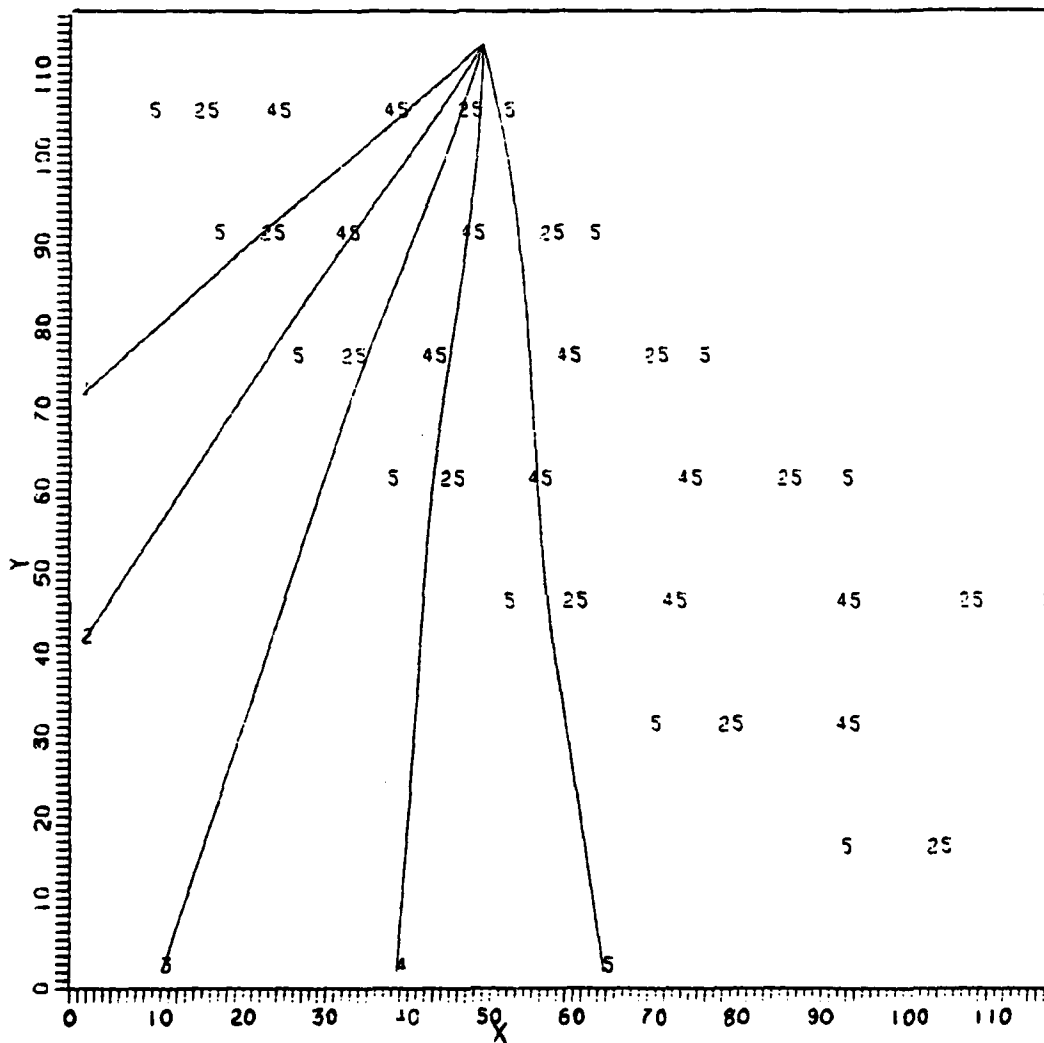


Figure 25. Ray trajectories for 14 second period waves in the Circumpolar Current model. The waves enter an opposing current from the inner radius side. Current speeds are given in cm/sec and  $N = 0.046$ . Grid spacing is 20 km.

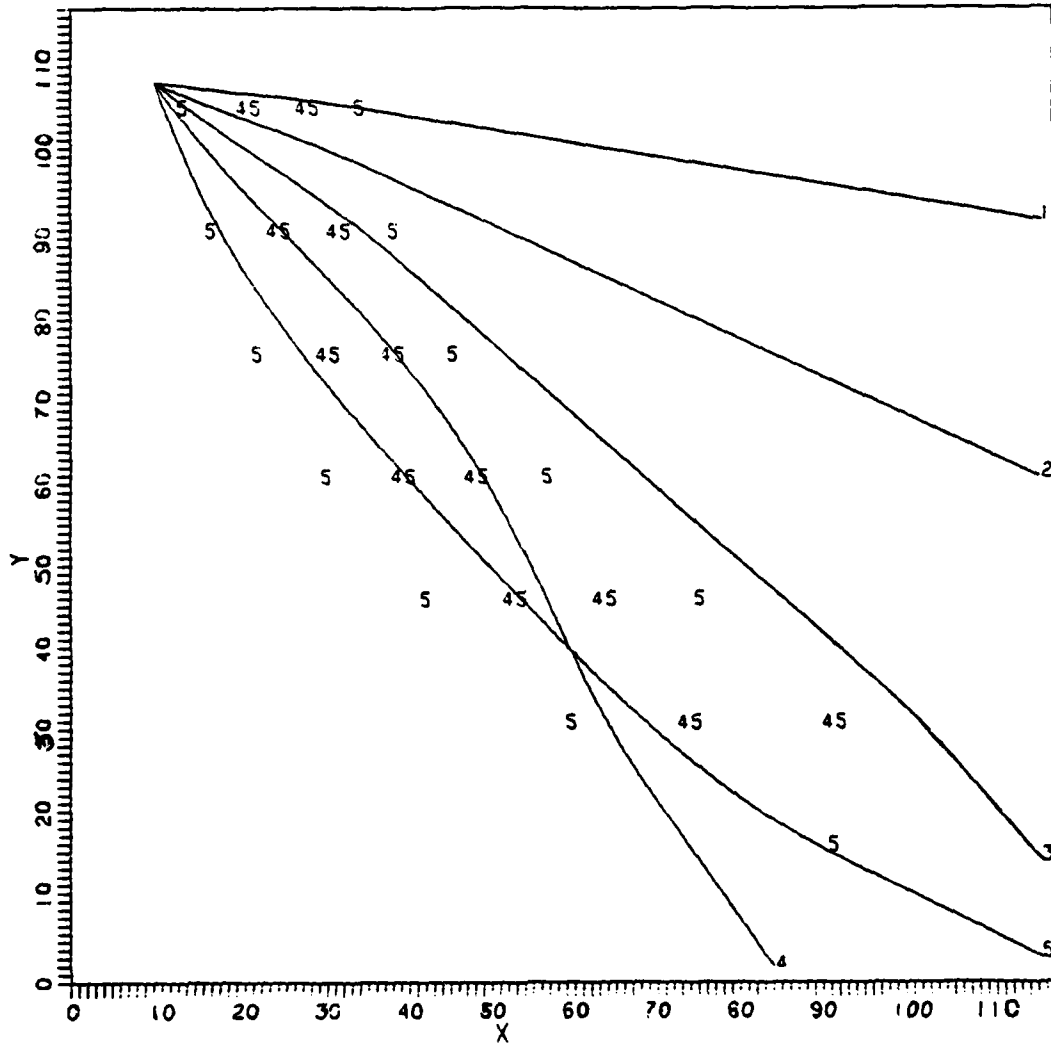


Figure 26. Ray trajectories for 14 second period waves in the Circumpolar Current model. The waves enter an opposing current from the outer radius side. Current speeds are given in cm/sec and  $N = 0.046$ . Grid spacing is 45 km.

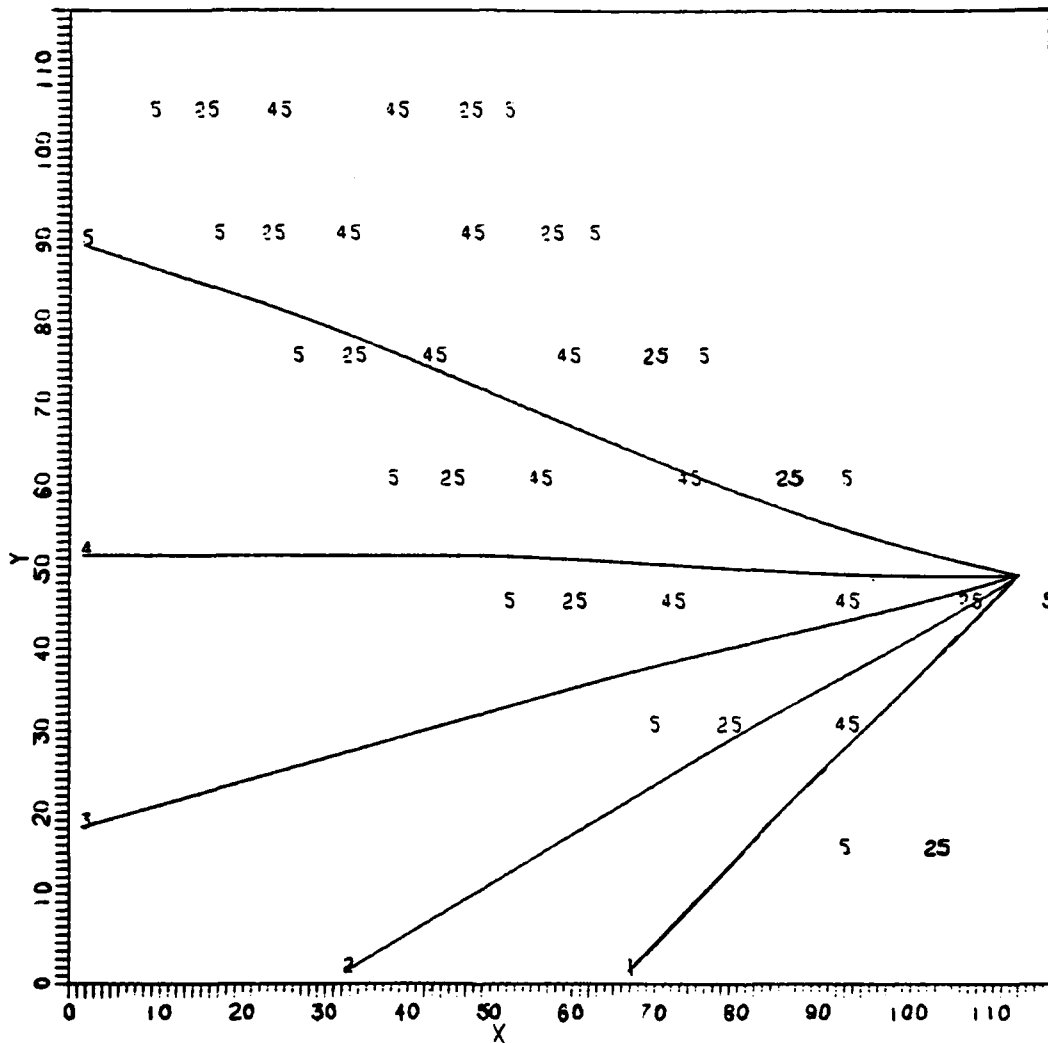


Figure 27. Ray trajectories for 17 second period waves in the Circumpolar Current model. The waves enter a following current from the inner radius side. Current speeds are given in cm/sec and  $N = 0.038$ . Grid spacing is 20 km.

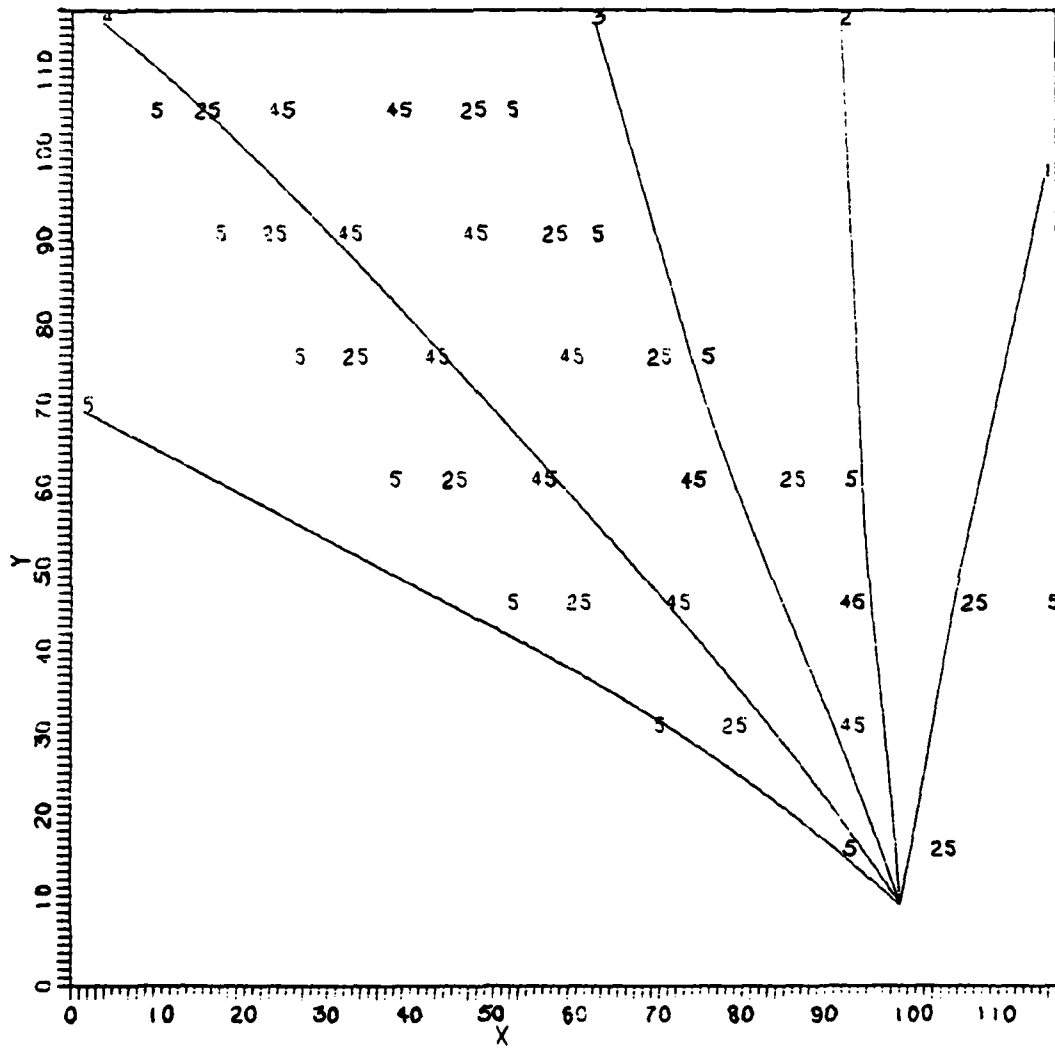


Figure 28. Ray trajectories for 17 second period waves in the Circumpolar Current model. The waves enter a following current from the outer radius side. Current speeds are given in cm/sec and  $N = 0.038$ . Grid spacing is 20 km.

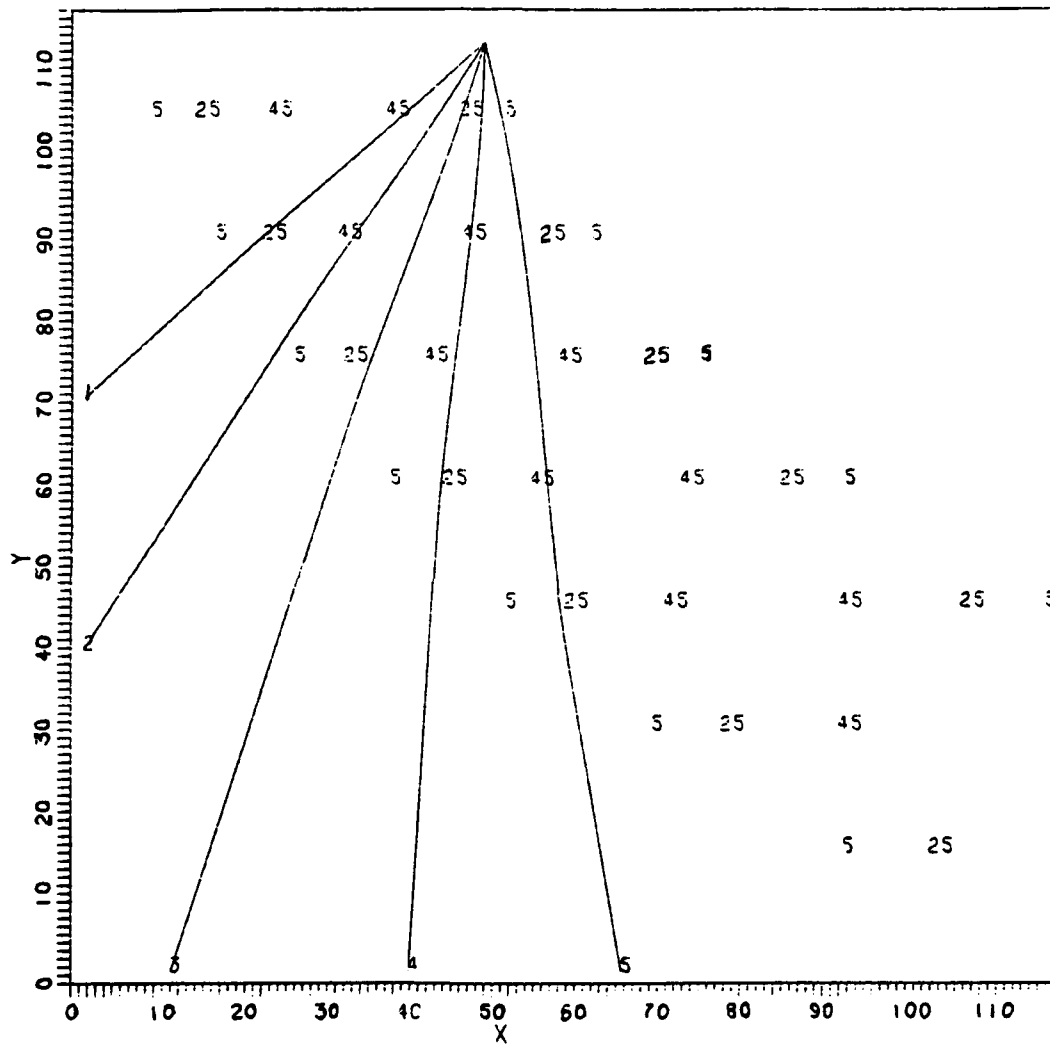


Figure 29. Ray trajectories for 17 second period waves in the Circumpolar Current model. The waves enter an opposing current from the inner radius side. Current speeds are given in cm/sec and  $N = 0.038$ . Grid spacing is 20 km.

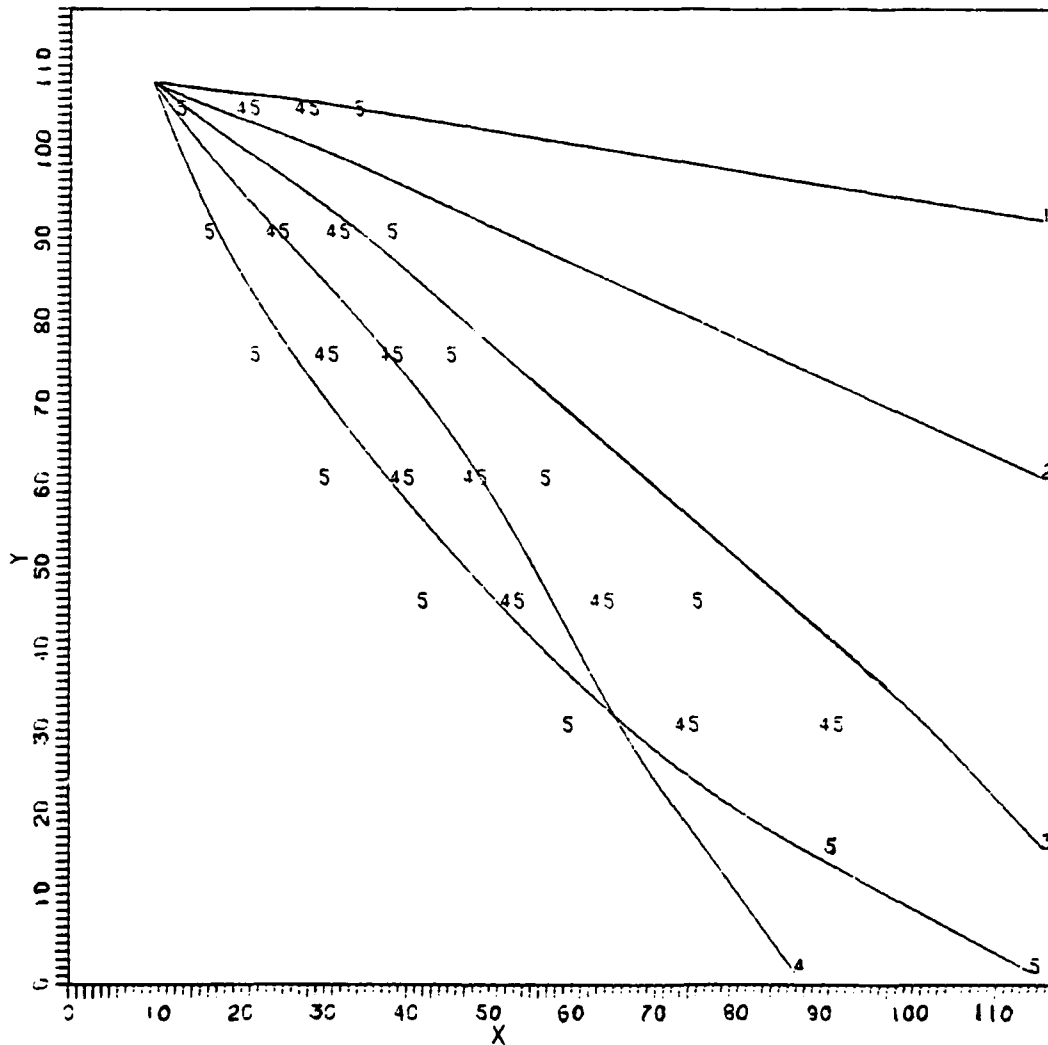


Figure 30. Ray trajectories for 17 second period waves in the Circumpolar model. The waves enter an opposing current from the outer radius side. Current speeds are given in cm/sec and  $N = 0.038$ . Grid spacing is 45 km.

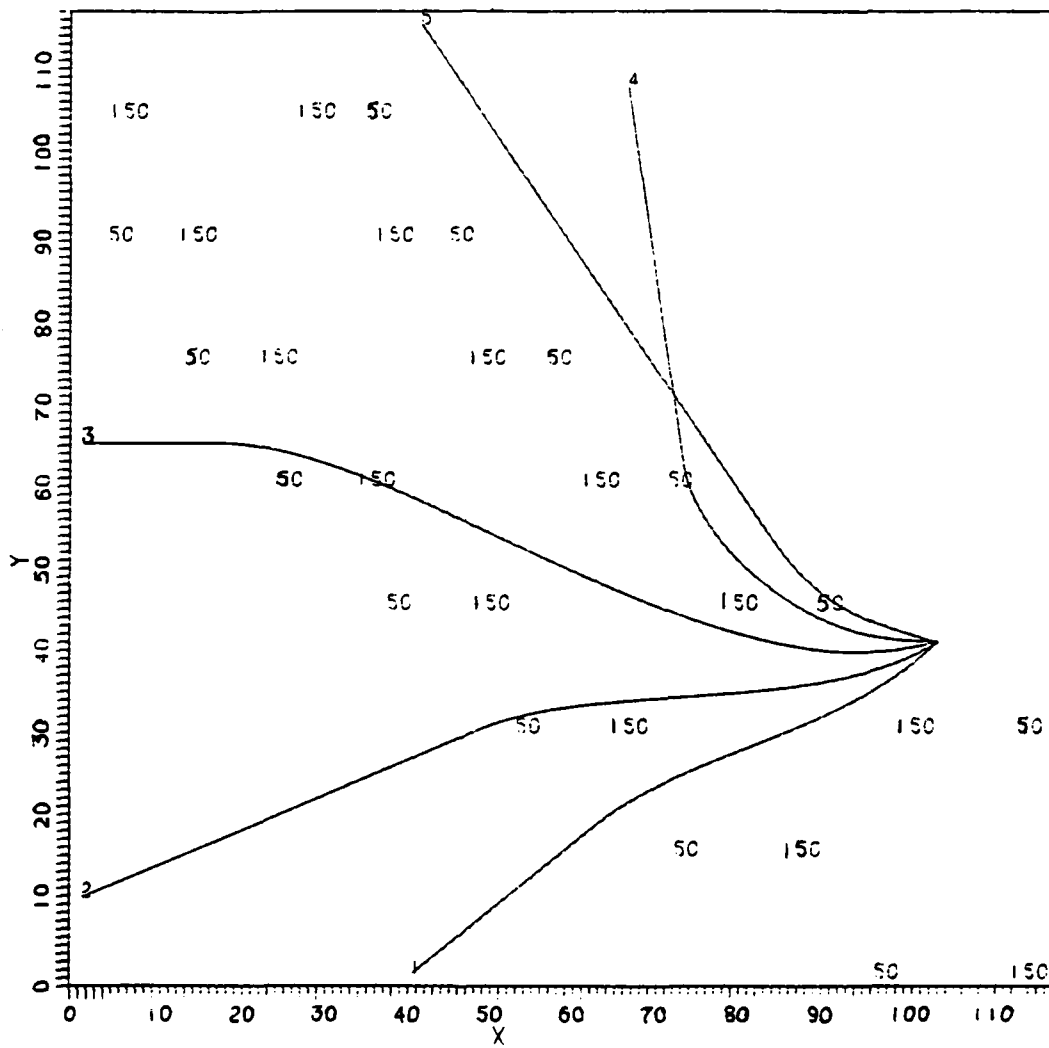


Figure 31. Ray trajectories for 7 second period waves in the curved Gulf Stream model. The waves enter a following current from the inner radius side. Current speeds are given in cm/sec and  $N = 0.366$ . Grid spacing is 2.5 km.

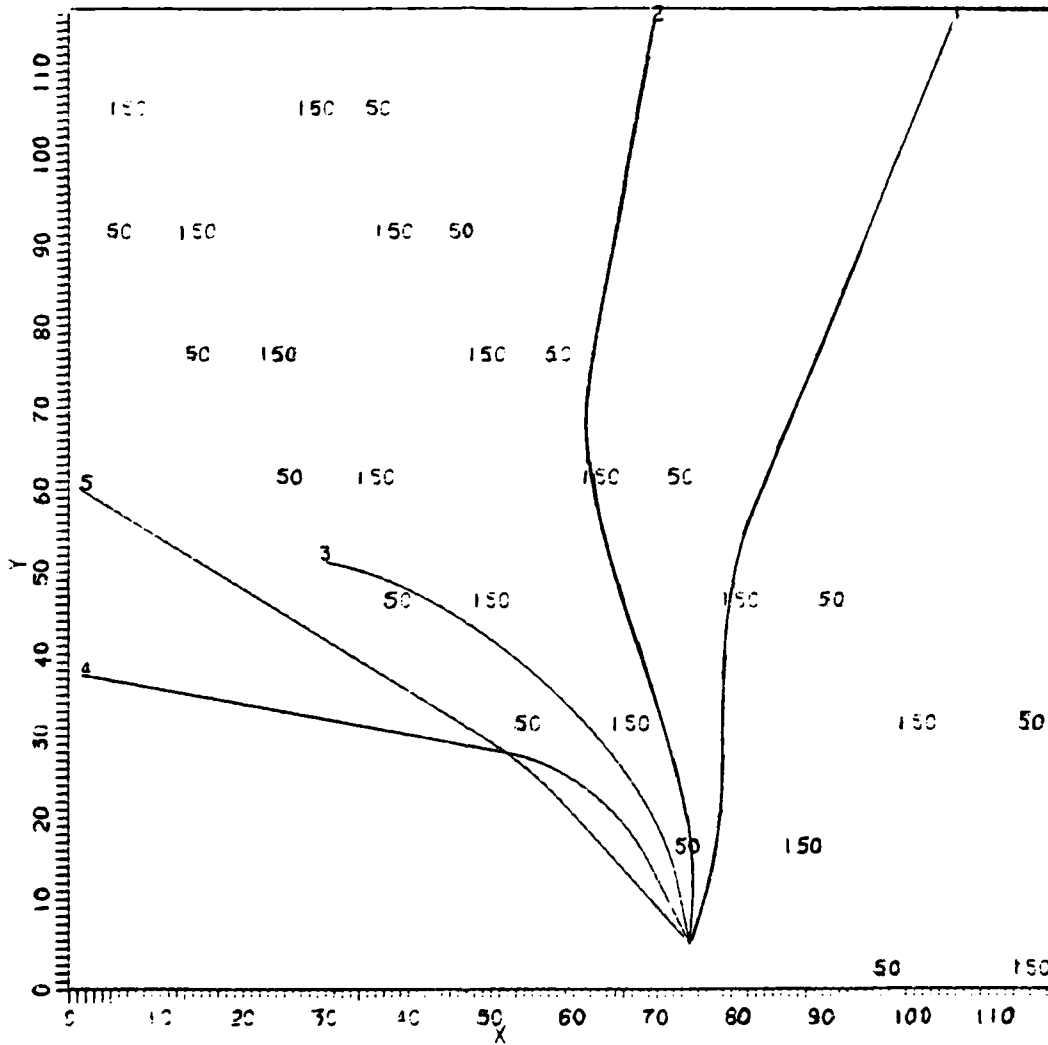


Figure 32. Ray trajectories for 7 second period waves in the curved Gulf Stream model. The waves enter a following current from the outer radius side. Current speeds are given in cm/sec and  $N = 0.366$ . Grid spacing is 2.5 km.

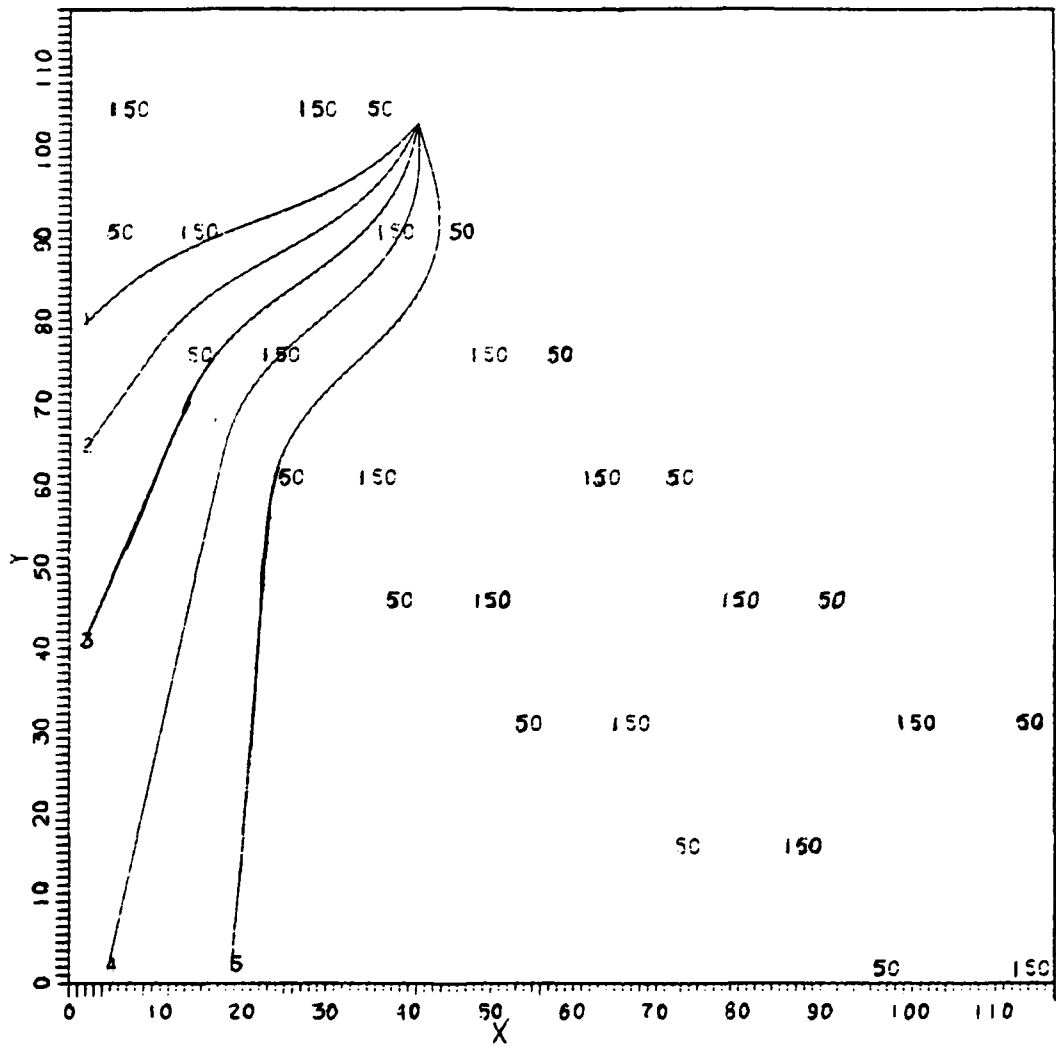


Figure 33. Ray trajectories for 7 second period waves in the curved Gulf Stream model. The waves enter an opposing current from the inner radius side. Current speeds are in cm/sec and  $N = 0.366$ . Grid spacing is 2.5 km.

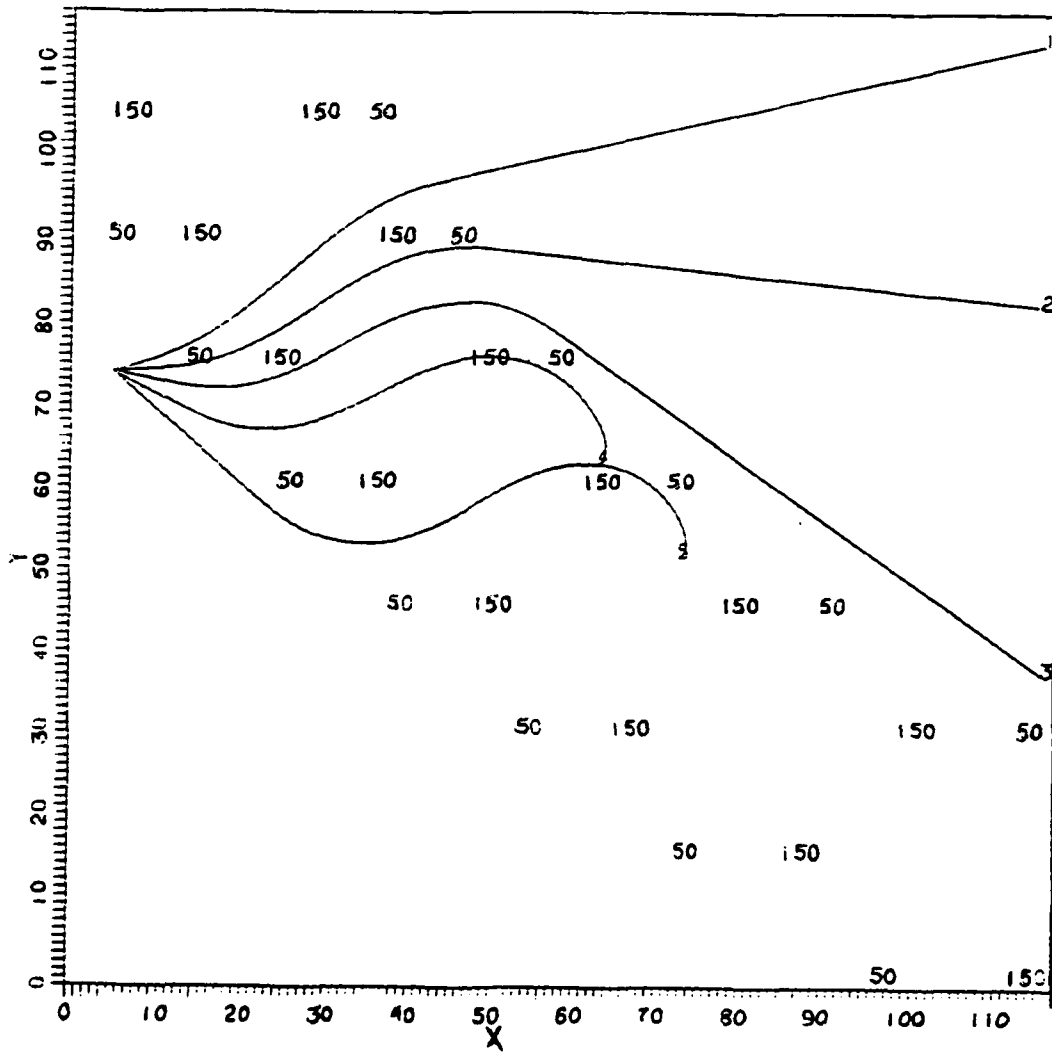


Figure 34. Ray trajectories for 7 second period waves in the curved Gulf Stream model. The waves enter an opposing current from the outer radius side. Current speeds are given in cm/sec and  $N = 0.366$ . Grid spacing is 2.5 km.

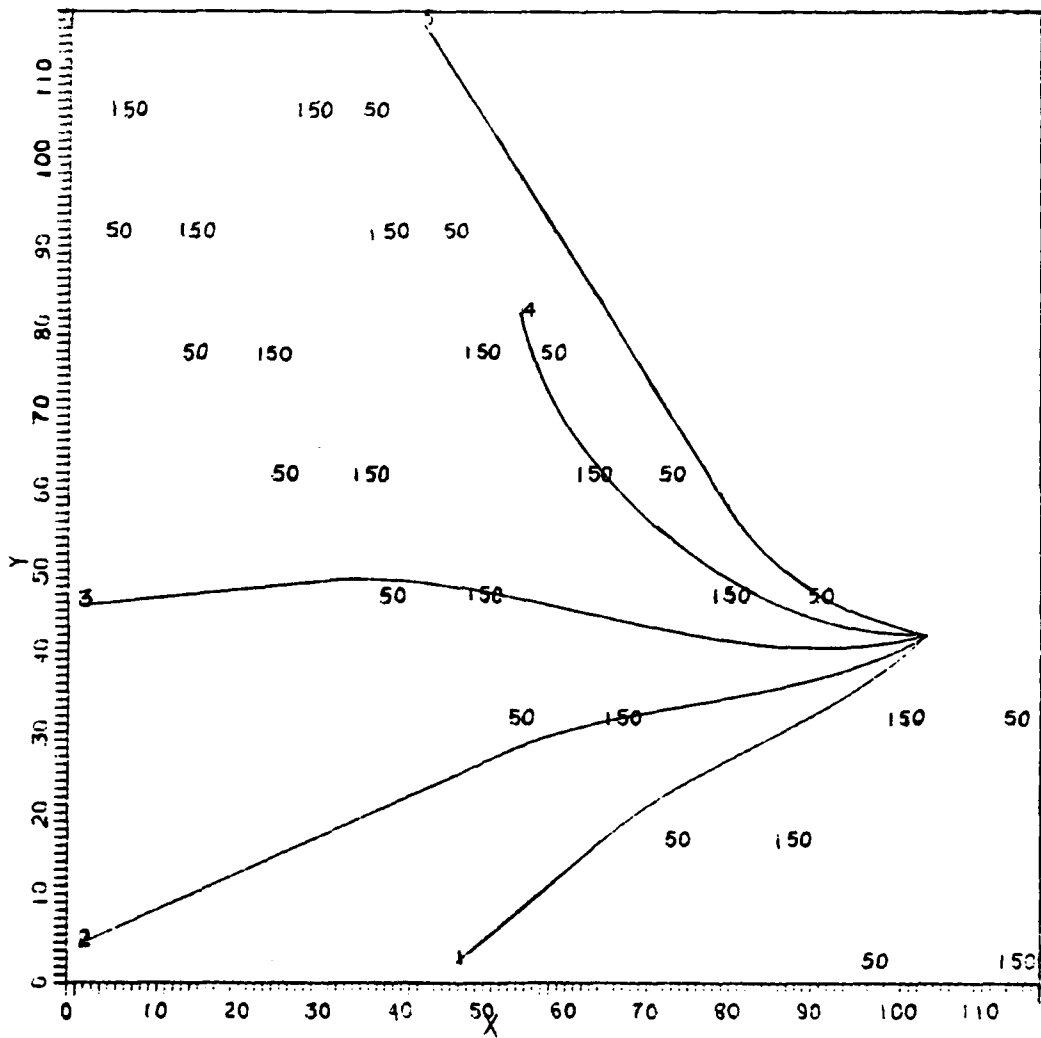


Figure 35. Ray trajectories for 10 second period waves in the curved Gulf Stream model. The waves enter a following current from the inner radius side. Current speeds are in cm/sec and  $N = 0.256$ . Grid spacing is 2.5 km.

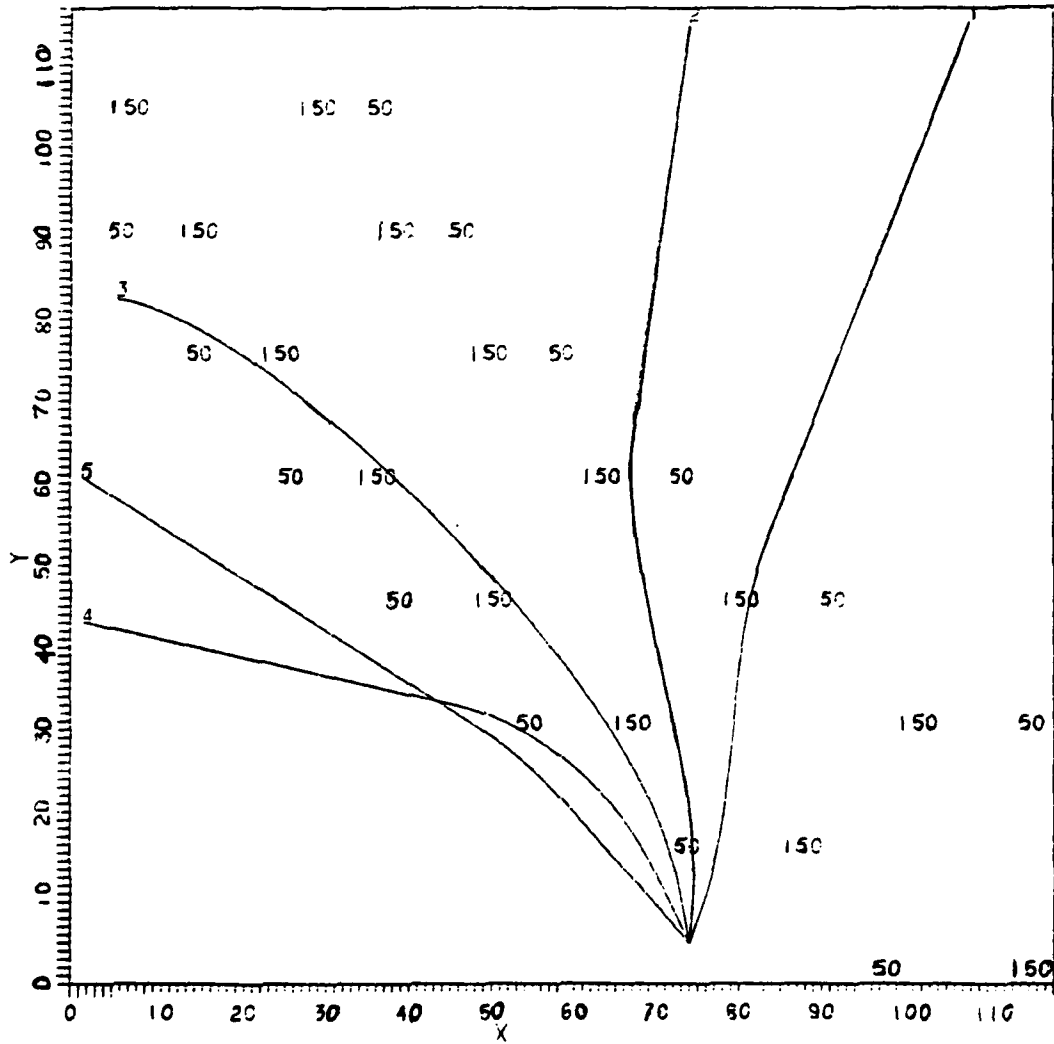


Figure 36. Ray trajectories for 10 second period waves in the curved Gulf Stream model. The waves enter a following current from the outer radius side. Current speeds are given in cm/sec and  $N = 0.256$ . Grid spacing is 2.5 km.

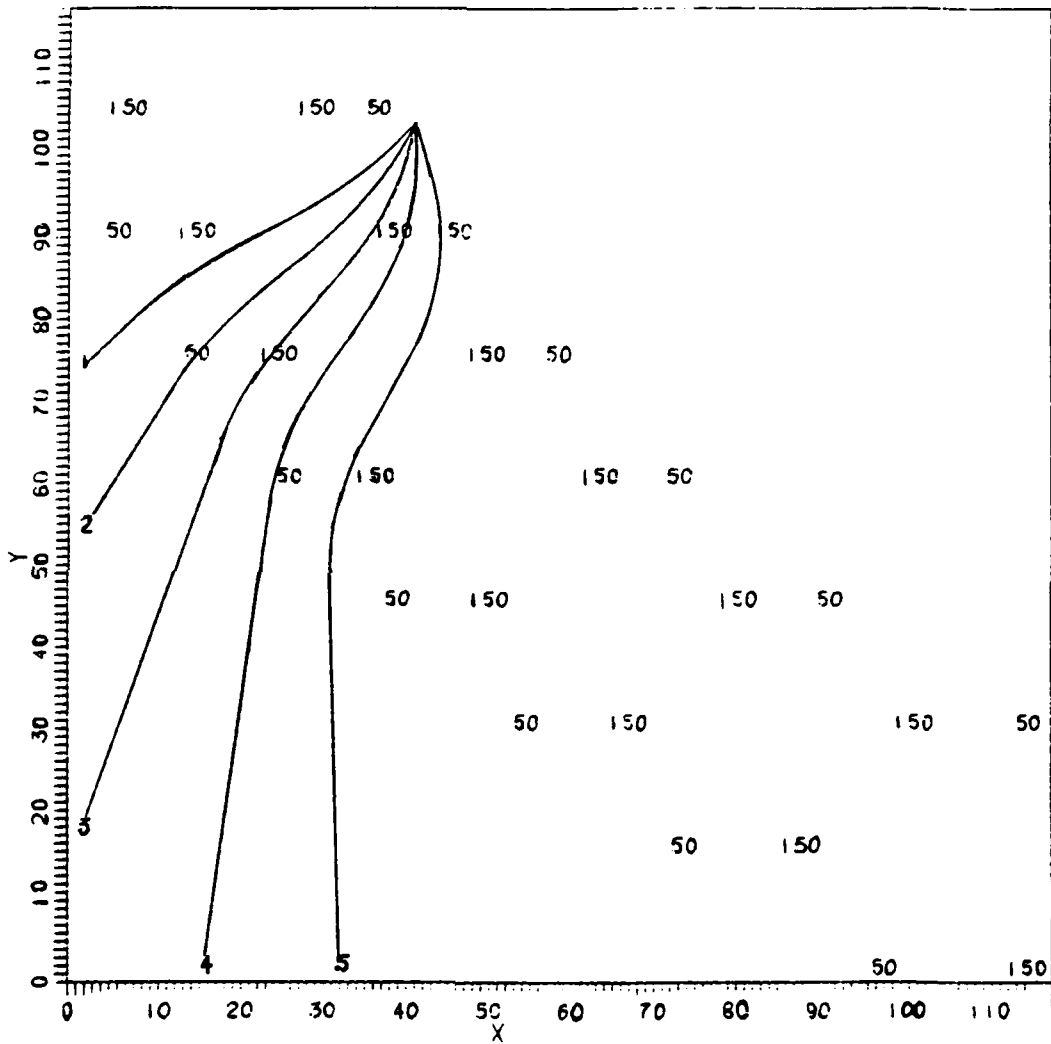


Figure 37. Ray trajectories for 10 second period waves in the curved Gulf Stream model. The waves enter an opposing current from the inner radius side. Current speeds are given in cm/sec and  $N = 0.256$ . Grid spacing is 2.5 km.

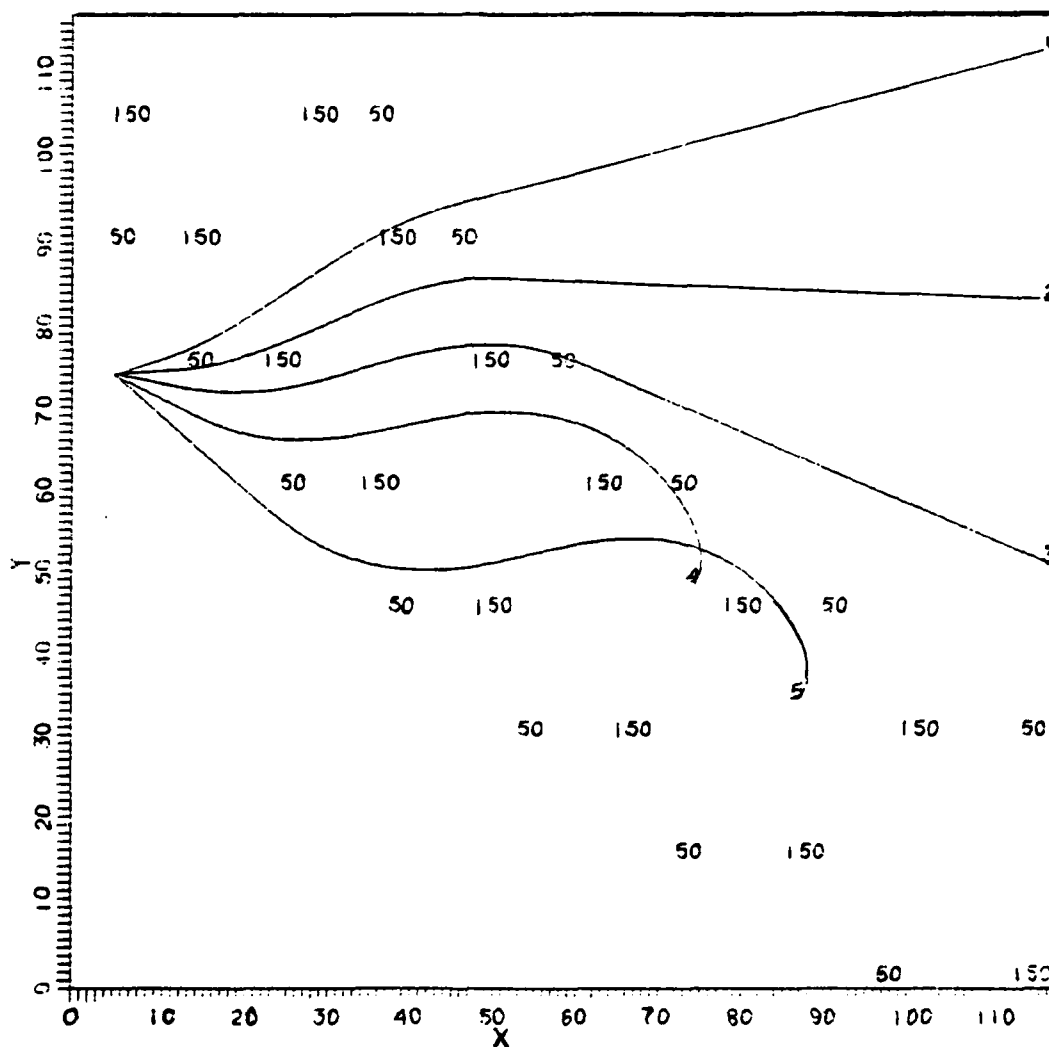


Figure 38. Ray trajectories for 10 second period waves in the curved Gulf Stream model. The waves enter an opposing current from the outer radius side. Current speeds are given in cm/sec and  $N = 0.256$ . Grid spacing is 2.5 km.

## V. COMPARISON OF REFRACTION METHODS

### A. Monochromatic refraction

Arthur (1950) considered the refraction of monochromatic waves by currents in shallow water. The equations he used and the results he obtained were discussed in Chapter II. In this section Arthur's approach is applied to deep water waves.

Monochromatic trajectories were computed using equation (26), which determines the direction of the waves along a ray, and

$$\tan\rho = \frac{u}{V' \cos\gamma} + \tan\gamma \quad (87)$$

which determines the direction of the ray. These equations are the same as equations (2) and (3) adjusted for deep water. Comparison of equations (33), for wave packets, and (87), for monochromatic waves, indicates that the ray directions for monochromatic waves changes less than the ray direction for wave packets, since  $G' < V'$ . Also, from these equations it is found that the monochromatic rays and monochromatic waves totally reflect at the same point, and that their critical angles are larger than the critical angles for packet rays (same as in Figure 2). These characteristics are clearly seen in Figures 39 thru 41, where the subscript  $m$  denotes monochromatic rays and the subscript  $p$  denotes packet rays. Since the ray equation for monochromatic rays has the same form as does the ray equation for wave packets the same general physical properties apply to both.

In Sections III.D. and IV.C., it was shown that  $\rho$ ,  $\theta$ , and  $\gamma$  are nearly equal when  $u \ll G'$ , since then little refraction occurs. This means that as  $u/G'$  approaches zero wave packet rays and monochromatic rays become nearly identical. However, they do not become identical, since  $G'$  is not equal to  $V'$ . The best agreement between monochromatic rays and wave packet rays is seen to occur for the rays with small initial angles, with differences increasing as the initial angle increases. The worst agreement is for rays which undergo total reflection. This occurs since the difference in the angles  $\theta$  and  $\gamma$  increases as the initial angle increases.

#### B. Vorticity approach

The vorticity equation (74) developed in Section III.G. is the same equation used by Teague (1974) to compute ray paths through eddy type currents. This equation was derived by assuming that  $u \ll G'$ , that  $U'$  is constant along a ray, and that the packet and wavelet directions are identical. Although  $U'$  is not actually constant along a ray, it changes so slightly when  $u \ll G'$  that there is no discernable difference between rays computed with  $U'$  constant and rays with  $U'$  allowed to vary. It was found that when  $N$  was 0.091, the conventional group speed changed by less than 4 percent along a ray and by less than 2 percent when  $N$  was 0.046.

Rays computed using the vorticity equation (74) are denoted in the figures by the subscript  $v$ . It is clearly seen from these figures that the best agreement between the vorticity rays and the

wave packet rays occurs when  $N$  is less than 0.05 (Figure 41), and when the initial angles are small. As  $N$  increases the vorticity rays become less reliable, with the worst agreement in Figure 39 occurring when  $N$  is 0.366. Vorticity rays and packet rays are seen to be identical or nearly so when the initial angles are 15 degrees or less, and to be significantly different when the initial angles equal or exceed the critical angles.

The vorticity rays shown in Figure 39 deviate appreciably from packet rays, since the assumptions made in deriving the vorticity equation (74) break down for such high values of  $N$ . In this case the speeds  $U'$  and  $G' = U' \cos(\theta - \gamma)$  change significantly along a ray. It was found that when  $N = 0.366$ ,  $U'$  changes by about 5 percent for a ray with an initial angle of 15 degrees and by as much as 13 percent for a ray with an initial angle of 45 degrees. The speed  $G'$  changes by 5 percent along a ray with an initial angle of 15 degrees to as much as 56 percent along a ray with an initial angle of 60 degrees.

Teague (1974) considered the refraction of wave packets by currents using the vorticity method. He investigated cyclonic eddies and swell waves with  $N$  values of 0.17, 0.08, and 0.02. From what has been shown here, it is evident that the vorticity method would result in reasonable ray trajectories for the second and third cases, but questionable trajectories for the first case.

### C. Kenyon's approach

Kenyon (1971) considered the refraction of wave packets by assuming that the packets travel in the same direction as the wavelets

within the packet. Thus, he used the conventional group speed instead of the geometric group speed. Kenyon determined ray trajectories by integrating the ray equations (4) for specific currents. He stated that his approach would be similar to the vorticity approach when  $u \ll G'$ .

A method of determining ray trajectories, which yields the same results as was obtained by Kenyon (1971), is to use equation (26) to determine the wavelet direction along a ray and

$$\tan \rho = \frac{u}{U' \cos \gamma} + \tan \gamma \quad (88)$$

to compute the ray direction. Trajectories computed using these equations are shown in Figures 39 thru 41. They are denoted by the subscript  $k$ . Comparison of equation (33) and equation (88) indicates that rays computed using these equations will differ as  $\theta$  and  $\gamma$  differ. It is also evident from these equations that the general physical properties discussed in Section III.D. and III.G. will also apply to rays computed using Kenyon's method. These features can be seen in the rays shown in the figures.

It is apparent from the figures that when  $N \leq 0.05$ , Kenyon's method and the one derived here give very similar rays. But, as  $N$  increases the difference in the ray trajectories increases, since then the difference in the directions of the wavelets and packets becomes significant. A similar relationship is found for initial angles. With small initial angles there is better agreement than for larger initial angles.

Lastly, it can be seen that when  $u \ll G'$  the vorticity method gives rays very similar to those determined by Kenyon's method.

#### D. Summary of refraction methods

In this chapter, it has been shown that the vorticity method is valid only under very limited conditions, with the best results occurring when  $N \leq 0.05$ . Reasonable trajectories, though, can be obtained even if  $N$  is as large as 0.10. Thus, it can be concluded that for swell waves (7 to 20 seconds) the vorticity method of wave refraction would not be applicable to currents like the Gulf Stream ( $N$  ranges from 0.366 to 0.13), but could be applied to currents like the Circumpolar Current ( $N$  ranges from 0.09 to 0.03). The vorticity method should, therefore, be confined to currents with speeds less than about 50 cm/sec for swell waves.

The results presented in this chapter indicate that the refraction methods discussed yield similar ray trajectories when  $u \ll G'$  and when the initial angles are small ( $< 30$  degrees). It has also been shown that as  $N$  increases and as the initial angle increases the ray trajectories become quite different using the various refraction methods. It can be seen from Figures 39 thru 41 that rays computed using the monochromatic method, vorticity method, or Kenyon's method agree more consistently with each other than any of them do with rays computed using the wave packet method presented in this study. In only the latter method is the difference in the wavelet and packet directions taken into account.

AD-A133 366

REFRACTION OF WAVE PACKETS BY CURRENTS(U) FLORIDA INST  
OF TECH MELBOURNE DEPT OF OCEANOGRAPHY AND OCEAN  
ENGINEERING S K HORTON APR 82 TR-JEB-9

2/2

UNCLASSIFIED

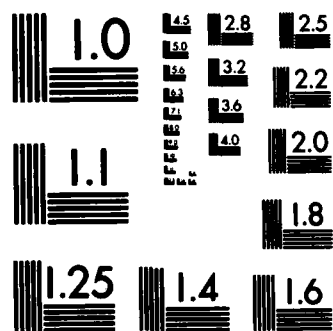
N00014-80-C-0677

F/G 8/3

NL



END  
FILMED  
SERIALS  
SECTION



MICROCOPY RESOLUTION TEST CHART  
NATIONAL BUREAU OF STANDARDS-1963-A

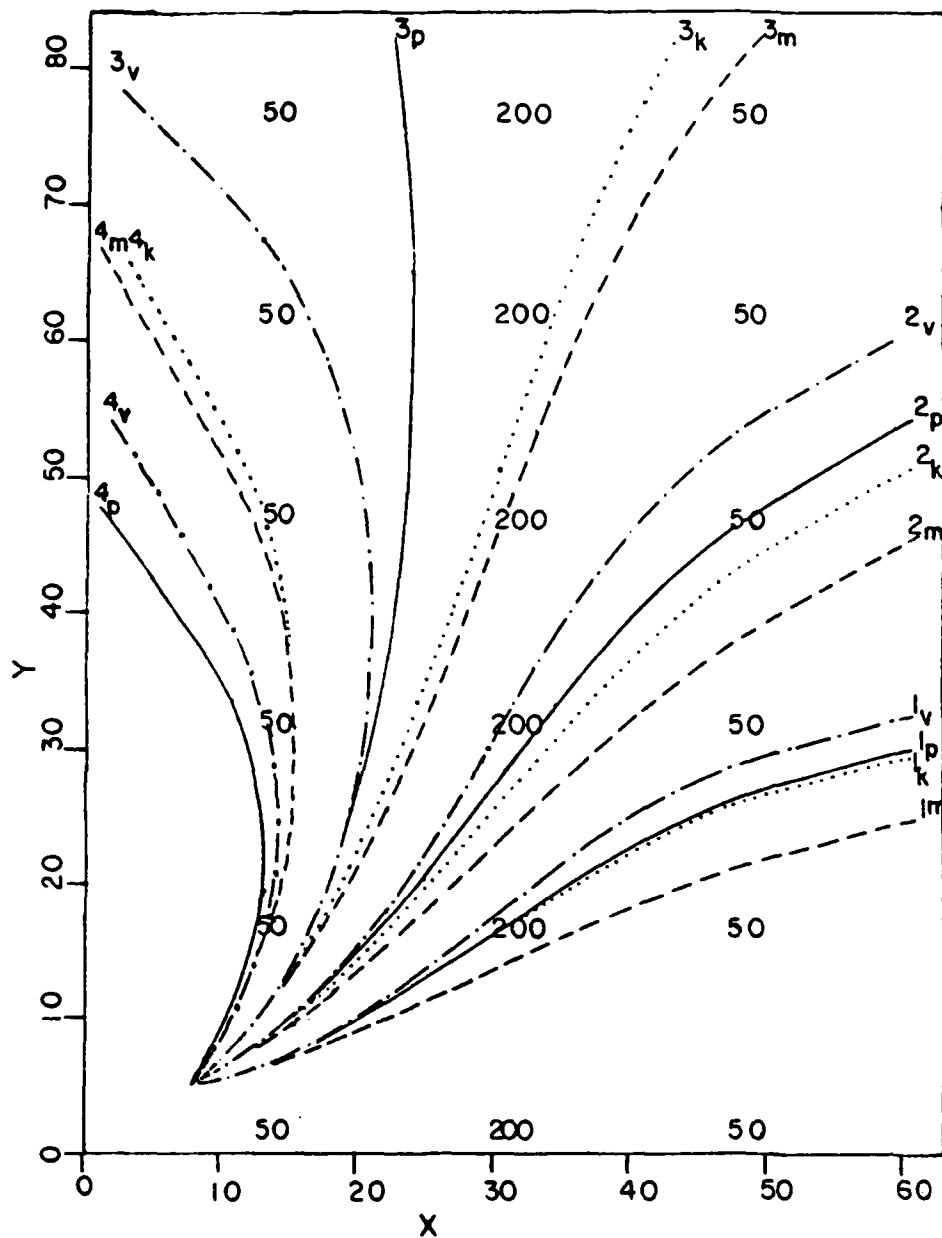


Figure 39. The rays in this figure were computed using the various refraction methods. The subscript p denotes the wave packet refraction method developed in this paper. The subscript k denotes Kenyon's method of wave packet refraction while the subscripts v and m denote the vorticity and monochromatic methods, respectively. Rays with initial angles of 15, 30, 45, and 60 degrees are shown. Current speeds are given in cm/sec and  $N = 0.366$ . Grid spacing is 2.5 km.

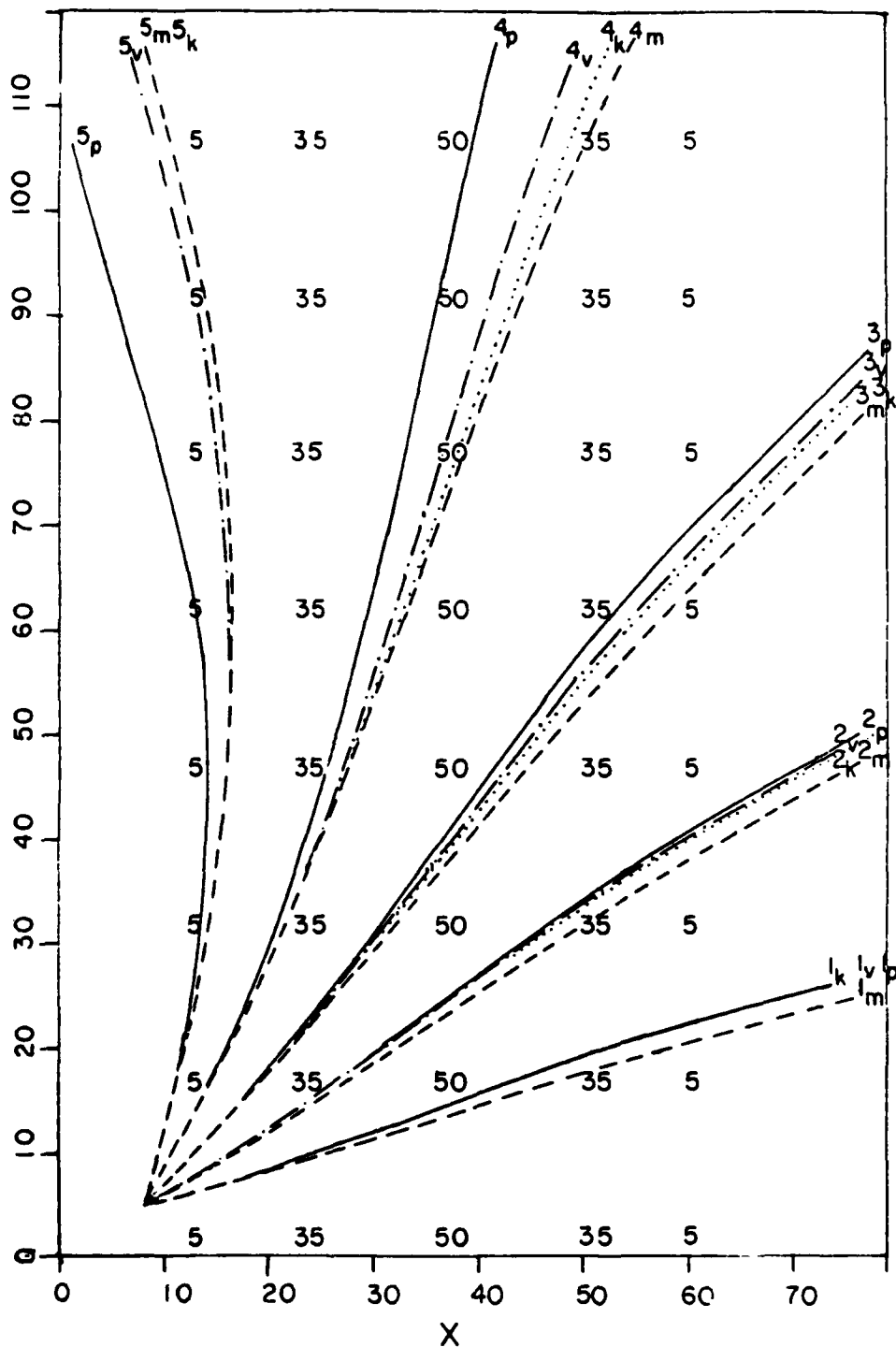


Figure 40. The rays in this figure were computed using the various refraction methods. The subscript p denotes the wave packet refraction method developed in this paper. The subscript k denotes Kenyon's method of wave packet refraction while the subscripts v and m denote the vorticity and monochromatic methods, respectively. Rays with initial angles of 15, 30, 45, 60, and 75 degrees are shown. Rays  $1_v$ ,  $1_k$ , and  $1_p$  are seen to be identical as are rays  $5_m$  and  $5_k$ . Current speeds are given in cm/sec and  $N = 0.091$ . Grid spacing is 20 km.

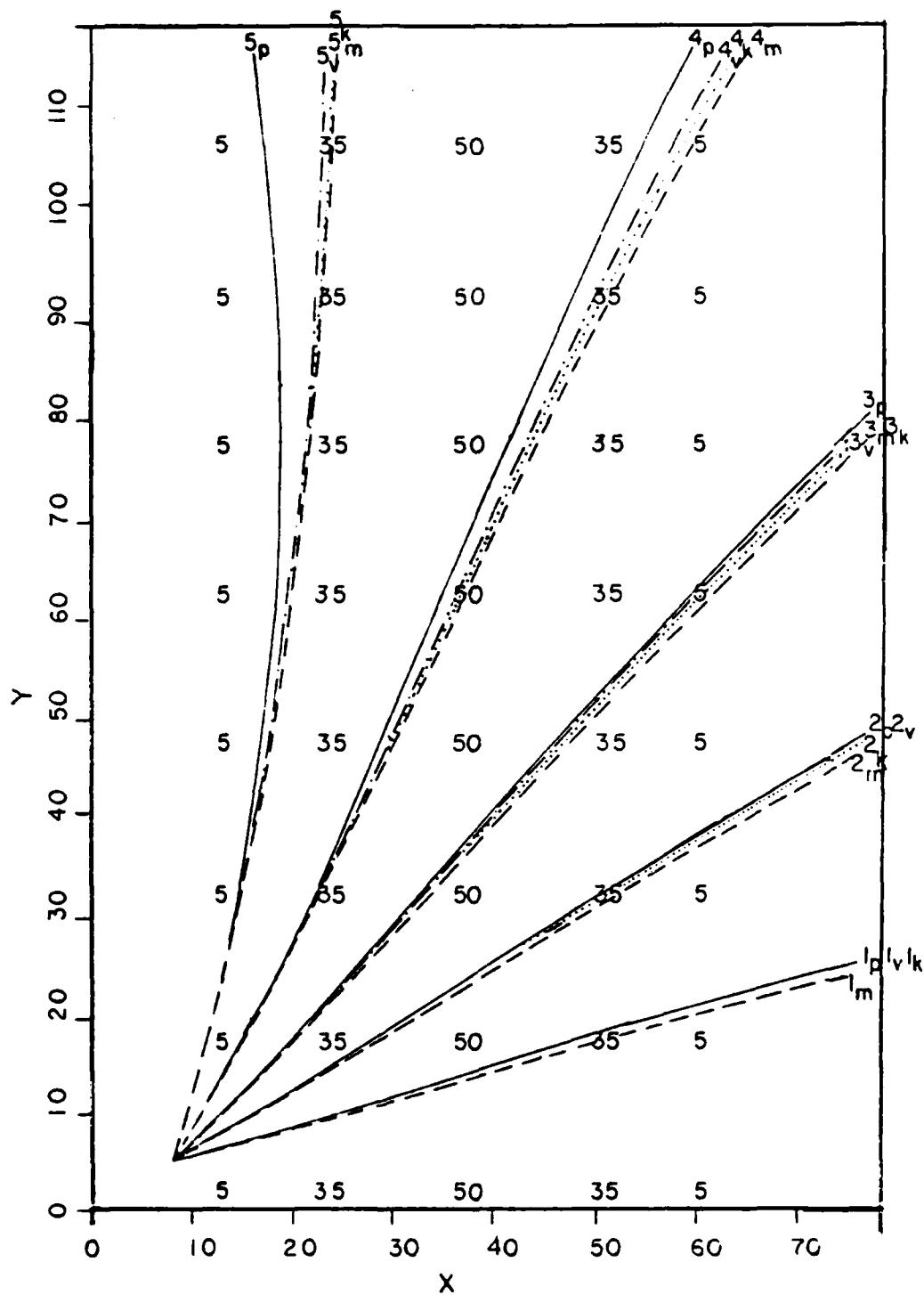


Figure 41. The rays in this figure were computed using the various refraction methods. The subscript p denotes the wave packet refraction method developed in this paper. The subscript k denotes Kenyon's method of wave packet refraction while the subscripts v and m denote the vorticity and monochromatic methods, respectively. Rays with initial angles of 15, 30, 45, 60, and 75 degrees are shown. Rays  $1_v$ ,  $1_k$ , and  $1_p$  are identical as are rays  $2_v$  and  $2_p$ . Current speeds are given in cm/sec and  $N = 0.046$ . Grid spacing is 20 km.

## VI. CONCLUSIONS AND RECOMMENDATIONS

### A. Conclusions

Breeding's method (1972, 1978, and 1981) of wave packet refraction has been applied in this study to the refraction of wave packets by currents. In this method, the direction of the wavelets and of the packets vary after refraction. Thus, curvature expressions for both wavelets and packets are needed for ray trajectory computations. It was found from the expression for the wavelet direction along a ray (equations 21 and 26) that the change in direction of the wavelets is dependent primarily upon the shear of the current and the phase speed relative to a fixed point. The change in direction of the packets (equations 27 and 28) was found to be dependent upon the current shear, the geometric group speed relative to a fixed point, the direction of the wavelets  $\gamma$ , and the difference in the direction between the wavelets and packets  $\phi$ .

Arthur (1950) and Kenyon (1971) pointed out that in a current rays are not generally orthogonal to the wave fronts. Thus, the direction of the ray is different from the direction of either the packets or the wavelets along the ray. It was shown that an advection equation (equation 30) patterned after Arthur's approach, or a vorticity equation (equation 73 or 74) could be derived to determine ray paths. The advection equation was found to be more general and more accurate than the vorticity equation. The best results from the

vorticity equation can be expected when  $N \leq 0.05$ . Values of  $N$  as large as 0.10 would give reasonable results, but  $N$  values greater than this would be questionable. Thus, it is concluded that a set of three equations is required to compute ray trajectories for wave packets refracted by a current. The ray is determined by simultaneously solving the curvature expression for the wavelets (equation 26), the curvature expression for the packets (equation 28), and the advection equation for the rays (equation 30).

The curvature equations for the wavelets and packets (equation 21 and 27) were derived from the ray equations of geometrical optics (equations 5 and 6), and from expressions for the angular frequencies of the wavelets and packets in a moving medium (equations 13 and 14). In geometrical optics, it is assumed that wave properties such as wavelength and direction change little over a distance of the order of a wavelength.

It was found that wave properties can be expressed as the sum of a component relative to the current and a component due to advection by the current. This is seen, for example, in equations (13) and (14) where the angular frequency is defined with respect to a fixed point. Further, it was found that the angular frequency relative to a fixed point is constant along a ray, but that the angular frequency measured relative to the current is Doppler shifted by the current. This latter frequency decreases in a following current and increases in an opposing current. Other wave properties are affected in a similar manner. In particular, the ray speed  $P$ , the geometric group speed  $G'$ , the wavelet speed  $V'$ , and the wavelength increase in a following

current and decrease in an opposing current.

Properties of wave packet rays were deduced from the ray equations (30) and (74). From these equations, it was found that swell waves are reflected or deflected from their original paths by a current with the short period waves being affected to a greater extent than the long period waves. Rays were found to bend away from (toward) the current normal in a following (opposing) current. This corresponds to saying that the sign of the curvature of a ray is the same as the sign of the vorticity of the current. The curvature of a ray was also found to increase as the vorticity of the current increased and to decrease as the value  $N$  decreased. Further, it was found that for a following and an opposing current the change in the direction of the ray is greater than the change in the direction of the packet, which is greater than the change in direction of the wavelets. If  $u \ll G'$ , then  $\rho \approx \theta$ . Wavelets and packets were found to remain normal to the current contours if they entered the current at normal incidence, but the ray was found to curve due to advection by the current. It was found that in a parallel current only rays in a following current are totally reflected, and at the turning point the ray, packet, and current directions are parallel. For a parallel, opposing current rays were found to bend toward the current normal and if sufficient refraction occurred rays would become perpendicular to the current contours. For curved currents, it was found that total reflection could occur in an opposing current. When this happens the ray and current are in opposite directions.

Snell's law equations for wavelets (equation 37) and for packets (equation 42) were deduced from the fact that relative to a fixed point the angular frequencies  $\omega$  and  $\sigma$  are constant along a ray, and that the components of the wave numbers  $\vec{k}$  and  $\vec{m}$  parallel to the current contours are also constant. When the transmitted value of the angle ( $\theta$  or  $\gamma$ ) is set equal to 90 degrees, the Snell's law equation can be rearranged to obtain an expression for the critical angle (wavelets, equation 51 and packets, equation 53). It was found that critical angles are dependent upon the value of  $M$  only. Thus waves of various periods may have the same critical angle if the current values are sufficient to cause the value of  $M$  to be the same. For example, a ray with an initial angle of 71 degrees is reflected if  $M$  is 0.046. This corresponds to a 14 second period wave and a current speed of 0.5 m/sec, or a 7 second period wave and a 0.25 m/sec current speed. This relationship is shown graphically in Figures 2 and 3. From these figures it was found that the critical angles for wavelets are greater than the critical angles for packets for any given  $M$  value. Since the packets and rays totally reflect at the same point, whereas the wavelets do not, the values of  $\theta$  and  $\gamma$  are appreciably different following a turning point. This would affect the geometric group speed  $G'$  causing it to be reduced in value. In fact,  $G'$  will vanish if  $\theta$  and  $\gamma$  differ by 90 degrees. Further, it was found that for swell waves (7 to 20 seconds), rays with initial angles less than 44 degrees are not reflected by open ocean currents since the current speeds are not sufficiently large. The critical angles computed from equations (51) and (53) are for currents with

parallel contours. It was found that the critical angle for waves which enter a curved current from the inner radius side are larger than the critical angles determined for the same waves in a parallel current, and that the critical angle for waves which enter from the outer radius side are less than those determined for parallel currents.

Four current models were considered in this study. These models were patterned either after the Gulf Stream or after the Circumpolar Current. Two of the models had parallel speed contours and two had curved speed contours (Section IV.A.). Ray trajectories computed using these current models demonstrated the physical properties determined from the ray equations. For the parallel current models, it was found that rays were deflected or reflected by a following current, and only deflected by an opposing current. Every ray which entered an opposing, parallel current passed through the current, but was deflected some distance upstream from its non-current path. Some rays in a following, parallel current passed through the current, and others were turned back and exited the current on the same side they entered the current. Similar results were obtained from the curved current models with a few exceptions. It was found that some rays were totally reflected by an opposing, curved current. Only rays which entered the opposing, curved current from the outer radius side could possibly be totally reflected. It was also found that some rays were focused by the current into a given area, that some rays exited and then re-entered the current, and that some rays were trapped within the current.

These results for the parallel and curved current models give some insight as to what could be expected for waves in the actual Gulf Stream or Circumpolar Current. All waves which enter the Gulf Stream from the northeast would be deflected some distance upstream from their non-current path. The degree of deflection would depend upon the value of  $N$  and upon the curvature of the current. Waves which enter the Gulf Stream from the southeast may pass through the current or may be totally reflected by the current. Rays with initial angles greater than about 44 degrees may be totally reflected. It was shown that the critical angle increases as  $N$  increases and as the curvature of the current increases. Waves which enter the Gulf Stream from the northwest or southwest may pass through the current or may be reflected by the current. The greater the curvature of the current contours the more likely the waves which enter from this side (outer radius side) of the current will be reflected. These results show that the Gulf Stream can act as a shelter for the coastline, keeping some swell waves from reaching the coast from the open oceans. However, it is also seen that some waves which approach from the slope water side will be turned back toward the coastline and possibly be trapped between the current and the coastline.

For the Circumpolar Current, it would be expected that waves which enter from the Antarctic side would pass through the current with some deflection from their non-current paths. Some rays may be totally reflected, but only if their initial angles are as large as about 75 degrees. Waves which enter the Circumpolar Current from the outer radius side (from the north) are more likely to be reflected

by the current. These rays may also be focused by the current or exit and re-enter the current on the Antarctic side. Thus, the Circumpolar current may significantly alter the path of waves which enter it.

Lastly, the wave packet refraction method developed in this study was compared to Arthur's (1950) monochromatic refraction method and to Kenyon's (1971) and Teague's (1974) wave packet refraction method. It was found that when the value of  $N$  is very small ( $\leq 0.10$ ) and when the initial angles of the rays are small ( $< 30$  degrees), that the various wave refraction methods give nearly identical trajectories. However, as  $N$  increases and as the initial angle increases the trajectories become considerably different. The differences in the trajectories are due primarily to the differences in  $\theta$  and  $\gamma$ , which are only accounted for in the wave packet refraction method presented in this study.

#### B. Recommendations

This study was confined to deep water currents, while Arthur (1950) considered shallow water currents. A natural extension of this study would be to investigate wave-current interactions at intermediate water depths. This study was also confined to considering ray and wave directions only. Thus, the effect of the current on wave heights was not considered. Johnson (1947) and Arthur (1950) have shown that wave heights are altered by a current. Wave heights may be enhanced by an opposing current or diminished by a following current. For example, Johnson (1947) discussed waves off

the coast of Washington which were observed to be diminished in height by a current. Arthur (1950) showed that wave heights could be increased such that breaking occurred within the current. Thus, to obtain a good understanding of wave-current interactions wave heights must be considered. Another area which needs to be investigated is the effect that waves have on the currents. Waves and currents probably affect each other. Teague (1974) mentioned the possibility that waves which break within an eddy may enhance the decay of the eddy. Finally, it should not be assumed that currents are constant to the depth of penetration of the waves. This assumption is good for the Circumpolar Current, since it is a deep current, but it may not be too good for the Gulf Stream.

It is highly desirable to conduct a field study in order to test the refraction theories for actual ocean currents. The Gulf Stream would be a good current for investigating wave-current interactions, since its current speeds are large. It has been found in this study that large current speeds show-up the differences in the various refraction methods quite well. To test these methods good directional wave data and current speed profiles would be required. Wave data should be taken on either side of the current and possibly at a couple of points within the current. Thus, the waves which pass through the current, those which do not, and the amount of deflection from their original paths could be determined. The study would be enhanced by considering waves with initial angles in the mid-range (30 to 70 degrees), since rays with these initial angles differ the most for the different refraction methods. Wave tank

experiments could also be conducted. This problem lends itself quite well to wave tank studies, since short period waves are affected the most by a current. It is necessary to use short period waves in wave tanks in order to have sufficiently short wavelengths.

## REFERENCES

- Arthur, R. S., Refraction of shallow water waves: the combined effects of currents and underwater topography, Am. Geophys. Union, 31(4), 549-552, 1950.
- Black, J. L., Hurricane Eloise directional wave energy spectra, paper presented at Offshore Technology Conference, Houston, Tex., April 30-May 3, 1979.
- Breeding, J. E., Jr., Refraction of gravity water waves, Ph.D. thesis, Columbia Univ., New York, 1972. (Also, Rep. 124-72, Nav. Coastal Syst. Lab., Panama City, Fla., 1972).
- Breeding, J. E., Jr., Refraction for hydrons considering bottom topography and currents, Rep. JEB-5, Florida Inst. of Tech., Melbourne, Fla., 1981a.
- Breeding, J. E., Jr., Ray curvature and refraction of wave packets, in Proceeding of the Seventeenth Coastal Engineering Conference, pp. 82-100, Am. Soc. of Civil Eng., New York, 1981b.
- Hayes, J. G., Ocean current wave interaction study, J. Geophys. Res. 85(c9), 5025-5031, 1980.
- Johnson, J. W., The refraction of surface waves by currents, Am. Geophys. Union, 28(6), 867-874, 1947.
- Kenyon, K. E., Wave refraction in ocean currents, Deep-Sea Res., 18, 1023-1034, 1971.
- Landau, L. D., and E. M. Lifshitz, Fluid Mechanics, 536pp., Addison-Wesley, Reading, Mass., 1959.
- Longuet-Higgins, M. S., and R. W. Stewart, The change in amplitude of short gravity waves on steady non-uniform currents, J. Fluid Mech., 10, 529-549, 1960.
- Shemdin, O. H., J. E. Blue, and J. A. Dunne, Seasat-A surface truth program: Marineland test plan, Doc. 622-6, Jet Propulsion Lab., Pasadena, Calif., 1975.
- Sokolnikoff, I. S., and E. S. Sokolnikoff, Higher Mathematics for Engineers and Physicists, 587pp., McGraw-Hill, New York, 1941.
- Stoneley, R., The refraction of a wave group, Proc. Cambridge Phil. Soc., 31, 360-367, 1935.

Teague, W. J., Refraction of surface gravity waves in an eddy, M.S. thesis, Univ. of Miami, Florida, 1974.

Thompson, E. F., Wave climate at selected locations along U.S. Coast, Tech. Rep. 77-1, U.S. Army Corps of Engineers, Fort Belvoir, Va., 1977.

Zermelo, E., Über das Navigationsproblem bei ruhender oder veränderlicher Windverteilung, *Z. angew. Math. Mech.*, 11, 114-124, 1931.

| REPORT DOCUMENTATION PAGE  |  | READ INSTRUCTIONS<br>BEFORE COMPLETING FORM                              |
|--|--|--|
| 1. REPORT NUMBER<br>JEB-9  | 2. GOVT ACCESSION NO.<br><b>A133 306</b> | 3. RECIPIENT'S CATALOG NUMBER  |
| 4. TITLE (and Subtitle)<br>REFRACTION OF WAVE PACKETS BY CURRENTS  |  | 5. TYPE OF REPORT & PERIOD COVERED<br>Technical                          |
| 7. AUTHOR(s)<br>Shelley Kay Horton   |  | 6. PERFORMING ORG. REPORT NUMBER   |
| 9. PERFORMING ORGANIZATION NAME AND ADDRESS<br>Department of Oceanography & Ocean Engineering<br>Florida Institute of Technology<br>Melbourne, Florida 32901   |  | 8. CONTRACT OR GRANT NUMBER(s)<br>N00014-80-C-0677                       |
| 11. CONTROLLING OFFICE NAME AND ADDRESS<br>Office of Naval Research<br>Coastal Sciences Program<br>Code 422CS, Arlington, VA 22217   |  | 10. PROGRAM ELEMENT, PROJECT, TASK AREA & WORK UNIT NUMBERS<br>NR388-165 |
| 14. MONITORING AGENCY NAME & ADDRESS (if different from Controlling Office)  |  | 12. REPORT DATE<br>April, 1982   |
|  |  | 13. NUMBER OF PAGES<br>109   |
|  |  | 15. SECURITY CLASS. (of this report)<br>Unclassified                     |
|  |  | 15a. DECLASSIFICATION/DOWNGRADING SCHEDULE                               |
| 16. DISTRIBUTION STATEMENT (of this Report)<br>APPROVED FOR PUBLIC RELEASE; DISTRIBUTION UNLIMITED   |  |  |
| 17. DISTRIBUTION STATEMENT (of the abstract entered in Block 20, if different from Report)   |  |  |
| 18. SUPPLEMENTARY NOTES<br>Master of Science Thesis, Florida State University,<br>Tallahassee, Florida   |  |  |
| 19. KEY WORDS (Continue on reverse side if necessary and identify by block number)<br>Refraction                      Total reflection<br>Snell's law                      Critical angle<br>Group velocity<br>Wave packet   |  |  |
| 20. ABSTRACT (Continue on reverse side if necessary and identify by block number)<br>The refraction of wave packets by ocean, surface currents is investigated using a refraction method based on Snell's law with geometric group velocity, $G' = U' \cos \phi$ (Breeding, 1978) where $U' = d\omega'/dk$ , $\phi$ is the difference in the direction of the wavelets and packets, and the prime denotes motion relative to the current. This refraction method requires curvature equations for the directions of the wavelets and wave packets, and an advection equation for the direction of the ray. Three equations are necessary, since after refraction the wavelet and |  |  |

packet directions differ, and a ray is not generally orthogonal to the wave fronts in a current. These equations are derived and applied to idealized current models. The current models are patterned after the Gulf Stream and the Circumpolar Current. Both parallel and curved current contours are considered. From this study, it was found that wave packets can be totally reflected or deflected from their original path by a current with the short period waves being affected to a greater extent than the long period waves. The curvature of a ray was found to have the same sign as the vorticity of the current and to increase as the vorticity increased. Rays were found to bend away from the current normal in a following current and toward the current normal in an opposing current becoming perpendicular to the current speed contours if sufficient refraction occurred. Wave refraction was found to be the least for rays with small initial angles and for currents where  $u_{\max}/G$  (maximum current speed to initial geometric group speed) is small. Further, it was found that the change in the direction of a ray was greater than the change in the direction of the packet, which was greater than the change in the direction of the wavelets. The ray angle increased in a following current, and decreased in an opposing current. Critical angles were computed for parallel current speed contours. From an analysis of these angles, it was found that wave packets totally reflect before the wavelets, and at the same point as do the rays. Also, critical angles were found to be a function of the ratio  $u/G$  (current speed at the turning point to the initial geometric group speed), and to increase as this ratio decreased. Further, it was found that rays with initial angles less than 44 degrees would not be totally reflected by open ocean currents, since extremely large current speeds would be required. An analysis of rays in currents with curved contours indicated that some rays are focused, that some rays exit and re-enter the current, and that some rays may be trapped within the current. These are features which cannot occur with parallel currents. Three additional refraction methods were considered and compared to the method presented here. They were a monochromatic refraction method patterned after Arthur (1950), a wave packet refraction method, using conventional group speed, developed by Kenyon (1971), and a vorticity equation used by Teague (1974) and presented by Kenyon (1971). It was found that there was very good agreement in the results of all the methods for small initial angles and small current speeds. However, differences between the results obtained by the different methods increased greatly for mid-range angles (30-75 degrees) and for large current speeds.

Unclassified

INITIAL DISTRIBUTION LIST

Office of Naval Research  
Coastal Sciences Program  
Code 422CS  
Arlington, VA 22217

Defense Documentation Center  
Cameron Station  
Alexandria, VA 22314

Director  
Naval Research Laboratory  
ATTN: Technical Information Officer  
Washington, D.C. 20375

Director  
Office of Naval Research Branch  
Office  
1030 East Green Street  
Pasadena, CA 91101

Commanding Officer  
Office of Naval Research Eastern/  
Central Regional Office  
Building 114, Section D  
666 Summer Street  
Boston, MA 02210

Office of Naval Research  
Code 422PO  
National Space Technology  
Laboratories  
Bay St. Louis, MS 39529

Office of Naval Research  
Code 422PO  
Washington, D.C. 22217

Office of Naval Research  
Code 100M  
Washington, D.C. 22217

Office of Naval Research  
Operational Applications Division  
Code 200  
Arlington, VA 22217

Commander  
Naval Oceanographic Office  
ATTN: Library, Code 1600  
NSTL Station, MS 39529

Commander  
Naval Coastal Systems Center  
ATTN: Library, Code 116.1  
Panama City, FL 32407

Central Intelligence Agency  
ATTN: OCR/DD-Publications  
Washington, D.C. 20505

Librarian  
Naval Intelligence  
Support Center  
4301 Suitland Road  
Washington, D.C. 20390

Officer in Charge  
Environmental Prediction  
Research Facility  
Naval Post Graduate School  
Monterey, CA 93940

Director  
Amphibious Warfare Board  
U.S. Atlantic Fleet  
Naval Amphibious Base  
Norfolk, Little Creek, VA 23520

Commander  
Amphibious Force  
U.S. Pacific Fleet  
Force Meteorologist  
Comphibpac Code 255  
San Diego, CA 92155

Commanding General  
Marine Corps Development and  
Educational Command  
Quantico, VA 22134

Office of Naval Operations  
OP 9870  
Department of the Navy  
Washington, D.C. 20350

Commandant  
U.S. Coast Guard  
ATTN: GECV/61  
Washington, D.C. 20591

National Oceanographic Data Center (D764)  
Environmental Data Services  
NOAA  
Washington, D.C. 20235

Defense Intelligence Agency  
Central Reference Division  
Code RDS-3  
Washington, D.C. 20301

Director  
Coastal Engineering Research Center  
U.S. Army Corps of Engineers  
Kingman Building  
Fort Belvoir, VA 22060

END

FILMED

10-83

DTIC